SOLUTE ATOM - DEFECT INTERACTIONS
IN
SILICON AND GERMANIUM

INTERACTIONS BETWEEN SOLUTE ATOMS AND DEFECTS
IN
SILICON AND GERMANIUM

By

RALPH CLARENCE DORWARD, B.Sc., M.Sc.

A thesis
Submitted to the Faculty of Graduate Studies
in Partial Fulfillment of the Requirements
for the Degree
Doctor of Philosophy

McMaster University

October 1967

DOCTOR OF PHILOSOPHY (1967)
(Metallurgy)

McMASTER UNIVERSITY
Hamilton, Ontario.

TITLE: Interactions between Solute Atoms and Defects in Silicon and Germanium

AUTHOR: Ralph Clarence Dorward, B.Sc. (University of Alberta)
M.Sc. (University of Alberta)

SUPERVISOR: Professor J.S. Kirkaldy

NUMBER OF PAGES: xvii, 190

SCOPE AND CONTENTS:

A thermodynamic investigation of interactions between solute atoms and defects (other solute atoms, electrons, phonons, and grain boundaries) has been conducted by solubility measurements of copper and gold in silicon and germanium. The major objective of the investigation was to gain a further understanding of the physical state of solute atoms and their interactions with defects in homopolar crystals. An attempt was also made to extend the theory and experimental results of equilibrium studies to kinetic phenomena associated with device manufacture. An experimental study of the kinetics of solute precipitation at dislocations was also carried out by electrical conductivity measurements.

Original contributions which have been obtained from the results of this program are listed below.

(1) The relative partial molar enthalpies and entropies of solution for the various systems are

$\Delta\overline{H}_{Cu}$(in Si)=37.3±0.5 Kcal./mole, $\Delta\overline{S}^{ex}_{Cu}$(in Si)=7.1±0.4 cal./mole-°K,

$\Delta\bar{H}_{Cu}$(in Ge)=41.3±0.7 Kcal./mole, $\Delta\bar{S}^{ex}_{Cu}$(in Ge)=10.3±0.6 cal./mole-°K,

$\Delta\bar{H}_{Au}$(in Si)=43.8±1.4 Kcal./mole, $\Delta\bar{S}^{ex}_{Au}$(in Si)=6.8±1.0 cal./mole-°K,

$\Delta\bar{H}_{Au}$(in Ge) $\gtrsim$ 45 Kcal./mole, and $\Delta\bar{S}^{ex}_{Au}$(in Ge) $\gtrsim$ 15 cal./mole-°K.

The partial molar enthalpy and entropy of copper in silicon with respect to Cu_3Si are 40.2±0.5 Kcal./mole and 9.7±0.5 cal./mole-°K, respectively.

(2) Solubility measurements, metallography, and X-ray studies yielded evidence for delayed nucleation of intermediate compounds in copper-silicon diffusion couples.

(3) The solubility of copper in vapor grown polycrystalline silicon is much greater than that in single crystal material below 800°C. The ratio of the grain boundary solubility to the single crystal solubility was estimated to be of the order of 5 x 10^5. The high interaction energy between copper and grain boundaries in silicon (approximately 1.5 eV) was ascribed to chemical bonding.

(4) Arsenic doping of germanium (such that the semiconductor remains intrinsic) enhances the solubility of copper in this material. This effect was quantitatively described by a theory of complex formation.

(5) A study of the solubility of copper in p-type silicon indicated that copper is incompletely ionized in intrinsic silicon at elevated temperatures (≈1000°C).

(6) The solubility of gold in silicon is decreased by boron doping,

and this was explained on the basis of a low (less than unity) donor/acceptor ratio of substitutional gold.

(7) The rate equation describing the precipitation of copper in silicon has a time exponent of 0.687 ± 0.043.

(8) Generalized phenomenological equations for ternary diffusion in covalent semiconductors were developed and it was demonstrated that information about diffusion phenomena may often be obtained from equilibrium measurements.

(9) A quasi-steady state experiment was designed whereby copper segregated to regions of high boron concentration (in silicon) during a heat treatment operation, in qualitative agreement with theory.

ACKNOWLEDGEMENTS

The author wishes to express his gratitude to Professor J.S. Kirkaldy for suggesting the field of research, and for his encouragement and help during the course of this project. Thanks are also due to many of the faculty, graduate students, and technical staff for helpful discussions and assistance. The assistance given by the staff and control committee of the McMaster nuclear reactor is especially appreciated. The author is also indebted to Dr. W.A. Pieczonka of Canadian Westinghouse Company Ltd. for beneficial discussions, and to Dr. T.W. Plaskett of the International Business Machines Corporation for supplying some of the materials.

The financial support provided by the National Research Council of Canada in the form of research grants and three studentships is gratefully acknowledged.

TABLE OF CONTENTS

Page

LIST OF TABLES*

---

* All the tables except those in Appendix B have been placed at the end of their respective chapters.

LIST OF ILLUSTRATIONS*

---

* The illustrations have been placed at the end of their respective chapters.

LIST OF COMMONLY USED SYMBOLS

A°	Angstroms
$^{\circ}C$	Degrees Centigrade
$\Delta\overline{C}_p$	Relative partial molar heat capacity
D	Diffusion coefficient (cm^2/sec)
E	Energy
E_c	Energy at the bottom of the conduction band
E_f	Fermi energy
E_f°	Intrinsic Fermi energy
E_r	Energy of dopant levels
E_v	Energy at the top of the valence band
G	Gibbs free energy
H	Enthalpy
ΔH_b	Binding enthalpy
ΔH^f	Enthalpy of fusion
J	Diffusion flux
K	Equilibrium constant
K_c	Interface transfer velocity
$^{\circ}K$	Degrees Kelvin
N	Total number of atoms (cm.$^{-3}$)
N_a	Concentration of acceptors
N_d	Concentration of donors
N_c	Concentration of complexes
N_i	Concentration and solubility of the ith component

N_o	Initial concentration of solute, concentration of neutral dopant
N_r	Concentration of dopantatoms of charge state r
$N(t)$	Number of solute atoms in solution at time t
$N°$	Intrinsic concentration, solubility
P	Pressure
$\Delta\overline{Q}_i$	Relative partial molar quantity ($Q = E, H, G, S, F$)
R	Gas constant (calories/mole - °K)
S	Entropy
$S°$	Absolute entropy
ΔS^{th}	Thermal entropy change, specific thermal entropy
ΔS^{f}	Entropy of fusion
ΔS^{M}	Molar entropy of mixing
T_m	Melting temperature
V	Volume
X	Mole fraction
a	Activity
a_o	Interatomic distance
e	Electronic charge
h	Planck's constant
i	i^{th} component (subscript)
k	Boltzmann's constant
k^e	Equilibrium distribution coefficient
l	Liquid phase designation (superscript)
n	Number, electron concentration, time exponent of a rate equation
n_i	Intrinsic carrier concentration

p	Hole concentration
r	Charge of dopant state
t	Time
u	Chemical potential
x	Distance
y	Fraction
α β η γ	Phase designations (superscripts)
β_r	Impurity level degeneracy factor
Φ	Electrostatic potential
γ	Activity coefficient
κ	Dielectric constant
μ	Shear modulus
ν	Frequency
Ω	Complexing equilibrium constant
ρ	Density
τ	Rate constant

CHAPTER 1

INTRODUCTION

Defects, and interactions between them, determine most of the technologically important properties of solids. Common examples of defect-determined properties are electrical and thermal conductivity, mechanical strength, and color. An understanding of defects in germanium and silicon is of great practical significance because the electrical characteristics of these materials are usually governed by solute atoms and their interactions with other defects. These interactions also play an important role in diffusion doping and heat treatment problems. A knowledge of the thermodynamic characteristics of the various interactions involved is often helpful in predicting the kinetic behavior of these operations.

From an academic point of view, silicon and germanium provide excellent media in which to study defect interactions. Crystals of very high purity and perfection are available due to the demands of semiconductor technology. Semiconductors are also very amenable to electrical measurements because their electron concentration is extremely sensitive to small variations in structure. In addition, the low electron densities in germanium and silicon are important since charged defects in these materials are much less effectively screened than in metals. Relatively large coulombic interactions are therefore possible. Studies of the interaction of defects also often provide useful information about the fundamental properties of the defects themselves.

Classical thermodynamics, which makes no reference to atomic models, has been instrumental in determining many macroscopic and phenomenological properties of materials. When combined with statistical thermodynamics, on the other hand, atomistic interpretations of solid state phenomena may be obtained. The combination of these two disciplines offers a powerful tool for the investigation and understanding of defects and their behavior in solids.

In this investigation the thermodynamic properties of copper and gold in germanium and silicon were examined primarily by solubility measurements. Interactions between solute atoms and defects (other solute atoms, electrons, phonons, and grain boundaries) affect the thermodynamic properties of a solution, and are therefore revealed by the solubility parameters. The kinetics of copper precipitation on dislocations in silicon, as determined by electrical conductivity measurements, have also been investigated. These investigations were made with two views in mind: the first was to gain a better understanding of the fundamental properties of solute atoms and their interactions with defects in covalent semiconductors; the second was to extend, if possible, the results to technically important problems in the semiconductor device industry such as diffusion and heat treatment.

Because of the interdisciplinary nature of this investigation, a summary of basic semiconductor principles and of solution thermodynamics and phase equilibria are included in the next chapter.

CHAPTER 2

REVIEW

This chapter is intended to provide a general background review of topics which are basic to an understanding of the theoretical and experimental problems involved in the present investigation. Included are discussions of defects in solids, the electronic structure of covalent semiconductors, the physical chemistry of solutions and phase equilibria, and experimental methods of solubility measurements in solids.

2.A Introduction to Defects in Solids.

2.A.1 Definition and Classification.

A general classification of imperfections in solids has been presented by Seitz (1952) in which he defines defects in relation to the conception of a perfect solid. A perfect solid is considered to be an hypothetical aggregate of atoms arranged in an unbroken lattice array with the condition that each unit cell possess an identical arrangement of the chemical constituents. Seitz also assumes that the perfect system is at the absolute zero of temperature and that the atoms are motionless except for zero-point oscillations. In addition, a perfect solid is realized only when the electronic configuration is in the lowest possible energy state for the particular system.

A defect is therefore any entity which constitutes a deviation from any of the above requirements for a perfect solid. Seitz lists the primary defects as:

(i) phonons

(ii) free electrons and holes

(iii) vacant lattice sites and interstitial atoms

(iv) excitons

(v) foreign atoms in either interstitial or substitutional positions

(vi) dislocations

(vii) surfaces (external and internal) *

This classification considers only the low density limit in which the defect concentrations are sufficiently small that their properties are independent of the presence of other like or unlike imperfections. In the high density situation primary defects may interact and combine to form secondary defects. Examples are:

(i) voids (vacancy clusters)

(ii) inclusions (clusters of foreign atoms)

(iii) sub-boundaries (alignment of dislocations).

A large number of defect complexes may also form by various combinations of unlike primary imperfections. In this way such complexes as color centers, grain boundary segregates, Cottrell atmospheres, ion-vacancy pairs and foreign atom - foreign atom pairs are produced. Such defects, and in particular those involving foreign atoms, will be discussed in greater detail in the next chapter.

---

* Seitz does not specifically include surfaces in his list of primary defects, but rather specifies in his requirements for a perfect solid that: "The surface of the ideal specimen will be regarded as determined by planar crystal faces which provide the aggregate with the lowest surface energy".

Seitz also discusses some other types of imperfections which will not be of concern in this investigation. These are "transient" defects (light quanta and charged and uncharged radiations) and those which arise from unaligned spins as in ferromagnetic materials.

Many other classifications of defects in solids may also be found in the literature. Van Bueren (1960)[a] classifies lattice imperfections according to spatial dimension as follows:

(i) zero-dimensional (point defects) - vacancies, foreign atoms, color centers, electrons and holes

(ii) one-dimensional (line imperfections) - dislocations

(iii) two-dimensional (surface imperfections) - grain boundaries, phase boundaries, external surfaces

(iv) three dimensional (volume imperfections) - voids,inclusions.

2.A.2 Thermal Properties

As stated in the previous sub-section, the perfect solid is hypothetical. Real crystals, which are usually grown at high temperatures from a liquid or a vapor, contain a certain number of irregularities.

Point defects may exist in solids in thermodynamic equilibrium since their introduction increases the entropy of the system. This is sufficient to compensate for their energy of formation thus making it possible to find a lower free energy in their presence. The equilibrium of a solid at constant pressure, P, and absolute temperature, T, is determined by a minimum in the Gibbs free energy,

$$G = H - TS,$$

where H and S are the enthalpy and entropy, respectively. The enthalpy is defined by

$$H = E + PV, *$$

where E is the internal energy and V is the volume. The entropy of a solid is comprised of thermal and configurational components, S^{th} and S^{cf}, and can be calculated from the Boltzmann relation

$$S = S^{th} + S^{cf} = k \ln (W^{th} W^{cf}),$$

where k is Boltzmann's constant, W^{cf} is the number of different ways in which the atoms may be arranged over the available lattice sites, and W^{th} is the number of different ways in which the total vibrational energy of the crystal may be distributed over the possible vibrational modes.

Creation and motion of many defects (in particular vacancies and interstitial atoms) are accomplished through lattice vibrations which interact with each other and combine at localized regions of the crystal to produce large displacements of one or two atoms. At low temperatures these vibration effects are not as important as they are at high temperatures, but a crystal which is cooled down from a high growth temperature may still contain a large number of non-equilibrium "quenched-in" defects. Lattice vibrations similarly excite electronic states to produce free electrons and holes in insulators, and excite free electrons to higher energy states in metals. Foreign atoms are often introduced intentionally during crystal growth procedures,

---

* H and E are often used interchangably in solid state theory since the PV term is generally negligible.

or they may arise due to contamination from starting materials and the crystal growing apparatus.

The dislocation is a defect which is not in thermodynamic equilibrium at ordinary temperatures since the entropy contribution to its free energy of formation is small compared to the contribution of its energy of formation (Cottrell, 1953). The reasons for their existence in "as-grown" crystals have not been completely elucidated. There is direct evidence, however, that stresses set up by thermal gradients (Penning, 1958)[a] and by foreign atom segregation (Tiller, 1958) during crystal growth increase dislocation densities. Frank (1953) has also pointed out that dislocations catalyze crystal growth from the vapor so that a crystal containing "accidental" dislocations grows faster than one which does not.

Grain boundaries are also non-equilibrium imperfections. They are generally formed by the impingement of separate crystals which have formed by a nucleation and growth process.

Defects of particular interest in the present study are electrons and foreign atoms in covalent semiconductors. These defects are discussed from the viewpoints of electronic structure and solution thermodynamics in the next two sections.

2.B Electrical Properties of Germanium and Silicon.

2.B.1 Intrinsic Semiconduction.

Germanium and silicon are elemental semiconductors having the diamond cubic structure in which each atom is tetrahedrally surrounded by four other atoms. These atoms are held together by covalent electron-pair bonds formed by the valence electrons (four per atom). The diamond structure gives rise to a filled Brillouin zone containing four valency electrons per atom (Hume-Rothery and Raynor, 1962). Since this zone and the next one of higher energy do not overlap in these materials, they have insulating properties. At temperatures above absolute zero electrons can be thermally excited into the second zone where they are free to act as conduction electrons. This is known as intrinsic semiconduction. For present purposes, the band structure of diamond cubic materials has been greatly simplified. A recent review of this complex subject is given by Blakemore (1962)[a] .

This phenomenon can also be qualitatively explained with reference to the atomic bonding scheme (See Figure 2.1(a)). Each atom contributes four valence electrons which are tetrahedrally bonded to four neighbouring atoms. All of the electrons, therefore, are used up in forming covalent bonds which comprise a band of quasi-continuous states known as the valence band. With all valence electrons in covalent bondage no excess electrons are free to drift throughout the crystal as electrical charge carriers. Lattice vibrations, however, may impart enough energy to these valence electrons to break them away from their parent atoms into conduction states where they are free to move. These states comprise a new quasi-continuum known as the conduction band. When a valence electron is excited (see Figure 2.1(b)), an unoccupied state, or "hole", is created in the valence band. Conduction is also possible, therefore, in the valence band via these available empty energy states. The net effect of this type of conduction is for the hole to move through the crystal in the opposite direction from the electrons. It thus behaves as though it were a positively charged particle.

As indicated above, electrical conductivity in semiconductors proceeds by two mechanisms-by electrons in the conduction band and by holes in the valence band. Between the two bands is a zone of forbidden energies known as the energy gap (see Figure 2.2 a) . This gap has a particular magnitude for each specific semiconductor, and if it is relatively large, the material may be classed as an insulator. Thermal excitation of valence electrons across this energy gap accounts for the characteristic property of pure semiconductors in which the electrical conductivity increases with increasing temperature.

Under equilibrium conditions the rate of electron and hole generation is equal to the rate of their recombination (see Figure 2.2 b) and the following reaction involving conduction electrons, e^-, and holes, e^+, and hole-electron pairs, $e^+ \cdot e^-$, may be written:

$$e^+ \cdot e^- = e^+ + e^- .$$

Following Swalin (1962), the law of mass action gives

$$K = \frac{a_{e^-} \times a_{e^+}}{a_{e^+ \cdot e^-}} ,$$

where K is an equilibrium constant and the a's are activities. If the concentrations of electrons, n, and holes, p, are small, as they usually are in most semiconductors at ordinary temperatures, the activities may be replaced by concentrations. Then since the concentration of electron-hole pairs remains relatively constant as n and p change,

$$n \,.\, p \equiv n_i^2 = AK, \tag{2.1}$$

where A is a constant and n_i is designated as the intrinsic carrier concentration. Through the thermodynamic relation

$$-\Delta F = kT \ln K,$$

where ΔF is the standard Helmholtz free energy of a reaction at constant volume and temperature, it follows that

$$n \cdot p = A \exp\left(-\frac{\Delta F}{kT}\right) = A \exp\left(-\frac{\Delta E}{kT}\right) \exp\left(\frac{\Delta S}{k}\right) \,, \tag{2.1a}$$

where ΔE is the magnitude of the energy gap. ΔE is not independent of temperature, however. An increasing amplitude of thermal vibrations, electrostatic interactions between charge carriers, and a change in the interatomic spacing due to thermal expansion generally cause a decrease in the energy gap. It has been found experimentally that the energy gap of germanium can be fairly well represented by (Morin & Maita, 1954)

$$\Delta E = \Delta E^\circ - \alpha T,$$

where ΔE° is the value of the energy gap at the absolute zero of temperature and α is a constant ($\alpha = 4.4 \times 10^{-4}$ eV per degree for germanium).

In order to make a complete description of the occupation of the electronic energy states in a solid, recourse must be made to Fermi-Dirac statistics. The Fermi-Dirac distribution law is given by

$$f(E) = \frac{1}{1 + \exp \dfrac{E - E_f}{kT}} \,,$$

where f(E) is the probability that a state of energy, E, is occupied and E_f is the Fermi energy. When E is equal to E_f, the probability for occupation is 1/2. It can be shown by classical thermodynamics that (Swalin, 1962)

$$E_f = T\left(\frac{\partial S}{\partial n}\right)_{E,V} = \left(\frac{\partial G}{\partial n}\right)_{p,T} \equiv u_e,$$

where u_e is called the chemical potential per electron.

The number of electrons per unit volume occupying states between the energies E and E + dE is given by (Dekker, 1957)

$$n(E)\, dE = N(E) f(E)\, dE,$$

where N(E) is the number of possible states per unit volume. The number of electrons in the conduction band of a semiconductor is thus

$$n = \int_{E_c}^{Top} n(E) dE = \int_{E_c}^{Top} N\,(E) f(E) dE, \qquad (2.2)$$

where E_c is the energy at the bottom of the conduction band and $N_c(E)$ is the density of states in the conduction band. Band theory shows that (Shockley, 1950)

$$N_c(E) = \frac{4\pi(2\,m_e)^{3/2}}{h^3} \quad (E - E_c)^{1/2} \quad ,$$

where m_e is the effective mass of the electron and h is Plank's constant. The solution of Equation 2.2 assuming

$(E_C - E_F) \gtrsim 4kT$ is (Dekker, 1957)

$$n = 2\left(\frac{2\pi\, m_e kT}{h^2}\right)^{3/2} \cdot \exp\left(\frac{E_f - E_c}{kT}\right). \qquad (2.3)$$

Similarly, the number of holes in the valence band is given by

$$p = 2\left(\frac{2\pi m_p kT}{h^2}\right)^{3/2} \exp\left(\frac{E_v - E_f}{kT}\right), \tag{2.4}$$

where m_p is the effective mass of a hole and E_v is the energy at the top of the valence band. For electrical neutrality at a given temperature, the number of holes must equal the number of electrons, so Equations 2.3 and 2.4 can be solved for E_f, and hence n and p may be determined also. In general, the Fermi energy of a pure elemental semiconductor lies almost halfway between the top of the valence band and the bottom of the conduction band. This intrinsic Fermi energy will be designated by E_f°. The electron and hole concentrations may also be determined by a comparison of Equations 2.3 and 2.4 with Equation 2.1a which yields

$$n = p = 2\left(\frac{2\pi kT}{h^2}\right)^{3/2} (m_e m_p)^{3/4} \exp\left(\frac{E_v - E_c}{2kT}\right)$$

and

$$A \exp\left(\frac{\Delta S}{k}\right) = 4\left(\frac{2\pi kT}{h^2}\right)^3 (m_e m_p)^{3/2}.$$

2.B.2 Extrinsic Semiconduction.

The discussion of electronic energy bands in the preceeding sub-section applies only to semiconductors which contain no defects other than electrons, holes and phonons. Real crystals possess various other types of imperfections which perturb the band structure by introducing new energy levels. The most important of these are introduced by foreign, or "dopant" atoms, but often dislocations and vacancies are also electrically active.

The simplest and best understood type of atomic defects in germanium and silicon are provided by dissolved atoms of Group III and Group V elements. Pearson and Bardeen (1949) showed by lattice parameter studies that boron and phosphorus form substitutional solid solutions in silicon. It is also believed (Geballe, 1959) that all Group III and V elements are incorporated substitutionally in germanium and silicon lattices. If a silicon atom is replaced by an atom of a Group V element such as arsenic, one electron will not be held in any chemical bond since five valence electrons are introduced and only four of them can form covalent bonds with the four nearest neighbor silicon atoms. As a result, this extra electron is relatively weakly bound to the arsenic atom and only a small amount of energy is required to set it free.* The arsenic atom may thus donate an electron to the conduction band and is therefore known as a "donor". On the other hand, the substitution of a silicon atom with an element of Group III, such as boron, leads to a deficiency of valence electrons. One of the four covalent bonds is now a one-electron bond, i.e. a hole, and an electron from the valence band may be easily excited into it. The boron atom thus accepts an electron from the valence band and is therefore known as an "acceptor". Electrical conduction via these impurity states is known as extrinsic semiconduction.

In Figure 2.3a the ionization energy of a donor atom is depicted by the difference between the bottom of the conduction band and the localized energy levels for the valence electrons of the donor atoms.

---

* Theoretical calculations of ionization energies are usually based on the model of a Bohr atom in a dielectric medium.

Similarly, acceptors can be shown to have energy levels just above the top of the valence band (Figure 2.3b). Figure 2.3c shows the situation when donors and acceptors are both present (as is usually the case). Under these circumstances the difference between the donor and the acceptor concentration determines the net carrier concentration. This effect is known as compensation. If the number of donors exceeds the number of acceptors, the semiconductor is said to exhibit n-type (electron) conductivity. The opposite case results in p-type (hole) conductivity.

Many elements from other groups of the periodic table also introduce energy levels into the band gaps of silicon and germanium. Possibly the simplest are those of Groups II and VI. In order for these elements to complete their tetrahedral bonding arrangement, double levels are formed, i.e. they may be singly or doubly charged. Zinc in germanium, for example, has two acceptor levels just above the valence band. The transition metals may also exist as singly or doubly charged acceptors. By the same reasoning, copper, silver and gold often introduce levels which may be triply charged. In a few cases substitutional impurities of valence less than four behave as donors as well as acceptors. These donor levels arise by ionization of valence electrons into the conduction band. Examples of such amphoteric impurities are gold and copper in germanium (Woodbury and Tyler, 1957) and gold in silicon (Collins et al, 1957).

The foregoing discussion applies only to foreign atoms which enter the lattice by substituting for solvent atoms. Since, however, the diamond cubic lattice is an "open" structure it is also possible for the atoms of many elements to reside in interstitial positions. Lithium (Fuller and Ditzenburger, 1953), hydrogen (Reiss and Fuller, 1959) and copper (Hall and Racette, 1964) are well known examples. In addition gold, silver and most of the transition metals appear to diffuse by an interstitial mechanism (Boltaks, 1963)[a] so a fraction of their atoms in solution must be located in interstitial sites. Interstitial lithium has a single valence electron which is easily removed if the atoms are imbedded in a dielectric medium. It thus behaves as a donor and when ionized, exists as a positive ion. The interstitial components of many other metallic dopants are also believed to act as donors since electron spin resonance studies have revealed the presence of mobile Fe^+, Cr^+, and Mn^{++} in silicon at room temperature (Woodbury and Ludwig, 1960). Interstitial acceptors have not been found, probably because large negative ions cannot be easily accommodated in interstitial sites.

The electronic levels associated with donor and acceptor atoms are populated according to Fermi-Dirac statistics. The Fermi function for the probability that an impurity level at energy E_r will contain an electron is (Blakemore, 1962)[b]

$$f(E_r) = \frac{1}{1 + \beta_r \left(\frac{E_r - E_f}{kT}\right)} ,$$

where β_r is an impurity level degeneracy factor which is the ratio of the number of ways a state can be unoccupied to the number of ways in which it can be occupied. The spin contribution to β_r is 1/2 for a Group V donor and 2 for a Group III acceptor. Silicon and germanium also have two degenerate valence bands (Blakemore, 1962)[a] so the total degeneracy factor for a Group III acceptor is 4. In addition to Equations 2.3 and 2.4 we now have for a semiconductor doped with N_a acceptor atoms and N_d donor atoms**

$$n_d = \frac{N_d}{1 + \beta_d \exp\left(\frac{E_d - E_f}{kT}\right)} \tag{2.5}$$

and

$$p_a = \frac{N_a}{1 + \beta_a^{-1} \exp\left(\frac{E_f - E_a}{kT}\right)},^{*} \tag{2.6}$$

where n_d and p_a are the number of neutral donors and acceptors, respectively, and E_d and E_a are the energies of the donor and acceptor level, respectively. The statistical problem for given dopant concentrations can then be solved by combining these equations with the electrical neutrality condition

$$n + n_d - p - p_a = N_d - N_a. \tag{2.7}$$

The solution of the five equations may be done graphically (Shockley, 1950) or by computer methods. A major simplification can often be made, however, because at temperatures of interest $(E_d - E_f)$ and $(E_f - E_a)$ are usually several times greater than kT so the dopants are essentially completely ionized, and Equation 2.7 reduces to

$$n - p = N_d - N_a. \tag{2.8}$$

---

* βa^{-1} is used in this instance because the expression refers to hole occupancy.

** Unless otherwise specified, the concentration symbol N will refer to number per cubic centimeter, and X will be reserved for mole fraction.

Combination of the above equation with the relation $n.p = n_i^2$ (a constant independent of doping for a given temperature (cf. Equation 2.1)) gives the following expression for the electron concentration:

$$n = 1/2 \left[(N_d - N_a) + \;(N_d - N_a)^2 + 4\, n_i^2\right]^{1/2} \quad . \tag{2.9}$$

If the electron concentration in doped material is known, then the Fermi energy may be related to E_f° and the intrinsic electron concentration, n_i, by (cf. Equation 2.3)

$$\frac{n}{n_i} = \exp\left(\frac{E_f - E_f^{\circ}}{kT}\right) \tag{2.10}$$

Similar expressions may also be written for the hole concentration:

$$P = 1/2 \left[(N_a - N_d) + \;(N_a - N_d)^2 + 4\, n_i^2\right]^{1/2} \quad , \tag{2.11}$$

and

$$\frac{P}{n_i} = \exp\left(\frac{E_f^{\circ} - E_f}{kT}\right). \tag{2.12}$$

It also follows that at temperatures and dopant concentrations such that N_d, $N_a < (np)^{1/2}$, the Fermi energy lies almost in the middle of the energy gap and the semiconductor behaves intrinsically. Figure 2.4 shows how the Fermi energy in doped semiconductors varies with temperature.

As was mentioned earlier, some impurities introduce into the energy gap a series of levels which differ in charge. Shockley and Last (1957) have presented a theory on the statistics of the charge distribution for impurities such as gold and copper in germanium which exist in charge states that may vary from +e to -3e depending on the position of the Fermi level. They derived relative occupation probabilities, W, for various charge conditions as listed below:*

Charge Condition	Relative Probability of Being in Charge Condition
Acceptor 3a (-3)	$W_{3a} = \frac{1}{\beta_{3a}} \exp\left[(3E_f - E_{1a} - E_{2a} - E_{3a})/kT\right]$
Acceptor 2a (-2)	$W_{2a} = \frac{1}{\beta_{2a}} \exp\left[(2E_f - E_{1a} - E_{2a})/kT\right]$
Acceptor 1a (-1)	$W_{1a} = \frac{1}{\beta_{1a}} \exp\left[(E_f - E_{1a})/kT\right]$
Neutral 0 (0)	$Wo = 1$
Donor 1d (+1)	$W_{1d} = \beta_{1d} \exp\left[(E_{1d} - E_f)/kT\right]$

Normalization to give the absolute probability for a given Fermi energy and temperature is accomplished by dividing each entry in the second column by the sum of column 2. Figure 2.5 shows how the charge per gold atom in germanium depends on the Fermi energy at low temperature (such that kT is small compared with the level spacing). At high temperature the change in charge state is less abrupt as the Fermi energy passes through an energy level.

To complete the general discussion of the properties of a semiconductor which contains a number of foreign atoms it is helpful to consider the physical chemistry of a solution. The next section is an

---

* Shockley and Last did not account for differences (explicitly) in the degeneracy factors of the various states, but they are included here for completeness.

introduction to the thermodynamic theory of two component solutions in which both classical and statistical treatments are employed to complement each other.

2.C Solution Thermodynamics

For simplicity the discussion of solution thermodynamics will be initially limited to binary (two-component) systems. The number of components of a system is the minimum number of chemically distinct constituents necessary to describe the composition of each phase (homogenous, mechanically separable, and physically or chemically different part of a system) in a system, i.e. those constituents whose concentrations may be independently varied under equilibrium conditions. The major emphasis will also be placed on the condensed state. Since semiconductor solutions are usually very dilute, attention will be given mainly to the thermodynamic properties of the solute (dopant) atoms which will be designated as component 2. These properties are described by partial molar quantities, $\overline{Q}_i$, which for a general multi-component system are defined by equations of the type (Denbigh,1966)

$$\overline{Q}_i \equiv \left(\frac{\partial Q}{\partial n_i}\right)_{p,T,n_j} ,$$

where Q represents any extensive thermodynamic parameter (E,V,H,S,G) and the n's are the number of moles of each component in the system.

From the definition of a partial molar quantity it follows that an extensive parameter change, dQ, caused by changing the number of moles in a two-component system by dn_1 and dn_2 at constant temperature and pressure is

$$dQ = \overline{Q}_1\, dn_1 + \overline{Q}_2\, dn_2 \ , \tag{2.13}$$

and then if $Q = Q(T,P,n_1,n_2)$,

$$Q = n_1 \overline{Q}_1 + n_2\overline{Q}_2 \ . * \tag{2.14}$$

Dividing through by the total number of moles in the system gives

$$Q_m = X_1\overline{Q}_1 + X_2\overline{Q}_2 \ , \tag{2.15}$$

where Q_m is a molar quantity and X_1 and X_2 are mole fractions. If the total differential of Equation 2.14 is taken and compared to Equation 2.13 we get, after introducing mole fractions, the expression

$$X_1 d\overline{Q}_1 + X_2 d\overline{Q}_2 = 0 \ . \tag{2.16}$$

This is known as the Gibbs-Duhem relation at constant pressure and temperature.

A specific reference state must be chosen for a complete definition of the thermodynamic functions. Relative partial molar quantities, $\Delta\overline{Q}_i$, are therefore defined as the difference between a partial molar quantity of a component in solution and the molar quantity of the pure substance, $Q_i°$, i.e.

$$\Delta\overline{Q}_i = \overline{Q}_i - Q_i° \ .$$

These functions are often called the partial molar quantities of mixing or solution. Usually, the reference state is chosen as the thermodynamically most stable state of a substance, although in certain cases supercooled liquids are also used (Wagner, 1952)[a].

---

* Mathematically, this integration is equivalent to the application of Euler's theorem to the homogenous differential expression.

For more convenient use in following sections, the reference state for a component in a solution will be chosen here as the pure chemical species in the same state of temperature and pressure as the solution under consideration. This means that superheated solids as well as supercooled liquids may serve as reference states.

In the theory of solutions it is convenient to define the activity, a_i, of each component in a system by the equation

$$\Delta\overline{G}_i = RT\ln a_i \ . \tag{2.17}$$

The above expression is often written in terms of the chemical potential, u_i, of a species.

Since $u_i \equiv \overline{G}_i$, then

$$u_i = u_i° + RT\ln a_i \ , \tag{2.18}$$

where $u_i°$ is the chemical potential of a species in its reference state. The molar free energy of mixing of a solution (a relative quantity) is given by

$$\Delta G_m = \Sigma_i \ X_i \ \Delta\overline{G}_i \ ,$$

or for a binary system

$$\Delta G_m = RT\ (X_1 \ln a_1 + X_2 \ln a_2). \tag{2.19}$$

A useful standard of comparison when considering solutions is the ideal solution, defined as one in which the activity of a solute is identical to its mole fraction (Raoult's law). Replacing the activities in Equation 2.19 with mole fractions and differentiating with respect to temperature yields

$$\left(\frac{\partial\ (\Delta G_m)}{\partial T} \right)_p = -\Delta S_m = R\ (X_1 \ln X_1 + X_2 \ln X_2)\ , \qquad (2.20)$$

and since $\Delta G_m = \Delta H_m - T\Delta S_m$,

$$\Delta H_m = 0$$

for an ideal solution.

Most real solutions do not fall into the ideal category, however, and it is useful to introduce an activity coefficient which is a measure of a solution's deviation from ideality. The activity coefficient, γ_i, is defined by

$$a_i = \gamma_i X_i\ .$$

If γ_i is independent of composition, the solution is said to follow Henry's law. Equation 2.17 may now be written as

$$\Delta\overline{G}_i = RT \ln X_i + RT \ln \gamma_i\ . \qquad (2.21)$$

The first term on the right hand side of this expression is an ideal part and the other is due to non-ideality. This extra term is often referred to as the excess partial molar free energy of solution, $\Delta\overline{G}_i^{ex}$, i.e.

$$\Delta\overline{G}_i^{ex} = RT \ln \gamma_i. \qquad (2.22)$$

Many non-ideal solutions exhibit the property that their partial molar entropies are the same as those of an ideal solution. Hildebrand (1929) termed these solutions as "regular". In this case

$$\Delta\overline{G}_i^{ex} = \Delta\overline{H}_i = RT \ln \gamma_i\ . \qquad (2.23)$$

In general, solutions also have an excess partial molar entropy of solution, $\Delta\overline{S}_i^{ex}$, and Equation 2.21 becomes

$$\Delta\overline{G}_i = RT \ln X_i + \Delta\overline{H}_i - T\Delta\overline{S}_i^{ex} . \tag{2.24}$$

It should be noted that if Henry's law is not obeyed, the last two terms in this expression will not be independent of X_i.

The foregoing thermodynamic discussion of solutions was completely classical in that no atomic model was invoked to describe the solution. An interesting problem arises when an atom exists in a solution as an ion and an electron. If the ion and the electron are considered as separate entities Equation 2.18 may be written per atom as

$$u_i = u_{ion}^{\circ} + kT \ln a_{ion} + u_e .$$

Replacing u_e with E_f and substituting the relation $a_{ion} = \gamma_{ion} X_{ion}$, the above expression may be written as

$$u_i = u_{ion}^{\circ} + kT \ln \left(\gamma_{ion} \cdot \exp \frac{E_f}{kT} \cdot X_{ion}\right).$$

This equation is identical to Equation 2.18 if

$$\gamma_i = \gamma_{ion} \exp\left(\frac{u_{ion}^{\circ} - u_i^{\circ} + E_f}{kT}\right) . \tag{2.25}$$

The significance of this relation is that non-ideality may arise from the electronic constitution of the system. This has especially important consequences in semi-conductors where very low concentrations of solute often have a marked effect on the Fermi energy of the solution.

To understand solutions on a more fundamental basis it is helpful to complement the classical thermodynamic description with statistical thermodynamics. The configurational molar entropy for random mixing of the atoms of a binary solution on identical sites can be determined by statistical methods as (Cottrell, 1955)

$$\Delta S_m = -R\,(X_1 \ln X_1 + X_2 \ln X_2)\ *.$$

This is identical to the entropy of mixing for an ideal solution given by the classical derivation (c.f. Equation 2.20). Two requirements for an ideal solution therefore are: 1) its atoms are randomly mixed on identical sites, and 2) the thermal entropy is the same as that for the pure components.

The energetics of solutions are often treated by a quasi-chemical approach in which the forces between atoms are assumed to be significant over short enough distances that only the interaction energies between nearest neighbors need be considered (Guggenheim, 1935). The molar enthalpy of mixing for a substitutional solution is then given by

$$\Delta H_m = -P_{12}\left[E_{12} - 1/2\,(E_{11} + E_{22})\right] ,$$

where P_{12} is the number of atom pairs of different type atoms and E_{11} E_{22}, and E_{12} are bonding energies between the three combinations of atom pairs. Since $\Delta H_m = 0$ for an ideal solution, then

$$E_{12} = 1/2\,(E_{11} + E_{22}).$$

The quasi-chemical theory is also easily applied to regular solutions. If the total number of lattice sites is N and Z is the

---

* This equation does not strictly apply for an interstitial solution but is a good approximation for dilute conditions.

number of nearest neighbors of a given atom, then

$$P_{12} = X_1X_2NZ \tag{2.26}$$

and

$$\Delta H_m = -X_1X_2\lambda, \tag{2.27}$$

where

$$\lambda = ZN\left[E_{12} - 1/2\ (E_{11} + E_{22})\right] .$$

Using Equations 2.15 and 2.16 and noting that $dX_1 = -dX_2$ it can be shown that Equation 2.25 transposes to

$$\Delta\overline{H}_1 = -\ (1-X_1)^2\ \lambda$$

and

$$\Delta\overline{H}_2 = -\ (1-X_2)^2\ \lambda .$$

Comparison of the above two expressions with the classical Equation 2.23 shows that for a binary solution

$$\ln\gamma_i = -(1-X_i)^2\left(\frac{\lambda}{RT}\right) . \tag{2.28}$$

Depending on the sign of λ, the activity coefficient may be less than or greater than unity. A net attraction between unlike atoms causes a negative deviation from Raoult's law ($\gamma_i<1$), whereas a repulsion results in a positive deviation. Equation 2.28 also shows that at low concentrations of solute ($X_i<<1$), $\ln\gamma_i$ is essentially independent of composition, i.e. Henry's law is obeyed. On the other hand, at high concentrations ($X_i\approx1$), $\ln\gamma_i$ is very nearly zero and Raoult's law is obeyed.

It can be reasoned intuitively that for finite values of ΔH_m a solution will not be strictly regular. Depending on whether ΔH_m is positive or negative, the system will tend to minimize or maximize the number of unlike bonds, thus increasing the degree of order and decreasing the configurational entropy. An excellent review of the quasi-chemical treatment of this problem is given by Christian (1965). The theory gives for the excess number of 1-2 bonds

$$P_{12}^{ex} \approx X_1^2 \; X_2^2 \; \frac{2N\lambda}{RT} \quad . \tag{2.29}$$

By comparing this expression with Equation 2.26 it can be shown that this effect will be negligible at low solute concentrations unless λ/RT is very large. Differences in atomic size may influence the regularity of a solution as well since strain considerations will affect the atomic configuration of a system. As will be shown in a later section, thermal entropy is also of considerable importance in most cases.

2.D Phase Equilibria and Solubility Parameters.

One of the easiest methods of determination of thermodynamic properties of a solution is by solubility measurements. From such experiments one can determine, for example, partial molar enthalpies and entropies of solution, and from these, activity coefficients. Interactions of solute atoms with defects affect the activity coefficient of the solute and the interaction should therefore be revealed by changes in the solubility limit and enthalpy and entropy of solution.

The thermodynamic requirement for equilibrium between contiguous phases at constant pressure and temperature is that the chemical potential of each component be constant throughout the system (Callen, 1960). A difference in chemical potential provides a generalized force for matter flow to restore the system to equilibrium.

Consider the hypothetical free energy vs. composition diagram (Figure 2.6) of two phases, alpha and beta. Since $u_i = \partial G/\partial n_i$, the requirement for equilibrium between two phases is

$$\left(\frac{\partial G}{\partial n_2}\right)^{\alpha} = \left(\frac{\partial G}{\partial n_2}\right)^{\beta} \quad ,$$

and the equilibrium concentrations are therefore given by the tangent common to both curves. Equating expressions for the chemical potential of component 2, say, in each phase gives (c.f. Equation 2.24)

$$u_2^{\circ}(\alpha) + RT \ln X_2^{\alpha} + \Delta\overline{H}_2^{\alpha} - T\,\Delta\overline{S}_2^{ex,\,\alpha}$$

$$= u_2^{\circ}(\beta) + RT \ln X_2^{\beta} + \Delta\overline{H}_2^{\beta} - T\,\Delta\overline{S}_2^{ex,\,\beta} .$$

Combination of terms yields

$$\ln \frac{X_2^{\alpha}}{X_2^{\beta}} = \frac{1}{R}\left[\frac{\Delta u_2^{\circ}}{T} + \frac{\Delta\overline{H}_2^{\beta} - \Delta\overline{H}_2^{\alpha}}{T} - (\Delta\overline{S}_2^{ex,\beta} - \Delta\overline{S}_2^{ex,\alpha})\right] , \quad (2.30)$$

where Δu_2° ($= u_2^{\circ}(\beta) - u_2^{\circ}(\alpha)$) is the difference in chemical potential of the chemical species in its respective reference states. The reference chemical potentials differ by an amount equal to the molar free energy required to transform the pure component from one state to the other. For example, if alpha is solid and beta is liquid (as is very often the case in semiconductor phase equilibria), Δu_2° will equal the molar free energy of fusion, ΔG_2^{f}, of pure component 2 at the temperature under consideration if the pure solid is used as the reference state for the complete system. Assuming that the difference in the heat capacity between liquid and solid solute is zero at all temperatures, Δu_2° is a linear function of temperature, i.e.

$$\Delta u_2^\circ = \Delta H_2^f - T\Delta S_2^f ,$$

where ΔH_2^f and ΔS_2^f are the enthalpy and entropy of fusion, respectively, of component 2. Equation 2.30 now becomes

$$\ln \frac{X_2^\alpha}{X_2^\beta} = \frac{1}{R}\left[\frac{\Delta H_2^f + \Delta\overline{H}_2^\beta - \Delta\overline{H}_2^\alpha}{T} - (\Delta S^f_2 + \Delta\overline{S}_2^{ex,\beta} - \Delta\overline{S}_2^{ex,\alpha})\right] . \tag{2.31}$$

The expressions derived in this section show that the solubility of a component in one phase with respect to another phase is dependent on certain enthalpy and entropy parameters. $\Delta\overline{H}_2^\alpha$ and $\Delta\overline{S}_2^{ex,\alpha}$, commonly called the heat and excess entropy of solution, respectively, will be referred to as the solubility parameters* of component 2 in the alpha phase. Similarly $\Delta\overline{H}_2^\beta$ and $\Delta\overline{S}_2^{ex,\beta}$ are the solubility parameters of component 2 in the beta phase. Corresponding expressions may also be written for component 1 in each phase.

It is often assumed that these parameters are temperature independent for dilute randomly mixed solutions. Hall (1957), however, proposed that as the temperature increases, the heat of solution decreases in systems which have a high degree of misfit between solvent and solute atoms. He attributed this effect to thermal

---

* These are not to be confused with the solubility parameters of Hildebrand and Scott (1950) which are used to predict miscibility of liquid solutions.

expansion which increases the interatomic distances in a crystal, thus making the substitution of solute atoms easier at high temperatures. Other contributions to the heat of solution may also be temperature dependent. In semiconductors the polarization energy of an ionized impurity atom must be considered (Weiser, 1962). The continuum expression for the polarization energy, U_p, is given by (Mott and Gurney, 1948)

$$U_p = -\frac{e^2}{D}\left(1 - \frac{1}{\kappa}\right) ,$$

where the ion is considered to be imbedded in a cavity of diameter, D, carved out of a medium with dielectric constant κ. Any variation of D or κ with temperature, therefore, would make U_p temperature dependent. Expressions for the repulsive energy arising from the Pauli exclusion principle (Born-Mayer equation) and for the chemical bond energy (Morse function) also involve interatomic distances. These contributions to the heat of solution may therefore also be temperature dependent.

In any case, Hall assumed relationships of the form

$$\Delta H = \Delta H°(1 + \theta T)$$

and

$$\frac{X^\alpha}{X^\beta} = C \exp\left(-\frac{\Delta H°}{RT} + \frac{\theta}{R}\right),$$

where $\Delta H°$ and ΔH are the enthalpies required to transfer a mole of solute from the external phase to the solid phase at zero degrees Kelvin and at T degrees Kelvin, respectively, θ is an arbitrary constant to be determined experimentally, and C is implied to be a temperature independent entropy factor.

Hall's theoretical and experimental analysis is an over-simplification of the problem, however, because it neglects the temperature variation of the entropy accompanying the change in the heat of solution. Use of the thermodynamic relation

$$\left(\frac{d(\Delta S)}{dT}\right)_p = \frac{1}{T}\left(\frac{d(\Delta H)}{dT}\right)_p$$

shows that measurements of $\ln \frac{X^\alpha}{X^\beta}$ as a function of 1/T actually measure ΔH, not $\Delta H°$ (Dekker, 1957).

The temperature dependence of the parameters in Equation 2.30 may also be discussed from a classical point of view by use of the relations

$$\frac{\partial(\Delta H)}{\partial T} = \Delta C_p$$

and
$$\frac{\partial(\Delta S)}{\partial T} = \frac{\Delta C_p}{T} ,$$

where ΔC_p is the heat capacity difference at constant pressure between products and reactants. Then

$$\Delta H_2{}^f = \Delta H_2{}^f(T_m) + \int_{T_m}^{T} \Delta C_p{}^f \, dT ,$$

$$\Delta \overline{H}_2{}^\alpha = \Delta \overline{H}_2{}^\alpha(T_m) + \int_{T_m}^{T} \Delta \overline{C}_p{}^\alpha \, dT \quad , \text{etc.},$$

where T_m is the melting point of pure solute, $\Delta C_p{}^f$ is the heat capacity difference between pure liquid and pure solid solute, and $\Delta \overline{C}_p{}^\alpha$ is the relative partial molar heat capacity of solute in the solid solution. It must be remembered, however, that the above expression for the partial molar heat of solution can not be applied at the solubility limit unless Henry's law is obeyed or $\Delta\bar{C}_p^{\alpha}$ is a known function of concentration.

General concensus of opinion suggests that the heats of solution of dopants in semiconductors are not highly temperature dependent providing Henry's law is obeyed (Lehovec, 1962; Trumbore et al, 1958, 1959). If an impurity exists in different states of ionization at different temperatures, however, it would appear logical that the heat of solution should be temperature dependent through polarization, Fermi energy, and size effects.

2.E Methods of Solubility Measurement in Semiconductors.

2.E.1 Equilibration Techniques.

Solubility determinations of solutes in semiconductors have generally been conducted by two methods - solidification and diffusion. The first method involves the determination of the equilibrium distribution coefficient between the liquids and the solidus near the melting point of the solvent. A review of this subject is given by Thurmond (1959). Distribution coefficients are usually obtained by Czochralski solidification of crystals at different temperatures (determined by the concentration of solute in the melt) followed by a measurement of the impurity concentration in the solid ingot. Since this is a kinetic experiment, care must be taken to achieve near-equilibrium conditions, because as the ingot solidifies, solute is rejected into the liquid. In order that an equilibrium distribution coefficient be found, the concentration gradient ahead of the solid-liquid interface must be eliminated. This is usually accomplished by ingot rotation and slow growth rates, however, a great deal of data obtained by this method is possibly in error (Trumbore, 1960). Dean et al (1961-62) described a more accurate method of determining equilibrium distribution coefficients in which they solidified ingots at different rates and extrapolated the measured coefficients to zero growth rate. Another solidification method, which has been used at low temperatures, is the thermal gradient technique (Trumbore, 1956). In this method solid silicon or germanium is dissolved in an impurity melt at a given temperature (an excess amount of semiconductor is used) and then precipitated on a seed crystal.

In nearly all cases solubility determinations by the diffusion method are conducted by exposing the semiconductor to an external source containing the impurity element. This source may be gaseous, liquid, or solid, and the impurity concentration obtained in the semiconductor will be the solubility with respect to the source phase. The kinetics of the reaction are often governed by the rate at which the dopant diffuses into the semiconductor.* For this reason, the solubilities of a number of elements in germanium and silicon have not been determined by this method, especially at low temperatures. After a sample has been diffused, the solubility may be determined by one of two ways. The simpler and more accurate method is a chemical or physical analysis of the complete sample, providing the diffusion time is long enough to ensure complete saturation. If such conditions are not realized, the diffusion profile must be determined and extra-

---

* Usually rate limitations at the interface have to be considered for a vapor source (Smits, 1958). They may arise from limitations in mass transport in the vapor or reactions at the surface.

polated to the surface where the concentration should equal the solubility limit.

If a true equilibrium solid solubility of one component in another is desired, the external phase must be that which is depicted by the phase diagram of the system as being in equilibrium with the solid solution in question. For example, the solidus of an equilibrium phase diagram must be determined by equilibration of the solid with a liquid of liquidus composition. This statement may be generalized further with the aid of the hypothetical phase diagram and corresponding free energy curves for a given temperature shown in Figure 2.7. As was shown in the previous section, the solubilities of the components in the various phases are given by common tangents to the free energy curves and are designated on the diagram by $C_{\beta\alpha}$, $C_{\alpha\gamma}$, etc. If component A is equilibrated with the gamma phase, the solubility, $C_{\alpha\gamma}$, of B in A will be obtained. Alpha of this composition is supersaturated with respect to the beta phase, however, and the system will attempt to lower its free energy by precipitating B atoms out of solution to form beta. In other words, alpha-gamma equilibrium is metastable and can only occur in the absence of beta. The true equilibrium solubility of B in A, therefore, is $C_{\alpha\beta}$.

On the basis of the foregoing discussion, care must be taken to equilibrate with the correct phase when determining equilibrium solubility data by the diffusion method. Diffusion determinations of dopant solubilities in semiconductors are often conducted by depositing a layer of the pure element on the surface of the semiconductor. The assembly is then diffusion annealed at the desired temperature and a "solubility" is obtained. Many investigators fail to stipulate, however, the phase with which the semiconductor is equilibrated. If intermediate phases (liquid or solid) exist in a given system at the temperatures concerned, a true equilibrium solubility is obtained only if the correct phase nucleates and grows in the diffusion region between the two materials.

Equilibration via a vapor phase is also frequently used for determining solubilities of impurities in semiconductors. Details of the techniques used are given by Trumbore et al (1962) who equilibrated germanium samples with liquidus alloys of Ge-Sb, Ge-As, and Ge-Bi, and by Kooi (1964) who saturated silicon with phosphorus supplied from a P_2O_5 source.

2.E.2 Determination of Solute Concentrations

The methods of determining impurity concentrations in germanium and silicon that have been used most extensively are electrical measurements and radio-chemical techniques. A review of resistivity and Hall coefficient measurements on semiconductors is given by Knight (1956). Koch (1960) and Leymonie (1963) review neutron activation and radio-tracer analysis, respectively.

Electrical measurements are satisfactory for analyzing shallow level impurities, but deep-level dopants pose a problem since they are only partially ionized at room temperature. This method also gives erroneous results if the impurity precipitates out of solution upon cooling, or if other compensating impurities are present. Radio-chemical techniques probably give the more accurate results of the two methods, but the number of elements which can be analyzed in this way is limited.

Electron probe microanalysis has also been used to a limited extent for impurity determinations in germanium (Wittry et al, 1960) but the sensitivity was found to be limited to about two parts in 10^4. A discussion of other methods of analyzing trace impurities in semiconductor materials including mass spectrometry, emission spectroscopy, and diffraction microscopy is given by Brooks and Kennedy (1962).

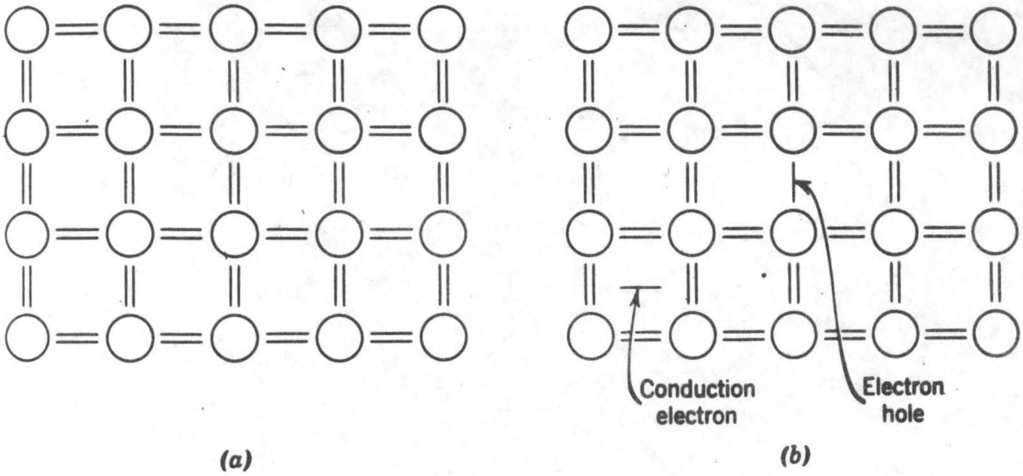

(a) (b)

Figure 2.1. Schematic view of covalent bonds in a semiconductor. (a) corresponds to no free electrons or holes, (b) corresponds to the existence of electrons in the conduction band and holes in the valence band. From R.A. Swalin, in "Thermodynamics of Solids", John Wiley & Sons, New York, 1962.

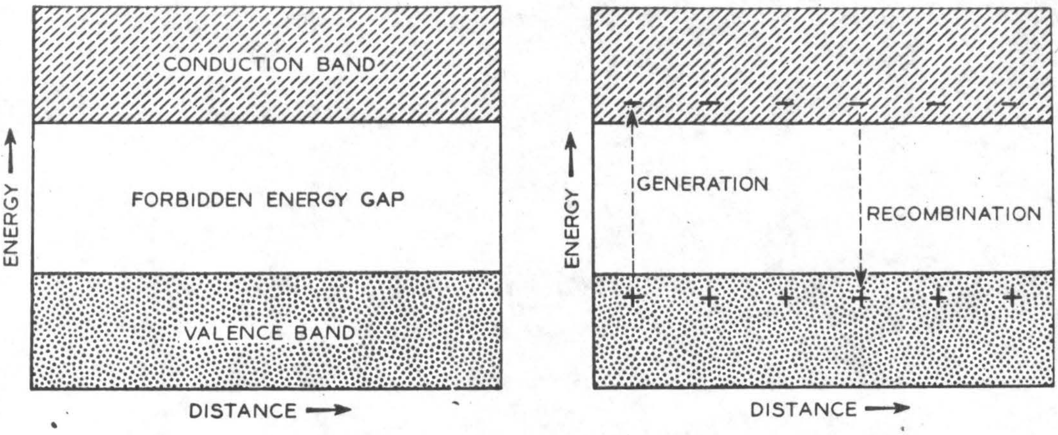

(a) (b)

Figure 2.2. Intrinsic semiconductor, (a) at low temperatures, (b) at elevated temperatures with thermal excitation of electrons and holes. From N.B. Hannay in "Semiconductors", Reinhold, New York, 1959.

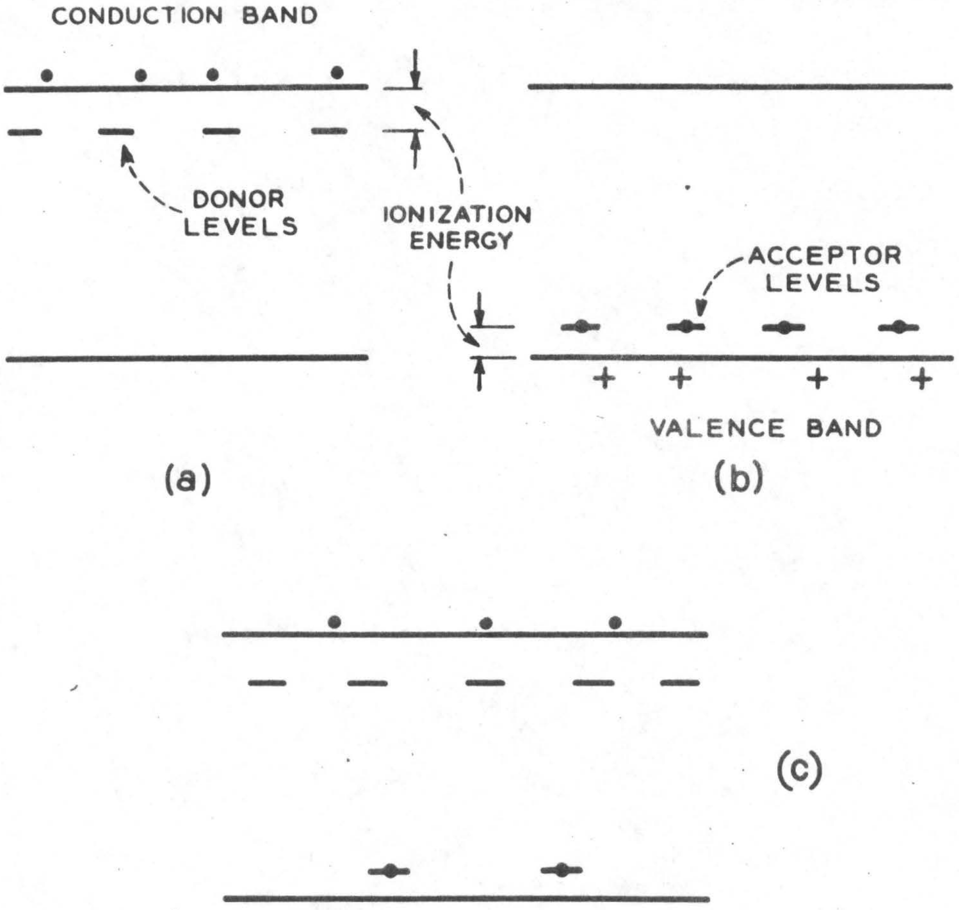

Figure 2.3. Energy levels for (a) donors, (b) acceptors, and (c) a partially compensated semiconductor. The solid circles and the crosses represent electrons and holes, respectively. From N.B. Hannay, in "Semiconductors", Reinhold, New York, 1959.

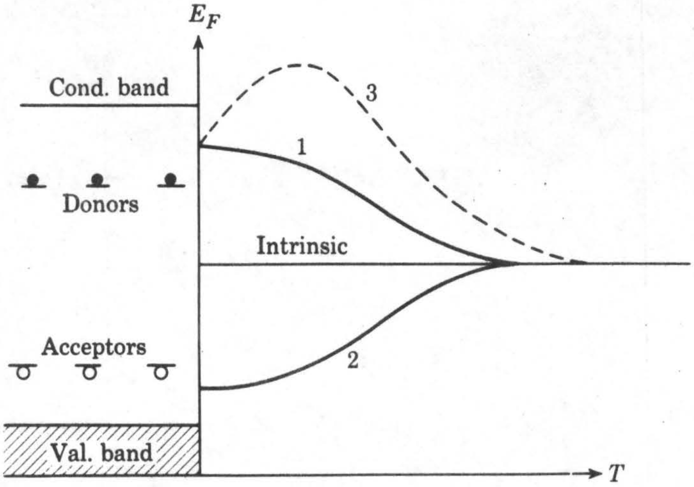

Figure 2.4. Schematic representation of the Fermi energy as a function of temperature; curve 1 for n-type, curve 2 for p-type. Curve 3 corresponds to the case when the electron gas is degenerate over a certain range of temperature. From A.J. Dekker, "Solid State Physics", Prentice-Hall, Englewood Cliffs, N.J., 1957.

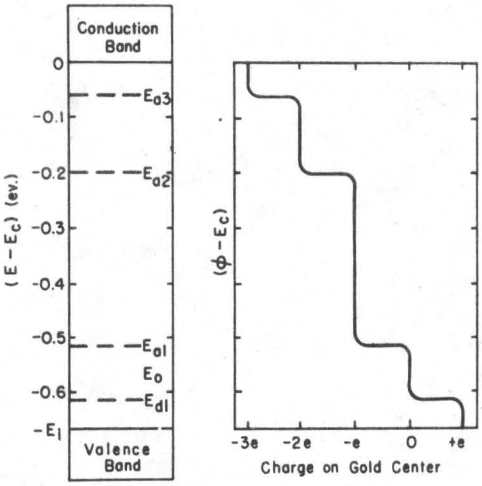

Figure 2.5. The energy levels of the amphoteric impurity gold in germanium showing how the charge per center depends on the Fermi energy at low temperatures. From J.S. Blakemore, "Semiconductor Statistics", Pergamon Press, New York, 1962.

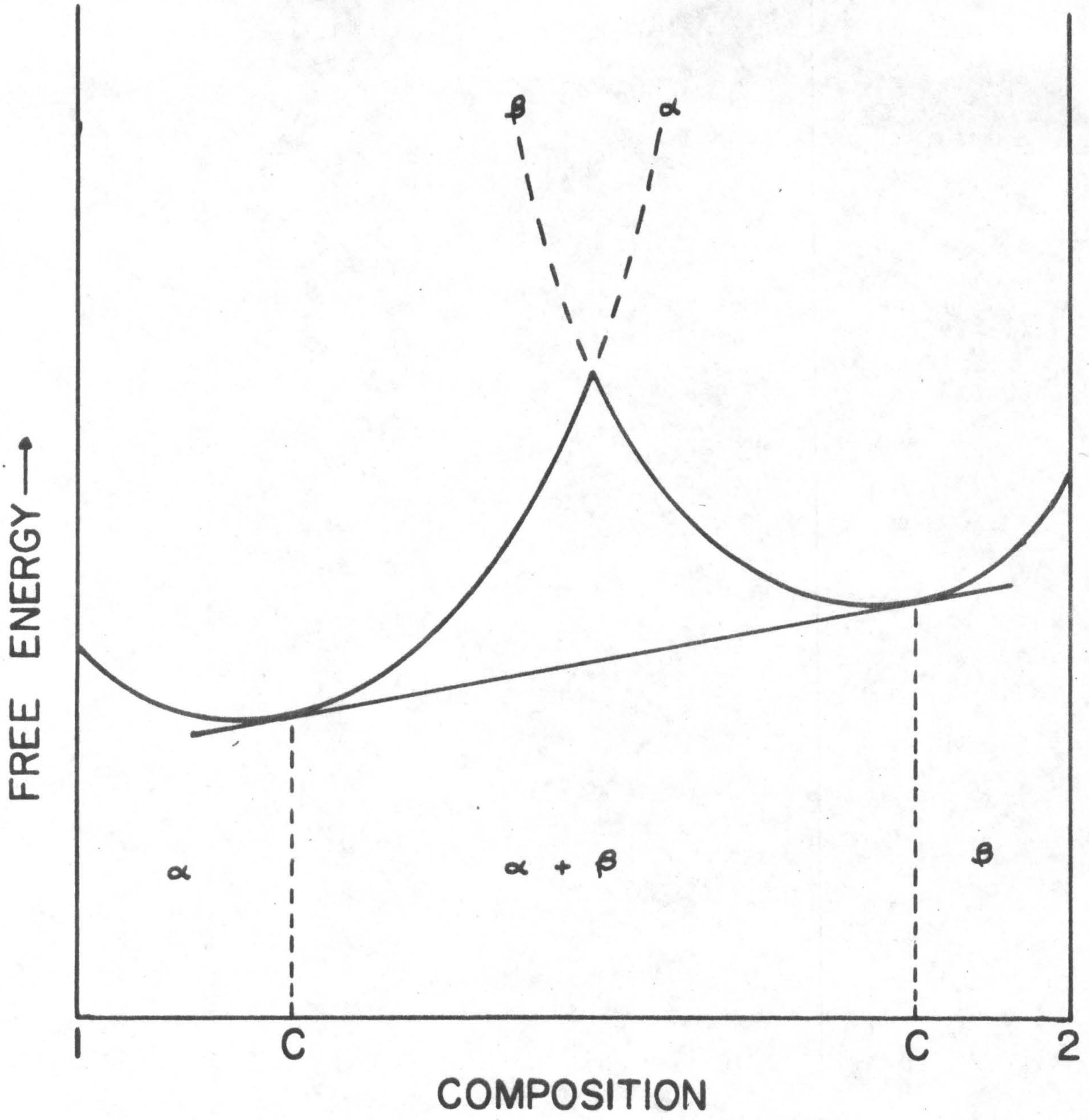

Figure 2.6. Free energy and equilibrium relations in an hypothetical two-phase system.

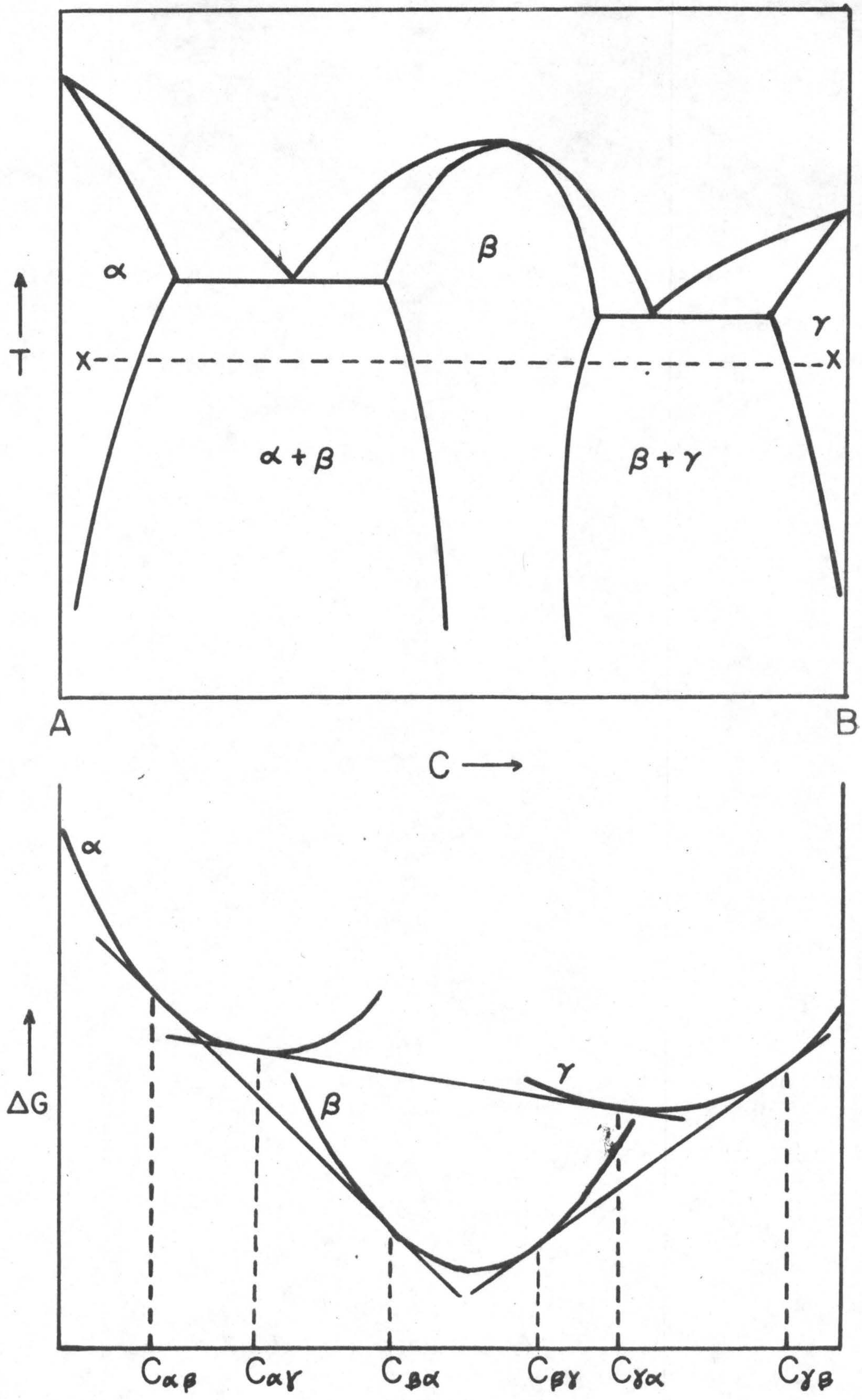

Figure 2.7. Phase diagram and corresponding free energy relations for an hypothetical three-phase system.

CHAPTER 3

THEORY OF INTERACTIONS

3.A Introduction

The following discussion of the theory of interactions of solute atoms with defects (other solute atoms, electrons, phonons, grain boundaries, and dislocations) in solid solution is generally thermodynamic in nature and particular emphasis is placed upon the effect of interactions on solubility parameters. An attempt is made, however, to apply information obtainable from equilibrium experiments to kinetic problems associated with device manufacture.

The central problem is to extend the solution theory presented in Section 2.C and determine the effect of the presence of defects on the activity of the solute atoms. It is convenient to divide defect interactions into two main categories: 1) direct and 2) indirect interactions. In the first group are those interactions which arise from the direct physical association of lattice defects. The second type is more subtle and it results from the law of mass action and not from physical association. In the discussion which follows, an indirect interaction is investigated first, and all the others are of the first type.

3.B. Electrons and Solute Atoms

Thermodynamic interactions between atomic and electronic defects in covalent semiconductors were first discussed by Reiss and his co-workers (1953, 1956)[a] on the basis of the law of mass action.

Wagner and Schottky (1930) established the foundation for this formalism by their investigation of the equilibrium properties of ionic solids. The basis of this approach is that lattice defects may be treated as chemical species and defect interactions may be considered to be chemical reactions. Reiss (1953) has shown that the law of mass action treatment for electronic defects is permissible only as long as the statistics satisfied by holes and electrons remain classical.

The law of mass action can be applied to the reactions shown below, each of which are characterized by equilibrium constants, K_1 and K_2 :

$$D^e \overset{K_1}{\rightleftharpoons} D^s \overset{K_2}{\rightleftharpoons} D^+ + e^- \quad ,$$

where D^e represents a donor species in an external phase, D^s is the non-ionized species in solid solution in the semiconductor, and D^+ and e^- are the ionized donor and electron in solution. It can be seen qualitatively from these reactions that an increase in the concentration of electrons will, through the mass action, reduce the ionization and therefore the solubility of the donor if it is extensively ionized. On the other hand, a decrease in the electron concentration would have the opposite effect. These two conditions could be achieved by the addition of other donors or acceptors. The mass action law gives for the above two reactions

$$K_1 = \frac{N_D^s}{N_D^e}$$

and

$$K_2 = \frac{N_D+ \cdot n}{N_D{}^s} \quad .$$

Therefore

$$N_D+ \cdot n = K_3 \ . \qquad (3.1)$$

Reiss and Fuller (1956)[a] solved the problem of acceptor enhancement of the solubility of a donor by combining Equations 3.1 and 2.1 with the condition for electrical neutrality to give

$$N_D+ = \frac{N_A-}{1+B}\left[\left(\frac{N_A-}{1+B}\right)^2 + (N_D{}^\circ+)^2\right]^{1/2} \quad , \qquad (3.2)$$

where $B = \left[1 + (2n_i/N_D{}^\circ+)^2\right]^{1/2}$, and $N_D{}^\circ+$ is the donor solubility in the absence of added acceptor, A^-, i.e. the solubility in the pure semiconductor.

Similar expressions may be derived for other combinations of dopants. The general result is that unlike dopants enhance each other's solubility, whereas like dopants have the opposite effect. The magnitude of this effect has a limit governed by the concentrations of dopants involved, however. If the condition

$$N_A- > N_D{}^\circ+ \text{ or } n_i$$

(using either n_i or $N_D{}^\circ+$, whichever happens to be larger) is not satisfied with reference to Equation 3.2, an acceptor addition will not have any significant effect on the solubility of a donor. This can be seen qualitatively with the help of Equation 3.1. If the electron concentration is large, either because the donor concentration or the number of intrinsic electrons is large, then a smaller number of acceptors cannot influence this concentration (c.f. Equations 2.3, 2.4 and 2.8) and Equation 3.1 therefore remains the same with n essentially unchanged.

Shockley and Moll (1960) have presented an alternate treatment of dopant atom-electron interactions by a statistical method in which they generalize the method to include dopant ions which have a possibility of existing in multiply charged states. According to the Shockley-Last theory (1957), the ratio of concentrations of impurity centers in any one of the possible charge conditions depends on the position of the Fermi level and is given by the ratio of Boltzmann factors shown in Section 2.B.2. These results can be extended to give the solubility of a dopant as a function of the Fermi energy. If the density of the neutral component of a solute species in a semiconductor is assumed independent of the Fermi energy, the concentration, N_r, of dopant atoms of charge state, r, is given by

$$N_r = N_o \exp \left[(rE_f - \Sigma E_r)/kT \right] ,$$

where N_o is the concentration of neutral dopant and

$$\begin{aligned} \Sigma E_r &= E_{1a} + E_{2a} + \ldots. + E_{ra}, \ r<0 \\ &= -(E_{1d} + E_{2d} + \ldots. + E_{rd}), \ r>0 \\ &= 0 \qquad . \ r = 0 \end{aligned}$$

The total concentration of dopant atoms is then

$$N = \Sigma_r N_r = N_o \Sigma_r \exp \ (-rE_f - \Sigma E_r)/kT \quad . \tag{3.3}$$

The value of N_o must be evaluated from an experimental determination of the solubility for a known Fermi energy.

If the intrinsic solubility, $N_i°$, of a simple donor (r=+1) or acceptor (r=-1) is known, the solubility, N_i, in material doped such that the Fermi energy is changed from $E_f°$ to E_f is given by

$$N_i = N_i° \exp\left[r(E_f° - E_f)/kT\right] \quad . \tag{3.4}$$

It can be seen that if the Fermi energy is lowered by the addition of an acceptor, say, the solubility of the donor is increased. If, on the other hand, another donor is introduced its solubility is decreased. Equation 3.4 therefore predicts the same behavior as does Equation 3.2. The exponential term in the above equation can be expressed in terms of the concentration of the second dopant by solving Equations 2.9 and 2.10 or 2.11 and 2.12, depending on whether a donor or an acceptor is added. If in the case considered previously (effect of an acceptor on the solubility of a donor), the dopants are essentially completely ionized and $N_a >> N_d$, n_i, the latter set of equations give

$$\frac{N_a}{n_i} = \exp\left(\frac{E_f° - E_f}{kT}\right) .$$

and then

$$N_d = N_d°\left(\frac{N_a}{n_i}\right) . \tag{3.5}$$

From a classical viewpoint the ΔE_f term in Equation 3.4 may be interpreted as a change in the partial electronic free energy of solution. This concept may be seen with the aid of Equation 2.25. If an intrinsic and an extrinsic semiconductor are equilibrated with an external phase containing a certain impurity, the chemical potential of this impurity must be identical in each for thermodynamic equilibrium, i.e.

$$kT\ln\gamma_{ion}^{\circ} N_i^{\circ} \pm E_f^{\circ} = kT\ln\gamma_{ion} N_i \pm E_F$$

or
$$N_i = N_i^{\circ} \frac{\gamma_{ion}^{\circ}}{\gamma_{ion}} \exp\left[\pm (E_f^{\circ} - E_f)/kT\right] ,$$

where the + and - signs refer to the ionization of a donor or an acceptor, respectively. This relationship is a generalization of Equation 3.4 since it also allows for a change in the ionic activity due to physical interactions with holes, electrons, or other ions. The above expressions could also be written as

$$kT \ln \gamma_i^{\circ} N_i^{\circ} = kT \ln \gamma_i N_i$$

or
$$\gamma_i^{\circ} N_i^{\circ} = \gamma_i N_i ,$$

where the γ_i's are now the activity coefficients of the atoms. Comparison with Equation 3.4 gives

$$\frac{\gamma_i^{\circ}}{\gamma_i} = \exp\left(\pm \frac{E_f^{\circ} - E_f}{kT}\right) \tag{3.6}$$

if, due to low concentrations, $\gamma_{ion}^{\circ} / \gamma_{ion}$ is assumed to be unity. Using the example considered in Equation 3.5 the activity coefficient of a donor, γ_d, in material doped with an acceptor is given by

$$\gamma_d = \gamma_d^{\circ} \frac{n_i}{N_a} \quad (\text{for } N_a >> n_i). \tag{3.7}$$

As will be shown in the next section, however, the assumption γ_{ion} =

γ_{ion}° is often a poor approximation because of ionic interactions.

3.C Solute Atoms and Other Solute Atoms

3.C.1 General

The study of solute atom-solute atom (different chemical species) interactions comes under the realm of the thermodynamic theory of ternary solutions. The basic problem is to determine the effect of an additional component (to be designated component 3) on the activity coefficient of a given solute (component 2) in a solvent (component 1).

One of the first theoretical treatments of the thermodynamics of multicomponent solutions was conducted in a classical manner by Wagner (1952)[b] who used a Taylor series expansion for the excess partial molar free energy (or equivalently the logarithm of the activity coefficient) of a component in solution. The activity coefficient of component 2, say, in a solution with mole fractions X_2, X_3, X_4, ... of the various components is then given by

$$\ln\gamma_2(X_2,X_3,X_4\ldots) = \ln\gamma_2^{\circ} + \left(X_2\frac{\partial\ln\gamma_2}{\partial X_2} + X_3\frac{\partial\ln\gamma_2}{\partial X_3} + X_4\frac{\partial\ln\gamma_2}{\partial X_4} + \ldots.\right)$$
$$+ \left(1/2\ X_2^2\ \frac{\partial^2\ln\gamma_2}{\partial X_2^2} + X_2X_3\frac{\partial^2\ln\gamma_2}{\partial X_2\partial X_3} + \ldots..\right) + \ldots.., \qquad (3.8)$$

where the derivatives are taken for the limiting case of zero concentration of all solutes and $\ln\gamma_2^{\circ}$ is the activity coefficient of component 2 at infinite dilution in the pure solvent. If the second and higher order terms are disregarded the above relation becomes a linear function of the various mole fractions:

$$\ln\gamma_2 = \ln\gamma_2^{\circ} + \varepsilon_{22}X_2 + \varepsilon_{23}X_3 + \varepsilon_{24}X_4 + \ldots.., \qquad (3.8a)$$

where the coefficients (interaction parameters) are

$$\varepsilon_{22} = \frac{\partial \ln \gamma_2}{\partial X_2} \quad \text{etc.}$$

Wagner also showed that these coefficients obey the reciprocity relation

$$\varepsilon_{ij} = \varepsilon_{ji} \; .$$

The coefficients in Wagner's equation must be determined experimentally and will in general include electronic as well as ionic interaction effects. If electronic effects due to changes in the Fermi energy are relatively important in a given system, the expression for the activity coefficient takes the form of Equation 3.6, i.e.

$$\ln \gamma_2 = \ln \gamma_2^{\circ} \pm \frac{\Delta E_f}{kT} \; .$$

In metallic systems it is possible that this relation may be represented by the Wagner formalism but this is not the case in semiconductors because Equations 3.6, 2.11 and 2.12 show that the activity of a donor in an extrinsic non-degenerate p-type semiconductor is given by

$$\ln \gamma_2 = \ln \gamma_2^{\circ} - \ln \left[\frac{fX_3}{2n_i} + \left(\frac{f^2 X_3^{\,2}}{4n_i^{\,2}} + 1 \right)^{1/2} \right] ,$$

where X_3 is the mole fraction of the acceptor and f is a factor which converts concentration units of atoms per cubic centimeter to mole fraction. This relationship is obviously not of the same form as Equation 3.8 even though the concentrations involved may be very low ($X_3 \geq 10^{-4}$ at 700°C in silicon). If a Taylor's series is used to expand this function, the first two terms obtained are

$$-\ln\gamma_2/\gamma_2^\circ = \frac{f}{2n_i} X_3 - \frac{f^3}{48{n_i}^3} X_3^3 + \ldots.$$

It can be seen that this series is only convergent for $fX_3 < n_i$ and therefore cannot be applied for concentrations of interest.

A number of recent publications (see for example Lupis and Elliott (1966a)) have been concerned with evaluating and measuring first and second order ternary interaction parameters and assigning to them enthalpy and entropy components. Most of the present experimental data are insufficiently accurate, however, to determine the Wagner coefficients with reasonable success unless the second order effects are small.

Ternary solutions have also been treated statistically by setting up an atomic model and applying quasi-chemical theories to ionic interactions and configurations. It must be stressed, however, that these theories are very approximate in that they consider only concentration independent nearest-neighbor interactions and thus disregard long range elastic forces, and both direct and indirect electronic interactions.

The simplest model of a ternary solution is one in which all the atoms are distributed in a completely random manner on identical lattice sites. The procedure for calculating the excess partial molar free energies of solution (and hence the activity coefficients) involves a determination of the heat of solution by summing the pair interaction enthalpies of all nearest neighbors in the lattice. If thermal entropy changes are neglected, the activity coefficient may then be obtained from the relation

$$RT\ln\gamma_i = \frac{\partial(\Delta G^{ex})}{\partial N_i} = \frac{\partial(\Delta H)}{\partial N_i} ,$$

where ΔH is the integral heat of solution (with reference to suitable standard states) of the lattice and N_i is the number of moles of the ith component. If the lattice sites are not identical, account must be also be taken of the excess configurational entropy. Ternary solutions containing one interstitial component have been treated by Kirkaldy and Purdy (1962)[a] and the case of two interstitials in a substitutional solvent has been considered by Burylev (1963). It is found for moderately dilute solutions of this type that the activity coefficients are represented by the first order Wagner equation. As in the simple binary, a net attractive force between unlike solute atoms results in a decrease in the activity coefficient. This means that if there is a negative interaction energy between two different solutes, they will mutually enhance each other's solubility.

The quasi-chemical theory becomes much more complicated if the atomic configuration is non-random. Depending on the signs and relative magnitudes of the various pair interaction energies, the different chemical species may cluster in a manner which lowers the free energy of the solution. If there exists a strong attraction between two solutes, for example, they will tend to become physically associated, thus lowering the enthalpy of solution at the expense of decreasing the entropy. Lupis and Elliott (1966)[b] give a detailed statistical analysis of the problem and show that the activity coefficients can be expressed by the Wagner formalism with the interaction parameters represented by complex functions of the various pair interaction energies.

3.C.2 Complex Formation and Solubility

In certain instances the theory of non-regular ternary solutions may be treated by a much simpler method than that of Lupis and Elliott. If the solutions are very dilute ($X \leq 0.01$) it may be assumed that the number of 2-2 and 3-3 bonds are negligible and that the atomic distribution is random except for an excess number of 2-3 bonds. This implies that only negative interaction energies between unlike solutes will affect their spatial distribution since the number of 2-3 bonds in a random dilute solution is negligible. This statement will not be true, however, if repulsive forces are extremely long-ranged. If strong attractive interactions between unlike solutes exist, distinct atomic (or ionic) complexes will tend to form in nearest neighbor sites.

Before any calculations can be attempted, a physical picture of the complexes must be postulated. If the interactions are coulombic in nature, a complex may be considered electrically neutral if

$$r_2 n_2 = -r_3 n_3,$$

where r_2 and r_3 are the charge states of the dopants and n_2 and n_3 are the number of ions of each component in a complex. The simplest case, therefore, is a complex of two ions of equal but opposite charge. It may be assumed then, that once a simple neutral complex forms, it does not interact to any significant extent with other "free" dopants, and its size is therefore fixed at two ions. Mobility studies by Reiss et al (1956)* lend support to this argument. They found that complex formation between singly charged dopants caused the elimination of charged scattering centers and a resultant increase in the mobility with no change in carrier concentration. If the charge states are not equal, the situation is more complicated, but the coulombic energy of interaction should be greater for a complex of two ions than for one containing more than this number. Under such conditions then, both enthalpy and entropy considerations favor two-ion complexes and they will probably predominate.

In many experimental studies of this subject a fast diffuser (to be designated component 2) is equilibrated in a semiconductor doped with conventional Group III or IV impurities which are slow diffusers. In such cases the slow diffusing dopant (component 3) may be considered to be stationary relative to the other, and only one atom of the former solute can exist in a complexed state. If $r_2 > r_3$ the resultant charge of a two-ion complex will have the same sign as component 2 and in this instance the assumption of two-ion complex should be quite good.

Swalin (1962) calculated by statistical means the number of complexes to be expected in a substitutional ternary solution containing N_2 ions of component 2 and N_3 ions of component 3 between which exists a binding enthalpy ΔH_b. The free energy, G, of the crystal, after the formation of N_c complexes, changes from G_{reg} to

$$G = G_{reg} + N_c \Delta H_b - N_c T \Delta S^{th} - T(S^m - S^m_{reg}) ,$$

where ΔS^{th} is the vibrational entropy change involved in the formation of a complex, and S^m_{reg} and S^m are the configurational entropies of mixing of the crystal before and after complex formation, respectively. It is assumed in this treatment that the complexing process does not change the electrical characteristics of the solution, i.e. the Fermi energy remains constant. At equilibrium G will be a minimum and thus $\partial G/\partial N_c = 0$.

The entropy of mixing after complex formation may be considered to consist of two terms: 1) the entropy of mixing, S_1^m, of the lattice minus the complexes, and 2) the entropy of mixing, S_2^m, of the lattice and the complexes. If the total number of lattice sites is N, the first component is given in the usual manner by

$$S_1^m = k \ln \left[\frac{(N - 2N_c)!}{(N_2-N_c)!\,(N_3-N_c)!\,(N-N_2-N_3)!} \right] .$$

Since there are 2 N_c sites occupied by complexes the second term is given by

$$S_2^m = \frac{1}{2} k \ln \left[\frac{N!}{(2N_c)!(N-2N_c)!} \right] ,$$

where the factor 1/2 is included because the entropy is desired in terms of entropy per complex and not per atom. After applying Stirling's approximation and differentiating the free energy expression with respect to N_c, the following equation is obtained:

$$\frac{N_c}{(N_2-N_c)\,(N_3-N_c)} = \frac{1}{2N} \exp\left(\frac{\Delta S^{th}}{k}\right) \exp\left(-\frac{\Delta H_b}{kT}\right) \equiv \Omega_c \,. \tag{3.10}$$

Since the solution was assumed to be very dilute, the solubility of component 2 at regions removed from the complexes may be expressed by N_2°, the solubility in the absence of complex formation, i.e.

$$N_2^{\circ} = N_2 - N_c \quad ,$$

where N_2 is the total solubility of component 2 and N_c is the number of complexes at the solubility limit of component 2. This statement is only true, however, if the addition of component 2 up to its solubility limit does not change the Fermi energy of the system. This means that one of the two following conditions must be satisfied:

$$\text{i) } N_2 \ll n_i \quad \text{or} \tag{3.11a}$$

$$\text{ii) } N_2 \ll N_3 \quad . \tag{3.11b}$$

Equation 3.10 may then be expressed at the solubility limit of component 2 by

$$\frac{N_2 - N_2^{\circ}}{N_2^{\circ}\,(N_3 + N_2^{\circ} - N_2)} = \Omega_c \quad . \tag{3.12}$$

If $N_3 \gg N_c$, this may be simplified to

$$\frac{N_2 - N_2^{\circ}}{N_2^{\circ}} = N_3\Omega_c \quad . \tag{3.13}$$

The above expressions may also be expressed in terms of activity coefficients. Using the relation $\gamma_2^{\circ}N_2^{\circ} = \gamma_2 N_2$, Equation 3.12 becomes

$$\ln\gamma_2 = \ln\gamma_2^{\circ} - \ln\,(1 + KX_3 - KX_2 + KX_2^{\circ}), \tag{3.14a}$$

where $K = \Omega_c f$ and f is again a factor converting units of atoms per cubic centimeter to mole fraction. Similarly, if $N_2 \ll N_3$ then

$$\ln\gamma_2 = \ln\gamma_2^{\circ} - \ln\,(KX_3 + 1). \tag{3.14b}$$

This may be expressed by the Taylor series

$$\ln\gamma_2 = \ln\gamma_2^{\circ} - KX_3 + \frac{(KX_3)^2}{2} - \frac{(KX_3)^3}{3} + \ldots\ldots,$$

but is convergent only for $0 \leq KX_3 \leq 1$.

A similar analysis can be conducted for complexing between interstitial (component 2) and substitutional (component 3) ions. In this instance the mixing entropy terms are:

$$S_1^{m} = k \ln \left[\frac{(N-N_c)!}{(N_2 - N_c)!\,(N - N_2)!} \cdot \frac{(N-N_c)!}{(N_3 - N_c)!\,(N - N_3)!} \right]$$

and $$S_2^{m} = 1/2k \ln \left[\frac{N!}{N_c!\,(N - N_c)!} \cdot \frac{N!}{N_c!\,(N - N_c)!} \right]$$

if the number of interstitial sites is equal to the number of regular lattice sites. The solution is then

$$\frac{N_c}{(N_2 - N_c)\,(N_3 - N_c)} = 2\,\Omega_c\,, \qquad (3.15)$$

and for the conditions assumed in Equation 3.13, the solubility of an interstitial impurity in a ternary solution may be expressed by

$$\frac{N_2 - N_2^{\circ}}{N_2^{\circ}} = \frac{N_3}{N} \exp\left(\frac{\Delta S^{th}}{k} - \frac{\Delta H_b}{kT}\right) . \qquad (3.15a)$$

It must be remembered that the expressions derived above apply only for negative interaction energies, and in addition, the solutions must be very dilute.

If the origin of interactions is coulombic, the binding enthalpy of a complex in an electrolytic solution is given by (Fuoss, 1934)

$$\Delta H_b = \frac{r_2 r_3 e^2}{\kappa a_\circ} , \qquad (3.16)$$

where κ is the macroscopic dielectric constant of the medium and $a_\circ$ is the equilibrium distance between the ion centers in the complex. Fuoss reasoned that the use of a macroscopic dielectric constant could be justified for aqueous solutions since $a_\circ$ is in general larger than the diameter of the ion and may include solvent molecules of solvation. This argument does not really apply for the calculation of interaction energies between nearest neighbors in a solid lattice, but Equation 3.16 has been extensively applied to this situation anyway (Reiss et al, 1956)[a].

It is also possible that interactions between dopants in semiconductors may arise due to elastic strain energy effects and from tendencies to form covalent bonds (Zaromb, 1957).

Reiss et al (1956)[a] attacked the problem of complex formation on the basis of the law of mass action. The complexing reaction between acceptors, A^-, and donors, D^+, may be written as

$$A^+ + D^- = C .$$

At equilibrium

$$\frac{N_C}{N_{A^-} N_{D^+}} = \Omega'_C ,$$

where Ω'_C is the ion-complexing constant. Combining the above expression with Equations 2.1 and 3.1 and the condition for electrical neutrality yields a complicated expression which generally must be solved numerically for the solubility of one dopant in terms of the concentration of another. The advantage of this method is that it accounts for changes in the Fermi energy and consequently conditions 3.11 do not have to be satisfied. Ω'_c was calculated using modified pair distribution functions due to Bjerrum (1926) and Fuoss (1934) for electrolytic solutions. Numerical calculations of Ω_c from Equations 3.10 and 3.16 (neglecting ΔS^{th}) and of Ω'_c yield practically identical results for given temperatures and inter-ionic spacings.

3.C.3 Complex Formation and Diffusion

In the absence of electrical and mechanical forces, Onsager (1945-46) proposed, as a generalization of Fick's first law of isothermal multicomponent diffusion, that the flux, J_i, of each component be assumed a linear function of all concentration gradients, ∇N_k, ie.

$$J_i = -\sum_{K=1}^{n} D'_{iK} \; \nabla N_K \; . \; (i = 1,2, \ldots\ldots n)$$

If the concentration units are chosen such that $\sum_{i=1} N_i$ = constant, then (Kirkaldy, 1958)

$$J_i = -\sum_{K=2}^{n} D_{iK} \; \nabla N_K \; (i = 2,3\ldots\ldots n).$$

For the special case when $\nabla N_3 = 0$ in a ternary system

$$J_2 = -D_{22} \frac{\partial N_2}{\partial X} \; .$$

Complex formation between solutes will render the diffusion coefficient strongly dependent upon the concentration of the third component.
If the complexes are considered immobile relative to the "free" components,

Reiss et al (1956) have shown that D_{22} can be related to D°_{22}, the diffusion coefficient of "free" component 2, by

$$D_{22} = \frac{D^{\circ}_{22}}{2} \left[1 + \frac{1/2\ (N_2 - N_3 + \frac{1}{\Omega_c})}{\sqrt{1/4\ (N_2 - N_3 - \frac{1}{\Omega_c})^2 + \frac{N_2}{\Omega_c}}} \right] . \qquad (3.17)$$

For the special case when $N_2 \ll N_3$ this relation reduces to

$$D_{22} = \frac{D^{\circ}_{22}}{1 + \Omega_c N_3} . \qquad (3.18)$$

It is seen that the diffusion coefficient of a solute (a kinetic parameter) is dependent on the complexing equilibrium constant, a parameter which may be obtained from equilibrium measurements. This is a good example of the application of information obtainable from equilibrium measurements to kinetic phenomena which, in general, are more difficult to investigate experimentally.

In Appendix A the flux equation is generalized for ternary diffusion in the presence of complex formation. An attempt is also made to include electrostatic potentials arising from electron-solute atom interactions.

3.D Phonons and Solute Atoms

The thermal entropy of a lattice arises from the vibration of atoms about a given point (neglecting electronic contributions) with which is associated a randomness in the distribution of the total vibrational energy of the crystal. If a crystal is treated as a collection of 3N harmonic oscillators of frequency ν_i, the thermal entropy,

S^{th}, is given at high temperatures by (Huntington et al, 1955)

$$S^{th} = -k \sum_{i=1}^{3N} \left[\ln \frac{h\nu_i}{kT} + 1 \right] \quad .$$

Defects which are present in a solid may interact with the lattice phonons and change the vibrational frequencies associated with the normal modes of the crystal. If the original lattice frequencies are $\nu_i°$ and the final frequencies after the introduction of the defects are ν_i', then the complete change in the entropy of the lattice is

$$\Delta S^{th} = k \sum_{i=1}^{3N} \ln \frac{\nu_i°}{\nu_i'} \quad . \tag{3.19}$$

In order to determine the specific entropy of a particular defect, the change in the elastic spectrum which results from the introduction of the defect must be evaluated.

Lifshitz (1956) has formally solved the dynamics of a crystal perturbed by a defect by assuming that the normal modes and frequencies were known for the unperturbed lattice, and by use of the dynamic Green's-function matrix was able to reduce the number of degrees of freedom of the perturbed lattice to a manageable size. Similar methods are outlined in a review paper by Maradudin et al (1963), but simpler, approximate methods of the solution of Equation 3.19 in which the vibrational spectrum is not explicitly determined will be given here.

Zener (1950) approached the problem qualitatively by treating a defect as a center of pressure in an infinite isotropic elastic continuum. In a previous paper Zener (1949) showed that the presence of residual elastic strain in a solid results in a lowering of its tensile and shear moduli which is proportional to the elastic strain energy. He also demonstrated that the lowering of these moduli in a region surrounding a solute atom results in a lower frequency of vibration in its vicinity. This lower vibrational frequency may be interpreted as a greater vibrational randomness and hence a positive change in vibrational entropy. Since the entropy change is dependent on the elastic strain through the elastic moduli, it can be seen that because strain energy often makes an important contribution to the heat of solution in solids, there should exist a correlation between the excess entropy and the heat of solution of solutes in solid solutions. Zener's treatment of the entropy of diffusion (1952), in which he assumed that the strain free energy is proportional to the shear modulus, μ, of a crystal, may also be applied to the analysis of excess entropies of solid solutions. From the thermodynamic relation $S = \left(-\partial G/\partial T\right)_p$, the change in vibrational entropy is therefore proportional to the temperature coefficient of the shear modulus, i.e.

$$\Delta S^{th} \propto -\left(\frac{\partial \mu}{\partial T}\right)_p \quad . \tag{3.20}$$

Since $(\partial \mu/\partial T)_p$ is negative for most solids, this relation shows that the change in thermal entropy due to defects is usually positive.

The problem of defect entropy has been considered in greater detail by Huntington et al (1955). They maintained that the elastic continuum treatment is valid only at relatively large distances from the defect, and considered the following three regions separately; 1) the atoms in the immediate neighborhood of the defect, 2) the region over which the defect sets up an elastic stress field, and 3) the surface of the solid. By using a Born-Mayer representation of the ion core interactions and an Einstein model for the elastic frequencies in the immediate neighborhood of the defect, they showed that when the atoms are crowded together closer than their normal equilibrium distances, the frequencies rise and the entropy change is negative. Conversely, a local expansion causes the frequencies to decrease resulting in a positive entropy charge. Huntington et al calculated the thermal entropies of a vacancy and an interstitial atom in copper as 1.47k and 0.8k, respectively, by determining the frequencies of vibrations near the defect as well as the strain energy contribution considered by Zener. They also accounted for a dilatation term arising from the boundary condition of zero pressure at the surface. This contribution is smaller than and of opposite sign to that of the term associated with the immediate region of the defect and thus partially compensates for the latter.

It should also be emphasized that when the defect entropies of solute atoms are being discussed, the difference in mass between the impurity and host atoms must be considered as well as the force constants between the atoms. Since the frequency of an oscillator is proportional to $(f/m)^{1/2}$ where f is a force constant and m is a mass, the thermal entropy of a lattice in the harmonic approximation may be expected to increase when the masses of the solute atoms are larger than the masses of the solvent atoms.

Freedman and Nowick (1958) pointed out the difference between ΔS^{th} in Equation 3.19 (the specific thermal entropy) and the excess partial molar entropy, $\Delta\bar{S}_2^{ex}$. ΔS^{th} is the entropy change relative to the pure solvent lattice so it is necessary to add to it the difference between the entropies of pure solvent and solute, $S_1°$ and $S_2°$, respectively.* Thus

$$\Delta\bar{S}_2^{ex} = k \sum_{i=1}^{3N} \ln \frac{\nu_i°}{\nu_i'} + (S_1° - S_2°) \ . \qquad (3.20)$$

Introducing an Einstein model for the pure defect-free solids gives

$$\Delta\bar{S}_2^{ex} = k \sum_{i=1}^{3N} \ln \frac{\nu_i°}{\nu_i'} + 3k \ln \frac{\nu_1°}{\nu_2°} \ .$$

They then reasoned that since there are 3N vibrational modes and $N\mathcal{Z}/2$ bonds, where $\mathcal{Z}$ is the coordination number, there are $6/\mathcal{Z}$ vibrational modes per bond. In a dilute solution the solute atom forms $\mathcal{Z}$ 1-2 bonds so six vibrational modes are related to these bonds. Thus the above relation becomes

$$\Delta\bar{S}_2^{ex}/k = \sum_{i=1}^{3N-6} \ln \frac{\nu_i°}{\nu_i'} + 6 \ln \frac{\nu_2°}{\nu_{12}} + 3 \ln \frac{\nu_1°}{\nu_2°} \ .$$

If the rather drastic assumption is made that the frequency ν_{12} is given by the geometric mean of ν_1 and ν_2, or

$$\nu_{12} = (\nu_1 \nu_2)^{1/2} \ ,$$

then

$$\Delta\bar{S}_2^{ex} = \sum_{i=1}^{3N-6} \ln \frac{\nu_i°}{\nu_i'} \ . \qquad (3.21)$$

Under such conditions the most important nearest-neighbor interactions

---

* It should be remembered that this statement is true only if the excess configurational entropy of mixing is zero.

have cancelled. Freedman and Nowick assumed that in such a case, the remaining vibrational modes could be treated in terms of Zener's strain theory. If strong 1-2 attraction exists, however, ν_{12} may be expected to be greater than $(\nu_1 \nu_2)^{1/2}$ with a corresponding negative contribution to $\Delta\overline{S}_2^{ex}$. The opposite will hold when a 1-2 repulsion predominates. It should also be kept in mind, however, that the atomic frequencies are also dependent on the degree to which the atoms in the neighborhood of a solute atom are removed from their equilibrium positions relative to a defect free solvent.

In dielectric media another contribution to the thermal entropy will arise from the polarization effect of an ionized impurity atom. The polarization entropy, ΔS^p, of a singly charged ion is given by (Weiser, 1962)

$$\Delta S^p = \frac{e^2}{D\kappa} \frac{d(\ln\kappa)}{dT}, \tag{3.22}$$

where an ion is considered to be embedded in a cavity of diameter, D, in a medium of dielectric constant κ. Using experimental values of

$\frac{d\ln\kappa}{dT} = (13.8 \pm 0.8) \times 10^{-5}\ (°K)^{-1}$ for germanium

and $(7.8 \pm 0.8) \times 10^{-5}\ (°K)^{-1}$ for silicon

(Cardona et al, 1959), the polarization entropies of charged defects are equal to 4×10^{-5} eV/°K and 6×10^{-5} eV/°K for silicon and germanium, respectively.

3.E Dislocations and Solute Atoms

According to Bullough and Newman (1963) in a review of this subject there are four possible contributions to the energy of long range interaction between a point defect and a dislocation: 1) an elastic interaction arising from the difference in size between solute and solvent atoms, 2) a second order elastic interaction which appears if the solute atom behaves like a small region with different elastic constants from those of the matrix, 3) an electrical interaction resulting from a distortion of the band structure in the neighborhood of the dislocation, and 4) another electrical interaction possible in covalent semiconductors in which dangling or broken bonds may act as localized acceptor sites. Van Bueren (1960)[b] also points out that once an impurity atom in a homopolar crystal arrives at the dislocation proper, it may form a chemical exchange bond with unpaired electrons.

Reference is made to the above mentioned articles for a detailed description of the nature of these interactions and emphasis will be given here to their thermodynamic and kinetic consequences in solution theory.

In order to determine the equilibrium concentration, X_2^d, of solute atoms associated with dislocations, the following Boltzmann relation is usually assumed:

$$X_2^d = X_2 \exp(U_b/kT), *$$

where X_2 is the concentration of impurity at large distances from the dislocation and U_b is the binding energy of solute atoms to the dislocation. Bauer (1966) has pointed out, however, that the binding

---

* This expression applies only if the concentration remains dilute everywhere.

free energy, ΔG_b, not the binding energy, is the parameter that reflects the degree of segregation of a specific species of point defect to dislocations, i.e.

$$X_2{}^d = X_2 \exp(\Delta G_b/kT). \tag{3.23}$$

This implies that the vibrational entropy change, ΔS_b, which is dependent on the normal modes of the lattice <u>and</u> the dislocation, must be evaluated. After decoupling the lattice and the dislocation vibrational modes, Bauer evaluated the following thermal entropy changes:

ΔS_l (lattice) $= S_l$ (defect at dislocations)
$- S_l$ (defect in lattice)

and ΔS_d(dislocation) $= S_d$ (defect at dislocation)
$- S_d$ (defect in lattice) ,

and by assuming that solute centers act as dislocation pinning points calculates the total binding entropy as

$$\Delta S_b = \Delta S_l + \Delta S_d = \Delta S' + k \ln (X_2{}^d)^{1/2} \quad ,$$

where $\Delta S'$ is a term independent of concentration. Letting $\Delta G_b = \Delta H_b - T\Delta S_b$ and substituting the above relation in Equation 3.23 gives

$$X_2^d = X_2^2 \exp\left(\frac{-2\Delta H_b}{kT}\right) \exp\left(\frac{2\Delta S'}{k}\right) \quad . \tag{3.24}$$

Substitution of the relations

$$\Delta H_b = -\Delta \overline{H}_2 + \Delta \overline{H}_2{}^d$$

and

$$X_2{}^2 \propto \exp\left(\frac{2\Delta\overline{H}_2}{kT}\right) ,$$

where $\Delta\overline{H}_2$ and $\Delta\overline{H}_2{}^d$ are the heats of solution of the solute in the bulk crystal and in the dislocation,respectively, gives

$$X_2{}^d \propto \exp\left(-\frac{2\Delta\overline{H}^d}{kT}\right) . \qquad (3.25)$$

It is difficult to investigate these equilibrium segregation relations by solubility measurements because normal dislocation densities will not usually affect the overall solubility of a solute. It may be possible, however, to get information about solute atom - dislocation interactions from kinetic measurements in supersaturated solutions since a more extreme phenomenon may occur under this condition whereby dislocations act as sites for nucleation of a new phase. Cahn (1957) has devised a classical model of nucleation on dislocations in which he assumed a cylindrical nucleus lying along the core of the dislocation. It was further assumed that the nucleus is incoherent with the matrix . The free energy of a nucleus then consists of three terms due to strain, surface, and volume. The strain energy and the volume energy terms tend to favor nucleation, whereas the surface energy term tends to oppose it. The overall effect is that the dissipation of strain energy achieved by replacing a segment of dislocation with a particle of a second phase results in a lowering of the activation energy for the formation of a stable nucleus. Depending on the relative magnitudes of the energy terms, it is conceivable that the barrier to nucleation could, in fact, vanish.

A great deal of theoretical work has been reported on the kinetics of migration of impurities to dislocations. The migration is normally controlled by diffusion processes assisted by drift flow resulting from the interactions mentioned previously. The solute flux is then given by an equation of the form

$$\vec{J} = -D \left(\vec{\nabla} c + \frac{c}{kT} \vec{\nabla} V\right) , \qquad (3.26)$$

where V is the interaction energy, D is the diffusion coefficient, and c is the solute concentration. The theories which have been advanced to date have only considered size-effect elastic interactions and electrical effects have been assumed negligible for temperatures at which substantial impurity migration can occur.

The kinetics of solute drift to edge dislocations was first investigated by Cottrell and Bilby (1949). They assumed that the $D\vec{\nabla}c$ term in Equation 3.26 could be neglected for short times (drift approximation) and obtained the following relation for the number of atoms, N_t, precipitated per unit volume of material in time, t, per unit length of dislocation:

$$N_t = 2N_o\left(\frac{\pi}{2}\right)^{1/2}\left(\frac{AD_t}{kT}\right)^{2/3} , \qquad (3.27)$$

where N_o is the initial number of solute atoms per unit volume and A is a constant dependent on the size of the atoms and the elastic properties of the solvent. Harper (1951) extended this relation to long periods of time by assuming that the decrease in the precipitation rate due to mutual interference of growing diffusion fields is proportional to the fraction already precipitated (Johnson and Mehl, 1939). Harper's expression for the fraction, y, of the original amount of solute which has precipitated as a function of time is

$$y = 1 - \exp\left[-2\left(\frac{\pi}{2}\right)^{1/3}\left(\frac{ADt}{kT}\right)^{2/3}\right] . \qquad (3.28)$$

Harper's analysis has been severely criticized by Ham (1959) who showed that the drift approximation is not accurate except at very small times for dislocation densities below 10^{12} cm./cm.^{3} . Ham proposed a model in which each dislocation and its stress field is replaced with a cylinder with an effective capture radius, the magnitude of which is assumed constant as precipitation proceeds. The effective capture radius is approximately the distance from the dislocation core at which the interaction energy equals the thermal energy, kT (≈10 to 100A°). The precipitated fraction is found to be proportional to (time)$^{2/3}$ only while the solute originally within the capture cylinders of the dislocations is precipitating. Ham also showed by a detailed mathematical analysis of diffusion of solute to an array of cylinders of fixed radius (see Carslaw and Jaeger, 1959) that the Johnson-Mehl assumption for matrix depletion is incorrect unless the density of dislocations is very low. He found that the long time part of the precipitation curve could be given quite accurately by

$$y = 1 - \exp\left(-\frac{t}{\tau}\right), \qquad (3.29)$$

where τ is a rate constant which is independent of concentration. It should be noted that this relation is the same as that for the "moving interface" cylindrical precipitate (Ham, 1958). Once the strain field of the dislocation is relieved, therefore, the precipitation rate law will still be of the same form.

A series of papers by Bullough and his co-workers (1959, 1960, 1961, 1962) also discusses this subject. In general, they support the arguments presented by Ham except that they made a full allowance for diffusion flow for migration of impurities very near the dislocation. They also investigated the physical nature of the precipitate particles which form at the dislocation core, and suggested that in the case of a continuous line precipitate, a transient variation in the transfer velocity across the matrix-core interface may occur. If the transfer velocity decreases with time then kinetics of the form

$$y = 1 - \exp\left(-\frac{t}{\tau}\right)^{n} \tag{3.30}$$

can be obtained, where n is less than unity.

Neither Ham nor Bullough and co-workers include in their theories the fact that the interaction energy progressively decreases as the dislocation strain is relaxed (Burke, 1965)[a]. This will have the effect of decreasing the effective capture radius as the precipitation reaction proceeds. It is also possible that if precipitation is accompanied by a volume change, the precipitate itself may set up a strain field.

3.F Grain Boundaries and Solute Atoms

Solute atoms interact with grain boundaries in a manner not dissimilar to the way they interact with dislocations. This is evident if one considers the low angle grain boundary which may be explained by a dislocation model. The physical nature of high angle grain boundaries is not yet defined by a complete theory; however, it is generally believed that they have a random misfit structure resembling a liquid and are not more than three atomic diameters wide (McLean, 1957)[a]. The thermodynamic difference between an interface and the interior of a homogenous phase is due to the surface tension that experiment shows exists at an interface. Solute elements which decrease the surface tension should therefore tend to adsorb to the surface (Gibbs, 1906). Little is known about the effect of solutes on grain boundary tension, however, so recourse is usually made to the statistics of occupancy of solute atoms in distorted and normal lattice regions.

Following McLean (1957)[b], the equilibrium concentration in a distorted region may be related to the concentration in a normal region (measure of the degree of grain boundary segregation) by determining the free energy, G, of the solute atoms which are distributed among N undistorted sites containing N_1 solute atoms and n distorted lattice sites containing n_1 solute atoms. If the enthalpies of the solute atoms in undistorted and distorted sites are $\overline{H}_1$ and $\overline{H}_1{}^b$ (both assumed independent of concentration), respectively, then the free energy due to the solute atoms is

$$G=n_1\overline{H}_1{}^b+N_1\overline{H}_1-kT\left(\ln n!N!-\ln(n-n_1)!n_1!(N-N_1)!N_1!\right) .$$

The minimum in G occurs when

$$\frac{n_1}{n-n_1} = \frac{N_1}{N-N_1} \exp \left(\frac{\overline{H}_1 - \overline{H}_1{}^b}{kT} \right) .$$

Upon introducing mole fractions, this relation becomes

$$X_1^b = \frac{X_1 \exp (Q/kT)}{1 - X_1 + X_1 \exp (Q/kT)} , \qquad (3.31)$$

where $Q = \overline{H}_1 - \overline{H}_1{}^b$. (3.32)

In the above derivation only the configurational entropy was considered. Strictly, the vibrational entropy should also be taken into account. If any vibrational entropy changes of the grain boundary due to solute segregation into it are ignored, then Equation 3.31 becomes

$$X_1{}^b = \frac{X_1 \exp (Q/kT) \exp (\Delta S/K)}{1 - X_1 + X_1 \exp (Q/kT) \exp (\Delta S/k)} , \qquad (3.33)$$

where $\Delta S = \overline{S}_1{}^b - \overline{S}_1$. If, however, solute segregation to a low angle boundary is under consideration, the problem should be treated by the method of Bauer (1966). It is rather difficult to estimate the effect of segregation on the vibrational entropy of a high angle grain boundary, but it is quite possible that it may be important since solute atoms are known to "pin" grain boundaries and inhibit their movement (Lücke and Detert, 1957). This effect then should influence the vibrational characteristics of the grain boundary probably in a manner analogous to the case of dislocation pinning.

Q in Equation 3.32 may be interpreted as a binding energy and it may arise from the same causes as were discussed in the previous section. If, for example, the strain energy of a solute atom can be relieved by segregation to a region that is already distorted, it provides a large driving force for segregation. This size effect interaction is usually the most important contribution to the binding energy in metals. Theoretical calculations of the elastic interaction energy based on dislocation models of grain boundaries were conducted by Lücke and Detert (1957) and by Webb (1957). A typical interaction energy for metals is in the order of 0.1 eV. An interaction due to the different electronic behavior of solute atoms in the interior of a crystal and in the grain boundary will also exist; however, calculations along these lines are difficult because very little is known about the electronic nature of a grain boundary. Lücke and Detert reasoned that since a grain boundary has liquid-like characteristics, an over-all estimate of possible grain boundary segregation for a given alloy system could be related to the ratio of the probability of finding the solute atom in the liquid to the probability of finding it in the solid. This ratio was assumed to be represented by the equilibrium distribution coefficient between the liquidus and the solidus near the melting point of the solvent, and could therefore be obtained directly from the phase diagram.

It is conceivable that in homopolar crystals, chemical exchange bonding between unpaired electrons will contribute significantly to the binding energy for grain boundary segregation in a manner analogous to the hypothesis of chemical bonding at dislocations in these materials.

Since grain boundaries in germanium and silicon are known to possess certain charged states (Sosnowski, 1959), it is also possible that electrostatic interactions may exist. This effect will probably be small at high temperatures, however.

CHAPTER 4

DISCUSSION OF PREVIOUS EXPERIMENTAL WORK

This chapter is a review of previous experimental work relevant to the study of the defect interactions discussed in the previous chapter. Particular emphasis is placed on the determination of thermodynamic properties of solute atoms by solubility measurements so a section is devoted to intermediate phase formation by interdiffusion between two phases not at equilibrium. Investigations of impurity precipitation at dislocations and of the effect of complex formation on diffusion are also included.

4.A Delayed Nucleation of Intermediate Phases in Diffusion Couples

Experimental observations of incubation periods for nucleation of intermediate phases have been made in diffusion couples of a number of systems. Care must be taken, however, to distinguish between behavior of this kind which is due to genuine nucleation difficulties, and that which is due to experimental problems associated with either initiating the diffusion reaction, or with detecting the presence of the new phase after small times of reaction. It is quite obvious, therefore, that oxide films must not be present between the two materials. Optical microscopic observations of this phenomenon must be treated with reservation because the nuclei may be too small to be visible at early times, especially if the growth rates of the phases are low. Using an electron micro-probe analyzer, Castaing (1951) noted the apparent absence of the beta phase in a copper-zinc couple reacted for one hour at 400°C. It seems quite likely, however, that this phase could have been present in a layer smaller than one micron thick, and therefore below the detection limit of the instrument. Electron microscopy is of little use for the detection of small particles of a new phase at a phase interface because replica techniques do not provide positive phase identification, and thin films of a section across a reaction zone are almost impossible to prepare by normal techniques because of electro-chemical problems associated with the presence of concentration gradients and of different phases.

Heumann and Heinemann (1956) made a metallographic study of the growth of the kappa phase in the copper-antimony system at 390°C by measuring the thickness of the precipitate as a function of time. If volume diffusion is the rate controlling process in a multiphase diffusion reaction and the interface concentrations are constant, then movement of the interfaces with time obey a parabolic law of the form (Crank, 1956)

$$x^2 = \text{constant} \times t .$$

By extrapolating to zero thickness in the early stages of growth these authors found that the corresponding diffusion time was greater than zero,thus indicating an incubation period for the nucleation of the kappa phase. At later stages, after the supersaturation was relieved, the growth rate decreased and extrapolated back to the origin of the graph. It has also been metallographically observed (Kidson and Miller, 1964) that in diffusion couples of aluminum and zirconium at 630°C the only detectable phase is $ZrAl_3$ whereas all the others (seven in number) appear to be absent even after annealing periods of ten hours.

Metal oxidation systems also form a class of multiphase diffusion reactions in which one of the initial phases is gaseous, and one or more phase layers of intermediate composition (metal oxides) form in the reaction zone. It has been observed by several workers that although the highest oxide is usually formed on metals of Groups IVa and Va of the periodic table, thermodynamically expected lower oxides often appear to be missing from the reaction zones of these metals. Kofstad (1963), in a study of tantalum oxidation over a wide range of temperatures, found that Ta_2O_5 is the predominant oxide under most conditions. Lower oxides were found in some ranges and not in others. Wallwork and Jenkins (1959) reported that during oxidation of titanium the only detectable oxide was TiO_2, whereas the equilibrium diagram indicates the presence of three other stable oxides between Ti metal and TiO_2. Sheasby (1963) found that during oxidation of niobium the predominant oxide under most conditions was Nb_2O_5 and the lower oxides did not form under some conditions.

In a more recent investigation, Cox (1965) studied intermediate phase formation in diffusion couples of the copper-zinc, silver-aluminum, and niobium-oxygen systems. Cox did not observe any nucleation inhibition for the beta phase in electro-plated copper-gamma brass couples. On the basis of orientation relationships observed between grains of the precipitate and the gamma phase he assumed that this phase acted as the parent phase for nucleation. He also found that in mechanically welded couples the precipitate grains formed as two separate layers which were oriented with respect to the phases on both sides of the original interface. This effect was interpreted as being due to vapor transport of zinc between the two halves of the couple before proper welding had occurred. Nucleation and growth of the precipitate then occurred in each phase independently of the other. Nucleation of the beta phase in alpha-gamma couples of the silver-aluminum system was found to be extremely difficult if care was taken to prepare deformation free samples of the gamma phase prior to electroplating with silver. Considerable inter-diffusion, as evidenced by large alpha-gamma interface displacements, took place before nucleation in deformation-free couples. Growth of the beta layer after nucleation was rapid so it was assumed that the non-appearance of the phase was a true indication that it had not nucleated. Additional evidence of inhibited nucleation was provided by the observation that the beta phase did not start growing at the original interface position.

Cox's study of niobium oxidation showed that Nb_2O_5 formed under most conditions but the lower oxides were often absent. He also observed in many cases a metastable phase which precipitated in the metal as a platelet, thus indicating supersaturation. At slow parabolic rates of oxidation it appeared that both nucleation and growth criteria for the formation of NbO were satisfied after a time, as evidenced by the relatively large layer of this oxide formed at the pentoxide-metal interface. If the rate of metal consumption was increased by reaction under different conditions after the NbO was once formed, the NbO layer then disappeared and the metal became supersaturated. At intermediate rates NbO particles were observed to nucleate, grow temporarily to relieve local supersaturation, and then be consumed again. Under these conditions the nucleation conditions were satisfied whereas the growth criteria were not. Under relatively rapid oxidation conditions, the NbO phase was not observed at all, even for long reaction times.

4.B Information from Solubility Measurements

4.B.1 Introduction

Reference to Equation 2.31 shows how the solubility of a component of a solution depends on certain enthalpy and entropy parameters. From an experimental determination of solubility as a function of temperature, one can often determine $(\Delta H_2^f + \Delta\overline{H}_2^\beta - \Delta\overline{H}_2^\alpha)$ from the slope of a plot of $\ln X_2^\alpha/X_2^\beta$ vs. $1/T$, and from its intercept the entropy factor $(\Delta S_2^f + \Delta\overline{S}_2^{ex,\beta} - \Delta\overline{S}_2^{ex,\alpha})$*. If the solubility parameters of a specific phase are desired, those of the other phase must be known, or at least be small enough that they are negligible.

In many instances, solubilities of elements in semiconductors are found by equilibration with an external liquid phase of liquidus composition. For convenience, Equation 2.31 may be rewritten as:

$$\ln k_2^e = \frac{\Delta H_2^f - \Delta\overline{H}_2^\alpha}{RT} - \frac{\Delta S_2^f - \Delta\overline{S}_2^{ex,\alpha}}{R} + \ln \gamma_2^l , \qquad (4.1)$$

where γ_2^l is the activity coefficient of component 2 in the liquid phase and $k_2^e (= X_2^\alpha/X_2^l)$ is the equilibrium distribution coefficient between the solidus and the liquidus. γ_2^l can often be estimated with the aid of the expression for the liquidus; if the liquid is in

---

* This statement is strictly true only if the solute in both phases obeys Henry's law over the concentration and temperature ranges considered.

equilibrium with essentially pure solid semiconductor and if the heat capacity of the pure supercooled liquid is the same as the pure solid, the liquidus is given by (Prigogine and Defay, 1954)

$$\ln\gamma_1^1 X_1^1 = \frac{\Delta H_1^f}{R}\left(\frac{1}{T_m} - \frac{1}{T}\right) \quad ,$$

where T_m is the melting point of the pure semiconductor.

An analysis of germanium and silicon liquidus curves by Thurmond and Kowalchik (1960) showed that in general the activity coefficient of the semiconductor along the liquidus can be described by

$$\ln\gamma_1^1 = \frac{a - bT}{RT}\,(1 - X_1^1)^2 \quad , \qquad (4.2)$$

where a and b are experimentally determined constants. If it is assumed that this relation applies at all temperatures and compositions, the Gibbs-Duhem relationship may be integrated to obtain (Darken and Gurry, 1953)

$$\ln\gamma_2^1 = \frac{a - bT}{RT}\,(1 - X_2^1)^2 \ . \qquad (4.3)$$

Thurmond and Kowalchik found that the predicted activity coefficients of second components at the eutectics of several semiconductor-metal systems agree very well with experimental determinations.

If solubility equilibrations are conducted with a phase for which thermodynamic data is unavailable (many intermediate phases for example), the partial molar quantities of a component of the solution in question must usually be evaluated with respect to this phase and not the pure substance. Information about an intermediate phase can obviously be obtained, however, by equilibrating with both a "known" phase and the intermediate phase.

4.B.2 Thermal Entropy of Binary Metallic Solutions

Zener (1950) has examined terminal solubility data for a number of aluminum-rich alloys and has shown that for these systems $\Delta\overline{S}_2^{ex}$ is always greater than zero, ranging from 2.3k to 4.1k. It was found that in general the greater the heat of solution, the larger is the thermal entropy. The systems studied, however, involve equilibrium between solid solutions and intermetallic compounds and consequently the enthalpies and entropies of solution were evaluated with respect to intermetallic compounds as reference states. Qualitatively, it might appear, therefore, that since intermetallic compounds often involve tight binding, the large positive values of $\Delta\overline{S}^{ex}$ quoted by Zener might be understood in terms of the looser bonding (and hence lower vibrational frequencies) that occur in the solid solutions relative to the intermediate phases.

Freedman and Nowick (1958) surveyed existing solubility data for binary alloy systems which show a two-phase region bounded by two terminal substitutional solid solutions and compared the results with systems for which there is equilibrium between a terminal solution and an intermetallic compound. These authors found a positive $\Delta\overline{S}^{ex}$ value for all but one of the systems examined giving qualitative agreement with Zener's predictions. They did not, however, establish a proportionality between the enthalpies and entropies of solution, indicating that nearest-neighbor considerations must be taken into account when calculating the thermal entropy of solute atoms. Care must also be taken when making correlations between enthalpies and entropies of solution because the enthalpy cannot usually be interpreted as being primarily due to strain energy.

Freedman and Nowick found that the thermal entropies obtained by equilibration with an intermetallic compound were approximately the same as those for the terminal systems. Again attention must be given to near-neighbor interactions because strong attractions lead to negative contributions to $\Delta\bar{S}^{ex}$ and may be enough to compensate for the positive contribution arising from the tight binding of the intermediate compound.

4.B.3 Thermodynamic Properties of Semiconductor-Metal Binary Systems

Over the past fifteen years a great deal of experimental work has been undertaken in this area, and no attempt will be made here to review all the data which has been accumulated. As was mentioned in the previous section, an excellent review paper by Thurmond and Kowalchik (1960) gives an analysis of all the important liquidus alloys of germanium and silicon systems. In another review article Trumbore (1960) collected all the solubility and distribution coefficient data available at that time for a large number of germanium and silicon systems. One of the most interesting features of the phase diagrams of germanium and silicon with most solutes is a retrograde solubility, i.e. if X_2^S is the composition of the solute along the solidus, dX_2^S/dT is positive over a certain temperature range. The requirements for Equation 2.31 to predict such behavior are a low eutectic (or peritectic) temperature relative to the melting point of the pure solvent and a large positive heat of solution.

A number of investigations have been made into the temperature dependence of the distribution coefficient, k^e, between solid solutions of solidus composition and liquid alloys of liquidus composition. Hall (1957) showed that plots of $\ln k^e$ vs $1/T$ for a number of systems, in particular Group 1b elements in germanium and silicon, are linear and exhibit large positive intercepts at $1/T = 0$. It was also observed that the greater the slope of the lines (corresponding to a higher enthalpy of solution), the larger is the value of the intercept. Hall explained these results on the basis of a temperature dependent heat of solution (see Section 2.C.2); however, in a later publication Oriani and Hall (1958) interpreted the large intercepts, after allowing for the $\ln\gamma_2{}^1$ term in Equation 4.1 and heat capacity effects, as arising from an excess thermal entropy of solution. Zener's qualitative prediction concerning the relationship between the heat and the entropy of solution appears to be upheld in the systems Hall investigated; however,the solubility data for some of the solutes are meager and somewhat scattered.

Similar analysis of solubility data for other semiconductor-metal systems have indicated that some distribution coefficients, are, in fact, temperature dependent in a non-linear manner. Trumbore et al (1958) found marked curvatures in $\ln k^e$ vs. $1/T$ plots for tin in germanium and silicon near the melting points of the pure solvents. They attributed this effect to a large deviation from ideality in the liquid solutions with which the solid materials were equilibrated. The number of systems in which this effect has been considered in the determination of solubility parameters is surprisingly limited, however. Trumbore et al (1959) determined the solubilities of aluminum and gallium in germanium and found that the logarithms of the distribution coefficients for these systems are also not linearly dependent on inverse temperature. Since gallium-germanium liquid alloys are nearly ideal, and departures from ideality in liquid germanium-aluminum alloys are of the wrong sign to predict the observed behavior, these authors presented another explanation for a temperature dependent distribution coefficient. Examination of Equation 4.1 shows that the only other variable large enough to account for the observations is the partial molar heat of solution since large deviations from random mixing should not occur at the concentrations under consideration. This means that the solid solutions do not obey Henry's law at concentrations near the solubility limit. As was shown in Section 2.C the activity coefficient of a solute is dependent on the Fermi energy. If the dopant concentration is large enough to affect this parameter, as is the case for aluminum and gallium in germanium, the activity coefficient, and hence the enthalpy of solution, will not be independent of concentration and $\ln K^e$ should be expected to vary with $1/T$ in a non-linear manner. Another factor which contributes to non-Henrian behavior is degeneracy arising from high dopant concentrations. Under this condition the degree of ionization changes along the solidus curve. These effects were not present in the work on Group 1B solutes reported by Hall (1957), however, because the solubility limits at all temperatures are not large enough to render the semiconductors extrinsic.

4.B.4 Solute Atom-Electron Interactions

The first experimental examination of this type of interaction in covalent semiconductors was conducted by Reiss and Fuller (1956) who determined the solubility of lithium (an interstial donor) in p-type silicon. The solubility of lithium was greatly enhanced and the results they obtained agreed very well with the theory outlined in Section 3.B. Reiss et al (1956) observed similar effects for lithium in p-type germanium. McCaldin (1965) demonstrated that the solubility enhancement of arsenic and antimony in p-type germanium could also be explained on the basis of the theory of solute atom-electron interactions.

An extensive study of the solubility of copper in extrinsic silicon and germanium has been conducted by Hall and Racette (1964). They showed that solubility enhancement could occur in both n- and p-type material and they attributed this to the fact that copper may be present in interstitial (singly charged donor) or substitutional (multiply charged acceptor) lattice sites. On the basis of their results they showed that in intrinsic silicon, copper is located predominantly in interstitial sites, whereas in germanium it resides mainly in substitutional sites. The dopant concentrations used to render the semiconductors extrinsic were in general quite high, and corrections had to be made for degeneracy effects and shrinkage of the energy gap due to heavy doping.

Another impurity which has received considerable attention in recent years is gold in silicon. Wilcox and LaChapelle (1964) have shown by diffusion measurements that the ratio of substitutional to interstitial gold is about 10 at 1000°C. Since substitutional gold is an amphoteric dopant its solubility should be increased in both heavily doped n- and p-type silicon. Numerous qualitative investigations have revealed such an enhanced solubility in heavily doped n-type silicon (Wilcox et al, 1964; Sprokel and Fairfield, 1965; Joshi and Dash, 1966). Wilcox et al did not observe similar effects in p-type silicon but they did not state the dopant concentrations used. If the acceptor/donor ratio of gold in intrinsic silicon is substantially greater than unity then a given p-type dopant level may decrease the acceptor concentration and increase the donor concentration in such a way that the overall gold solubility remains relatively unchanged.

4.B.5 Complex Formation

The first observation of complex formation in covalent semiconductors was made by Reiss et al (1956)b in boron and lithium doped silicon. They found that at high temperatures (900 - 1200°C) a boron concentration of 2×10^{18} atoms per cm^3. enhanced the lithium solubility to an extent which could not be explained on the basis of either an electronic or an inter-ionic coulombic interaction and attributed their results to covalent bond formation between boron and substitutional lithium. Reiss and Fuller (reported by Fuller, 1959) also investigated complex formation between lithium and gallium in germanium and discovered that experimentally determined lithium solubilities could only be explained by a combination of the electronic and the complex formation theories. In the same publication Reiss and Fuller reported lithium solubilities in zinc doped (doubly charged acceptor) germanium and found the extent of complex formation was substantially greater than in gallium doped material.

To the author's knowledge the above-mentioned investigations have been the only quantitative solubility studies of complex formation in germanium and silicon. Hall and Racette (1964) found evidence for ion pairing between copper and arsenic in germanium because the solubility enhancement in this system was greater than could be explained by an electronic interaction, but no quantitative estimate of complex formation was conducted. Joshi and Dash (1966) also found that complexes involving gold may form in silicon doped to a high level with phosphorus ($\approx 2\times10^{20}$ atoms per cm.^{3}).

4.C Equilibrium Grain Boundary Segregation

An extensive review of this subject is given by Westbrook (1964) in which he discusses both the theoretical and experimental aspects of this phenomenon. The present discussion will be limited to the various experimental techniques that have been used to study grain boundary segregation. It should also be stressed that a great deal of care must be taken to ensure that room temperature observations are representative of equilibrium conditions at the temperature in question. Quenching rates, for example, must be great enough to prevent grain boundary precipitation effects.

Means of investigating foreign atom segregation at grain boundaries may be divided into direct and indirect methods. Direct methods allow identification of the segregating element and often provide a quantitative measure of the amount and distribution of such species. Examples of this method are chemical and autoradiographic techniques. Arkharov et al (1956) etched the fracture samples of a nickel-chromium steel which was broken intergranularly. Chemical analysis of an etchant solution indicated a concentration of phosphorus in a 0.3 micron thick layer from 70 to 75 pct. higher than that of the bulk sample. Ainslie et al (1960)[a] have demonstrated sulfur segregation in grain boundaries of high purity iron by autoradiography and solubility measurements. A calculation based on reasonable parameters for grain boundary widths and matrix absorption coefficients has shown that for tracer segregation to be demonstratable, the ratio of grain boundary concentration to grain interior concentration must exceed 10^3 (McLean, 1957).[b]

Indirect methods are limited to a qualitative assessment of the existence of segregation and any calibration ultimately rests upon the development of a direct technique for the same system. A number of these methods are metallography, X-ray techniques, surface energy measurements, electrical properties, microhardness, and ultrasonic absorption. Reference is made to Westbrook's paper for the details of these methods. Interesting results are often obtained from micro-hardness profiles of grain boundaries. Westbrook and Wood (1961), for example, found increases in hardness up to 30 microns away from grain boundaries in sulfur-segregated iron. It is difficult to correlate these results with the commonly accepted view that grain boundary regions are only two or three atom diameters across; however, electron micrographs reveal extensive networks of dislocations adjacent to the grain boundaries (Ainslie et al, 1960)[b] probably caused by lateral sulphur diffusion. The abnormal sulfur segregation obtained from their autoradiography and solubility study (1960)[a] - enough to coat the boundaries with 100 - 150 atom thicknesses of sulfur - is then explained by assuming that sulfur is adsorbed by dislocations in the boundary networks.

4.D Kinetic Studies

4.D.1 Nucleation and Precipitation on Dislocations

The first experimental work in this field was conducted by Davenport and Bain (1935) who studied strain ageing by measuring the increase in hardness of a low-carbon steel with time at various temperatures. By assuming a direct proportionality between hardness change and the fraction of carbon atoms precipitated, Cottrell and Bilby (1949) showed that Davenport and Bain's results fit their theoretical prediction (Equation 3.27) quite well. Harper (1951) investigated the precipitation of carbon and nitrogen in cold-worked iron by internal friction techniques and found that the kinetics are described accurately by his theoretical relation (Equation 3.28) which was derived as an extension of the Cottrell and Bilby theory of strain ageing. He also showed that the activation energy for the precipitation reaction of each solute corresponds to their diffusion activation energies. Thomas and Leak (1955) also found that the kinetics of carbon precipitation on dislocations follow the Harper equation.

Bullough and Newman (1962) explained this fortuitous behavior on the basis of a transient rate limitation (see Section 3.E). Direct evidence for a rate limitation of some kind does exist because the time required for complete ageing obtained by Thomas and Leak was about fifty times the mean diffusion time for the dislocation densities employed. Bullough and Newman ascribed the transient rate limitation to a local increase in pressure as the number of carbon atoms in the core region increases, which then leads to the presence of a local transient hydrostatic compression at the core-matrix interface. They proposed that the interface transfer velocity, K_c, could be given by

$$K_c = K_c{}^{\circ} \exp \left[- \frac{\gamma\, y(t)}{kT} \right] \tag{4.4}$$

where γ is a constant, $K_c{}^{\circ}$ is the value appropriate to an unstrained interface, and $y(t)$ is the fraction of solute precipitated at a given time. Recent work by Carpenter and Baker (1965) and Hartley (1966) on the strain ageing of tungsten-carbon and tantalum-oxygen alloys, respectively, also indicates that the validity of Harper's equation as an empirical representation of experimental data appears to extend beyond its theoretical limitations.

Doremus (1960) found that the time exponent, n, in the rate equation for carbon precipitation in iron decreases with the degree of cold work. He attributed this behavior to the presence of subgrain boundaries formed by cold work which tend to become surface sinks for which n is 1/2. The overall value of n is then determined by the distribution of carbide particles in boundaries and on isolated dislocations and their spacing along the dislocations.

Copper precipitates on dislocations in silicon have been directly observed by Dash (1956) who established conclusively by infra-red microscopy the correlation between surface etch pits and emergent dislocations. Dash found that fast quench rates produced homogenous dislocation decoration whereas screw dislocations were not always decorated when cooling was carried out within a few minutes.

Schwuttke (1961) has studied the location and shape of copper precipitates in silicon as a function of oxygen content. All the precipitates in vacuum float-zone-refined crystals formed on dislocations as a single set of parallel needles lying along a <110> direction. Oxygen doped crystals, however, contained some starlike random precipitates, often coincident with growth striations, and the precipitates on the dislocations also often had a complex dendritic or star form. It was assumed that these stars are nucleated at impurity clusters, probably SiO_2, which formed on the dislocations at some period of the crystal's history. This hypothesis was confirmed by the fact that fresh dislocations introduced by plastic deformation were decorated by needles only.

In an electron microscope investigation of copper precipitation in silicon Rieger (1964) found that precipitates which appear to be compact and continuous in a light microscope actually consist of irregularly arranged spherical particles which occupy sharply bounded regions. The size and concentration of these particles are independent of the original copper concentration, but the volume which they occupy was found to increase with increasing supersaturation. Rieger also observed that regions of precipitation contain a large number of spiral dislocations and proposed a growth mechanism based on climb of the original dislocation. According to Weertman (1957) the equilibrium form of a dislocation acted on by an ordinary stress and a chemical stress produced by a deviation of the vacancy concentration from the equilibrium is a helix. During the formation of helical dislocations on quenching, jogs which have formed from the precipitation of vacancies will in turn generate more vacancies by non-conservative motion. These regions of high vacancy concentration then act as nucleation centers for copper precipitates. In addition, Rieger assumed that the strain induced by the precipitates is a supplementary source of vacancies, and in this sense the proposed mechanism is auto-catalytic.

Fiermans and Vennik (1965) examined the growth mechanism of isolated copper precipitates in silicon with the intention of correlating it with the decoration mechanism active on dislocations. They proposed that precipitates containing oxygen act as indentation centers during the quenching operation resulting in the formation of small dislocation loops. X-ray diffraction micrographs and etch pitting experiments indicated that the presence of copper causes these indentation patterns to grow and form large strained regions. The fact that precipitation of interstitial copper requires an appreciable amount of vacancies indicates that climb of the freshly formed loops is the predominant factor in the growth mechanism of the precipitates, i.e. by climbing the fresh dislocations produce the required number of vacancies and leave copper specks on their trails. These authors also believe that grown-in dislocations are sufficiently pinned to prohibit the amount of climb required to form precipitates of the dimensions normally encountered.

It is obvious that a great deal of confusion exists about the mechanism of copper precipitation in silicon since many visual observations contradict each other and the chemical composition and physical structure of the precipitates are not even known.

Electrically active donors due to copper have been observed in silicon by Hall and Racette (1964). The room temperature precipitation kinetics were not analyzed quantitatively, but these authors did conclude that the rate constant increases with increasing supersaturation. This is not consistent with the current theories of precipitation on dislocations. The above conclusion is based on the assumption that no pre-precipitation occurs upon cooling from high supersaturation temperatures, however, because such an effect could make the observed reaction rate appear faster than the actual rate. It is difficult to extrapolate an initial concentration at time zero from the data of Hall and Racette (presented as the ratio of hole concentration in p-type silicon after and before copper diffusion vs. ln (time) plots); however, Figure 4.1 shows the author's interpretation of these data on $\ln (N_o/N(t))$ vs. $t^{2/3}$ and t^1 curves. An initial concentration (N_o) was chosen for each supersaturation temperature such that the curves pass through the origin of the graph. Only three sets of data are presented for which it was believed the diffusion time was long enough for complete saturation. The scatter in these plots is quite pronounced but they do tend to indicate that the time exponent is less then unity and that the rate constant is independent of N_o.

A number of kinetic investigations have indicated that copper and nickel precipitate at dislocations in germanium. A review of these studies is given by Van Bueren (1960). Both these elements diffuse in germanium by a dissociative mechanism (Frank and Turnbull, 1956) whereby rapidly diffusing interstitials combine with vacancies and are converted to substitutional sites. Tweet (1957) found that kinetics for copper precipitation in germanium samples containing a high dislocation density have the form of Equation 3.28. At low temperatures the observed rate constant was independent of dislocation density and he attributed the rate limiting process to be the dissociation of substitutional copper to interstitials and vacancies. As a consequence of the dissociative diffusion mechanism, Penning (1958)[b] showed that at high temperatures the rate of removal of copper and nickel in germanium is equal to the rate of annihilation of vacancies at the dislocations.

4.D.2 Diffusion in the Presence of Complex Formation

No controlled experiments on the diffusion behavior of a solute in the presence of a concentration gradient of a third interacting solute (see Appendix A) have been conducted in covalent semiconductors. This is undoubtedly because of the complex theoretical and experimental nature of the problem. A few investigations have been conducted for the special case where the concentration gradient of the third component is uniform, however.

Reiss et al (1956)[a] qualitatively investigated the diffusion of lithium in germanium doped with p-type impurities. A gallium concentration of 2.8×10^{17} atoms per cm.^3 and an indium concentration of 6.4×10^{17} atoms per cm.^3 reduced the diffusion coefficient by factors of approximately 10 and 20, respectively at 25°C. Zinc (a doubly charged acceptor) doped to a level of 2.7×10^{16} atoms per cm.^3 reduced lithium's diffusion coefficient by a factor of about 300 at

100°C. Potemkin and Potapov (1960) studied the electrical mobility of copper in antimony doped germanium. Their investigation indicated that an antimony concentration of 3×10^{17} atoms per cm.^3 decreases the diffusion coefficient as determined from the Einstein relation by a factor of 2 in the temperature range 550 - 600°C.

4.E Summary

The literature pertaining to thermodynamic properties of solute atoms in covalent semiconductors is extensive but many investigators have not been duly concerned with the establishment of true equilibrium conditions when conducting solubility measurements. Effects of non-ideality of equilibration phases have also been largely neglected in the determination of solubility parameters. The solubility data for many systems is insufficiently accurate to derive therefrom meaningful solubility parameters. The concentrations involved are usually very low and a small error in the slope of a $\ln k^e$ vs. $1/T$ plot results in a relatively large error in the determination of the excess entropy term.

Very few quantitative solubility investigations have been conducted to study complex formation. In most cases the dopant concentrations required to make this effect significant also render the semiconductor extrinsic, and thus quantitative calculations are difficult because of interfering electronic interactions. One possible means of avoiding this problem may be to study complexing of multiply charged dopants.

A great deal of work has been reported on solute atom-grain boundary interactions. Most of the studies have involved indirect experimental methods, however, and little direct evidence exists for enhanced grain boundary solubility. It has been suggested that strong chemical bonding may occur between solute atoms and grain boundaries in homopolar crystals so it may be expected that such an effect could result in measurable solubility differences between single crystal and polycrystalline material.

The precipitation kinetics of interstitial solutes at dislocations appear to follow a $t^{2/3}$ rate law which cannot be explained on the basis of a diffusion controlled reaction. An analysis of existing data has indicated that the time exponent in the equation describing the precipitation of copper in silicon may also be less than unity. Further work is necessary, however, to support this finding.

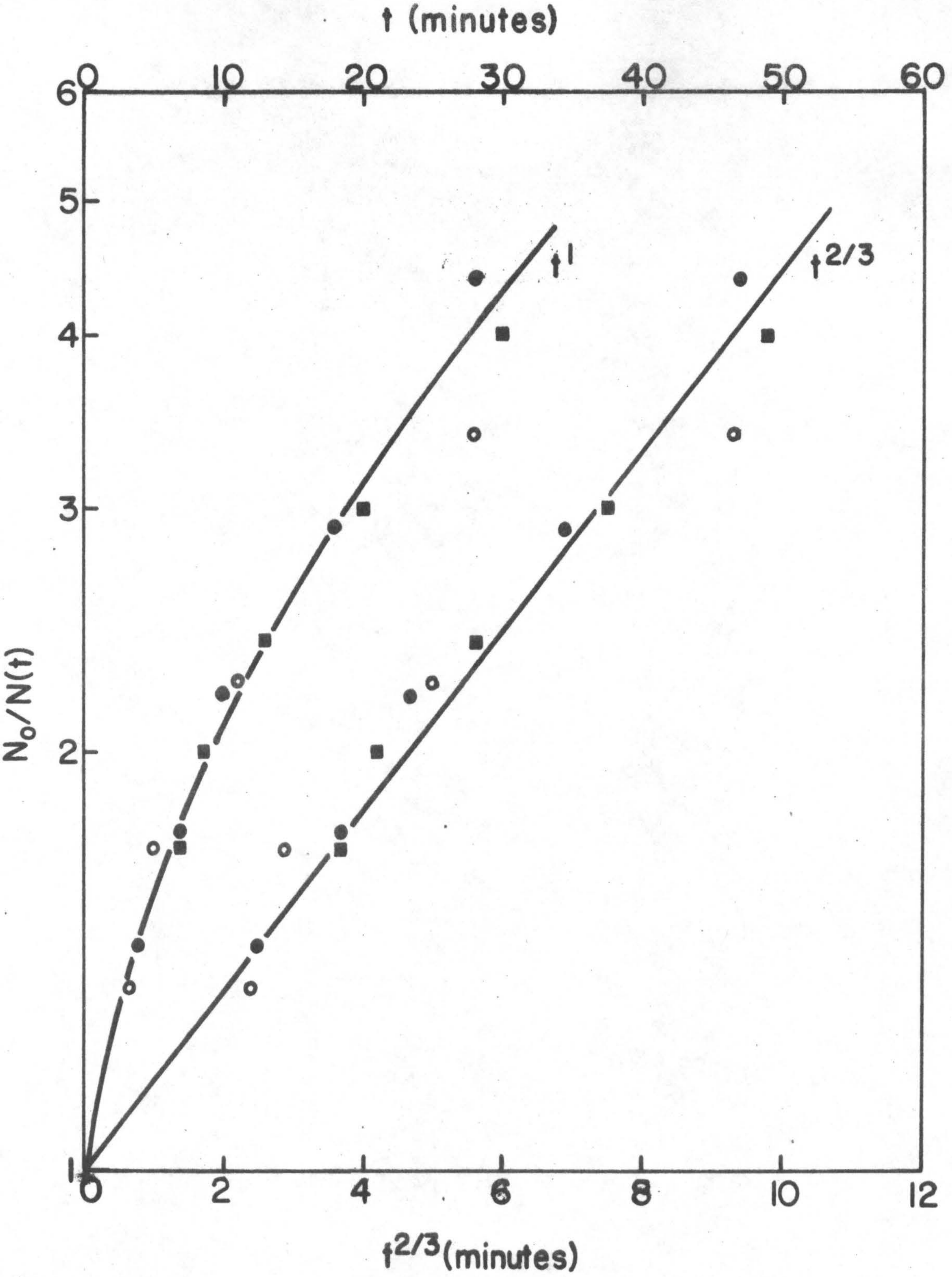

Figure 4.1. Plots of $\ln(N_o/N(t))$ vs. t^1 and $t^{2/3}$ for precipitation of copper in silicon at room temperature. The data is taken from work by Hall and Racette (1964). The symbols represent the following saturation treatments: open circles - 450°C for 3.5 hr.; solid circles - 472°C for 4 hr.; squares - 575°C for 2 hr. The initial copper concentration at zero time was taken as 6.75×10^{12}, 8.75×10^{12}, and 1.2×10^{13} atoms/cm.^{3} respectively.

CHAPTER 5

EXPERIMENTAL

5.A Introduction.

5.A.1 General Objectives

The general objective was to investigate by equilibrium measurements the interaction characteristics of solute atoms with defects in covalent semiconductors in order to gain a better understanding of the fundamental properties of solute atoms and defect interactions in these materials. It was also hoped that the results obtained by equilibrium measurements could be extended to diffusion problems associated with the semiconductor device industry. Kinetic phenomena are usually more difficult to investigate experimentally than are equilibrium properties, but in many cases thermodynamic information may be used to predict certain kinetic characteristics of a system (see Appendix A).

As was shown in the previous chapters many thermodynamic properties of solutions may be determined through solubility measurements. It was our desire, then, to study by this method as many of the previously discussed interactions as possible. To the author's knowledge no controlled measurements of the solubility of a solute in both a single crystal and a polycrystalline solvent over a range of temperature have previously been conducted in either metals or semiconductors. With the choice of a suitable dopant the kinetics of precipitation on dislocations could be easily studied at the same time by electrical resistance measurements. A great deal of work has been done on impurity precipitation in germanium and silicon (Reiss and Fuller, 1959) and these materials appear to be excellent media for such studies.

Of interest too are the equilibrium phase relationships for simple binary systems. Most of the previous solubility determinations in germanium and silicon have involved equilibria between solid and liquid phases, i.e. the solubilities were measured at temperatures greater than the eutectic temperatures of the systems involved. A few investigators have measured solubilities below the eutectic temperature (Hall & Racette, 1964 - Cu in Ge and Si; Struthers, 1956 - Cu in Si; Wertheim, 1959 - Ni in Ge), but no evidence was given that equilibrium was obtained with the correct phase. In all cases a slice of the semiconductor material was plated with a quantity of the elemental second component and subsequently annealed at the desired temperature. If the phase diagram of the two elements shows an intermediate phase(s) at a given temperature, then this phase(s) must nucleate and grow in the diffusion zone between the two materials in order that a true equilibrium solubility be obtained (see Figure 2.7) It proved feasible to investigate non-equilibrium "solubilities" by a comparison with equilibrium solubility measurements and by interface metallography studies.

5.A.2 Choice of Systems

The choice of systems for a quantitative investigation depends on many factors, the two most important being: 1) ease of accurate chemical analysis and 2) a sufficiently high diffusion coefficient so that the equilibration times required for samples of a reasonable size are experimentally practical. It is also desirable that the solubility limit at all temperatures of interest be low enough that Henry's law is obeyed. This constitutes a serious limitation in semiconductor systems because, as is shown in Chapter 2, the dopant concentration must not be great enough to render the semiconductor extrinsic. As a practical example, the impurity concentration in silicon at 600°C should not exceed one part per million. The sensitivity of the method of chemical analysis is therefore exceedingly important. Electrical resistance measurements and radio-chemical techniques have been used extensively for determining impurity concentrations in silicon and germanium, the latter proving to be the more accurate method.

Due to the availability of the McMaster Reactor facilities, it was decided to utilize either neutron activation analysis (NAA) or a radio-tracer technique. This naturally restricts the number of systems that may be studied since those chosen must have suitable radiochemical characteristics, the most important of which are suitable isotope lifetimes of the unknown elements. In radio-tracer applications this is especially important because a long time often elapses between irradiation and counting steps. For the greatest accuracy in determining minute quantities of an unknown in a given matrix by NAA, it is usually advisable that the matrix be non-interfering, i.e. it should not contribute any background to the counting procedure. It is therefore convenient to analyze for γ-ray emitting isotopes in silicon by NAA since Si emits only β-rays which can be screened in a γ-ray counting apparatus. Neutron irradiated germanium, however, is a strong γ-ray emitter of fairly long half-life and is also difficult to chemically separate from most other elements of interest. A tracer technique would therefore appear to be the more favorable method.

The study of equilibrium phase relationships and the determination of solubility parameters for a given system also requires that its phase diagram be known. In order to investigate the interesting possibility of obtaining meta-stable solubilities in certain instances, a system must be chosen which has a measurable solubility below the eutectic temperature and also exhibits one or more intermediate phases. It would be advantageous if this intermediate phase were readily available or at least easily manufacturable so that it could be used for equilibration purposes. One of the simplest methods of preparing an intermediate phase, providing it has a congruent melting point, is to solidify it from a melt of suitable composition.

A study of precipitation on dislocations naturally requires a system in which a second phase containing impurity atoms nucleates and grows at dislocations under conditions of supersaturation. The solute atoms also must be mobile at temperatures where experimental measurements are possible.

The silicon-copper system appears to satisfy all of the criteria discussed above. Copper in silicon (an interstitial donor) is easily analyzed by NAA and it has a very high diffusion coefficient and a low, but detectable solubility limit. It has also been observed to precipitate out of solution on dislocations (Dash, 1956). The phase diagram of the system is well established (Hansen, 1958; Elliot, 1965) and it shows a congruently melting intermediate compound, Cu_3Si, in equilibrium with silicon rich solid solution below a eutectic temperature of 802°C. It should also be possible, therefore,to compare thermal entropies evaluated with reference to both a pure metal (Cu) and an intermediate compound (Cu_3Si) in this system.

Copper in germanium is attractive because it also is a fast diffuser, has a low solubility, and can be readily analyzed by radiotracer techniques. Since it can exist in three different charge states, strong coulombic interactions with donor ions are quite likely. Complex formation in extrinsic arsenic doped germanium has been observed (Hall and Racette, 1964) but has not been studied quantitatively. It would therefore be desirable to investigate this effect in material doped lightly enough that electronic interactions are absent.

Gold in silicon also has a number of attributes which render it a favorable dopant for solubility studies - it is easily analyzed by NAA and has a fairly high mobility and a low solubility limit. In addition, it is amphoteric, i.e. it may behave as a donor or an acceptor. This should have important consequences regarding the dependence of the solubility limit on the Fermi energy (Bullis, 1966). Since present qualitative data indicate that the acceptor/donor ratio in intrinsic material is greater than unity (see Section 4.B.4), solubility measurements in lightly doped p-type material may further elucidate this hypothesis. Gold in germanium, however, has a low diffusion coefficient (Dunlap, 1955) and is therefore not very amenable to solubility measurements at temperatures far removed from the melting point of the solvent. The solubility of gold in germanium has only been determined near the melting point by solidification methods (Tyler, 1959; Syed, 1964).

Copper and gold in elemental semiconductors are also important from a technical standpoint. They are not normally used to provide silicon and germanium with their useful primary electrical characteristics as are the Group III and V elements, but they may have both beneficial and detrimental secondary effects. Since gold and copper in silicon, and copper in germanium are rapid diffusers, they are often easily introduced as contaminants during heat treatment and diffusion doping operations. If they interact with certain defects, they may also segregate in localized regions of device structures. Experiments have indicated that copper, by acting as a recombination center, reduces the lifetime of both silicon (Collins and Carlson, 1957) and germanium (Burton et al, 1953)a. Gold is an important impurity in silicon because of its effectiveness in the control of lifetime and resistivity in both n- and p-type material. Since copper and gold in silicon and germanium often exist in multivalent states, they are also effective scattering centers and may therefore reduce electron and hole mobilities. It has even been suggested (Hall and Racette, 1964) that copper precipitates in silicon introduce the energy levels normally assigned to this impurity.

5.A.3 Specific Experimental Proposals.

The experimental program adopted to gain a further understanding of solute atoms and their interactions in homopolar crystals was as follows: i) A redetermination of the equilibrium solubility of copper and gold in pure single crystal silicon and germanium so that the partial molar enthalpies and entropies of solution could be determined accurately. It will be seen that a good deal of scatter exists in most of the data gathered from the literature. It was also necessary that the solubility be known accurately in pure material in order that a comparison could be made with defect-containing material. ii) A determination of the solubility of gold and copper in boron doped (extrinsic) silicon to investigate interactions of solute atoms with electrons and other solute atoms. iii) A study of the effect of boron diffusion doping on the redistribution of copper in a uniformly copper doped silicon wafer. This experiment was conducted to investigate the effect of electronic interactions on the segregation of mobile impurities during device heat-treatment operations. iv) A determination of copper and gold solubilities in arsenic doped (intrinsic) germanium to study solute atom-solute atom interactions in the absence of electronic effects. v) Measurements of the solubility of copper in pure polycrystalline silicon. vi) A kinetic study of copper precipitation in silicon near room temperature.

It was also decided to conduct solubility measurements of copper in silicon below the eutectic temperature of this system by the plate-and-anneal method and compare the results with those obtained by equilibration with Cu_3Si. Metallography and X-ray studies were also used to detect the presence of Cu_3Si in the interface region.

The phase diagrams of the various systems as given by Hansen (1958) are shown in Figures 5.1 to 5.4.

5.B. Apparatus and Materials

5.B.1 Furnace Assembly.

The samples were diffusion saturated in the horizontal electrical resistance furnace shown schematically in Figure 5.5. Power was supplied through a 1300 watt variable transformer to a Kanthal heating element. The temperature was maintained to ± 1°C by a Pt-13 pct. Rh themocouple placed near the heating element and a Honeywell "Pyr-O-Vane" controller which activated the high-low power circuit. The 1.25 inch inside diameter furnace working tube was constructed of re-crystallized quartz and was suitably connected to provide an atmosphere of argon. The argon was purified by passing it through another furnace containing titanium chips at 1000°C. The samples were contained in either a pyrophyllite boat or evacuated and argon back-filled quartz capsules. A quartz tube for manipulating the boat was fitted through one end plug and was also used to house a Pt-10 pct. Rh measuring thermocouple.

5.B.2 Gamma-ray Spectrometer.

The apparatus used to measure the gamma activity from samples was a single channel spectrometer purchased from Phillips Industries Limited. A flow drawing of the assembly is shown in Figure 5.6. The components are:

a) PW 4111/03, a scintillation probe consisting of a 37.5 millimeter diameter well-type scintillation crystal (thallium activated NaI) for detecting the radiation, a photomultiplier tube and a cathode follower. The scintillation probe projected through a hole in the bottom of a 2 inch-wall lead counting castle. Figure 5.7 is a sectional diagram of the crystal-source configuration used to measure the radioactivities of liquid solutions.

b) PW 4025/10, a high voltage unit stable to ± 0.03 pct. supplying the voltage required by the radiation detector.

c) PW-4071, a pre-amplifier designed as a link between the radiation detector PW 4111/03 and the main amplifier/analyzer PW 4280. It ensures the lowest possible susceptibility to interference of the measuring arrangement.

d) PW 4280, a linear amplifier/pulse-amplitude analyser used to analyse the composite pulse signal from the scintillation detector. The discriminator may be used to "tune-in" on a specific energy level thus reducing the effects of background radiation.

e) PW 4242, a linear count ratemeter used to measure the average rate of randomly occurring pulses. The count-rate is directly indicated on a visual panel meter and a loud speaker.

f) PW 4231, a 7-decade electronic display scaler.

g) PW 4260, an electronic timer to be operated in conjunction with the scaler.

h) PW 4211, a supply of stabilized 12 volt d.c. power for components (d) to (g).

5.B.3 Cu_3Si Preparation Apparatus

The intermediate compound was prepared in the apparatus depicted in Figure 5.8. The raw materials were heated inductively in a recrystallized alumina crucible around which was placed a 1/8 inch thick suscepting graphite sleeve. The crucible assembly was supported within a quartz tube which was suitably connected for an inert atmosphere of argon.

5.B.4 Electrical Resistance Measurement Assembly

Samples for resistance measurements were clamped in the holder shown schematically in Figure 5.9b. The holder was placed in a rubber envelope which was immersed in a constant temperature water bath (Figure 5.9a). The temperature of the bath was maintained to ± 0.1°C by a Haake off-on control heater and was measured with a Hg thermometer. Resistance changes were determined by imposing a known d.c. voltage across the sample and measuring the current with a Conway ammeter.

5.B.5 Silicon and Germanium Material.

The germanium single crystals were purchased from Semimetals, Inc. High purity polycrystalline silicon grown from the vapor by Dow Corning was supplied through the offices of Dr. T. S. Plaskett of the I.B.M. Corporation. Czochralski grown single crystals of pure and phosphorus doped silicon were also obtained from Semimetals, Inc. Pure and boron doped crystals of float zoned silicon were purchased from Texas Instruments, Inc. A summary of the resistances and growth methods of the single crystals obtained is given below.

Material and Dopant	Resistivity (ohm-cm.)⁻	Growth Method	Dopant Concentation (atoms/cm.^{3})
Si (pure)	500 (n-type)	Czochralski	1×10^{13}
Si (pure)	2000	Float Zoned	-
Si (boron)	0.02	Float Zoned	5×10^{18}
Si (phosphorus)	0.03	Czochralski	7×10^{17}
Ge (pure)	10.0 (n-type)	Crucible	2×10^{14}
Ge (arsenic)	0.012	Crucible	5×10^{17}

Resistances and dopant concentrations of silicon were correlated with the condensed data of Irvin (1962). The arsenic content of the doped germanium crystal was obtained from work by Fritzsche (1958).

The Cu_3Si compound was prepared from polycrystalline silicon and 99.999 pct. pure copper supplied by A.D. MacKay, Inc. The matrix material for the NAA standards was 99.9999 pct. pure aluminum which was provided by the Department of Metallurgy and Materials Science of the University of Toronto.

5.C Methods and Procedures

5.C.1 Equilibration for Solubility Determinations

The samples for the solubility measurements were slices of semiconductor material weighing approximately one gram. They were cut about one millimeter thick from purchased ingots with a diamond saw. After slicing, the wafers were lapped on 600 mesh silicon carbide paper and cleaned and degreased with high purity "Transist AR" grade acetone supplied by the Mallinckrodt Chemical Works.

For determinations above the eutectic temperatures of the systems concerned, the semiconductor slices were displacement plated with a copper (or gold) film about two microns thick. The plating solutions were copper sulfate (for silicon), copper nitrate (for germanium) and gold chloride (for silicon and germanium). Standard commercial electroplating baths (Safranek and Winkler, 1953; Weisberg and Graham, 1953) were used for plating the silicon samples, but those for germanium were prepared from neutron-irradiated copper and gold, and were not of a fixed composition. All the solutions also contained a small amount of hydrofluoric acid to reduce the oxide layers on the samples, thereby insuring an adherent film.

After plating, the silicon samples were placed in a pyrophyllite boat in a cool region of the annealing furnace. The furnace system was purged with purified argon for about one hour and the boat was then pushed into the hot zone with the quartz manipulating tube. When the samples were saturated, they were cooled quickly in air by quenching on a copper block. Since the germanium samples were plated with radioactive isotopes, they were sealed off in evacuated and argon back-filled quartz capsules and then placed in the furnace and diffused. When the anneal was over, the capsules were quenched in water.

The annealing times for all samples were determined from an equation for diffusion from a constant source into a slab of thickness, l, (Boltaks, 1963)[b]. The diffusing species is assumed to enter the body through both boundaries ($x = 0$ and $x = l$) at which the concentration is held constant at the value $N°$, the solubility of the diffusand in the body. At long times, the concentration profile, $N(x,t)$, is described by the equation

$$N(x,t) = N° \left[1 - \frac{4}{\pi} \exp -\left(\frac{\pi^2 Dt}{l^2}\right) \sin\left(\frac{\pi}{l}\,x\right) \right],$$

where D is the diffusion coefficient of the diffusand. In order for $N(l/2,\, t)$ to have a value of $0.99\,N°$, the time required is given by

$$t \simeq \frac{l^2}{2D}\,. \tag{5.1}$$

The diffusion coefficients for the various systems were taken from the experimental data of Boltaks (1963)[a] - Cu and Au in Si; Fuller et al (1954) - Cu in Ge; and Dunlap, (1955) - Au in Ge. Annealing times were calculated on the basis of achieving 99pct. saturation. Since copper in silicon has a very high diffusion coefficient, most of the samples in this system were annealed for much longer times than were required. The gold-germanium samples, however, had to be annealed for two weeks, even though they were only 0.5 millimeters thick. For this reason, only one temperature was considered for this system (850°C). A number of the gold-silicon samples were also less than one millimeter thick and had to be diffused for periods of up to two weeks.

The solubility of copper in pure single crystal silicon below 802°C was determined by two different equilibration methods. The first was by the technique described above, except that a series of runs for various annealing times at a given temperature was conducted. This was carried out to determine whether the "solubility" was time dependent because of possible retardation in the nucleation and growth of Cu_3Si in the diffusion zone. Care was taken to ensure that all the samples were of the same initial thickness and that they were chemically dissolved to the same thickness before chemical analysis. In the other method, the silicon was equilibrated with powdered Cu_3Si. The silicon slices and the Cu_3Si powder were sealed in evacuated quartz capsules which were then placed in the furnace. Equilibration by this method occurred via the copper vapor phase, and in this way the true equilibrium solubility could be compared with that obtained by the "plate and anneal" method. Since a rate limitation is possible for equilibration with a vapor phase, two samples were equilibrated for different periods of time at 700°C.

The solubility of copper in polycrystalline and boron doped silicon below the eutectic temperature was also determined by the latter method. All the solubility determinations in the other systems were made above the eutectic temperature so they were conducted by the first method.

5.C.2. Chemical Analysis of the Solubility Samples

For reasons discussed earlier, copper and gold concentrations in the silicon samples were determined by neutron activation analysis and the germanium samples were analysed by a radio-tracer technique. The basic difference between these two methods is that NAA involves the irradiation of the whole sample (matrix plus unknown) after an experimental test, whereas in radio-tracer analysis, the unknown is irradiated prior to the experimental test. In both cases, the final step is to correlate the measurable radio-activity with the amount of unknown present.

Most materials, when placed in a nuclear reactor, become radioactive through the absorption of thermal neutrons. The activity, or the number of disintegrations of an isotope per unit time after removal from the reactor, is proportional to the amount of the element present and to the neutron flux. By using samples of known composition to determine the activity to be expected from a given amount of an isotope throughout an irradiated assembly, the composition of unknown samples in the assembly can be calculated by a direct comparison of the measured activities of each.

(a) Neutron Activation Analysis of Copper and Gold in Silicon

After the samples were removed from the furnace, the external phase was chemically removed with a mixture of nitric and hydrofluoric acid. To ensure the attainment of a true bulk solubility and to eliminate possible out-diffusion effects from cooling, about half the sample was also dissolved. The samples were then cleaned by a light etch with a mixture of high purity "TransistAR" grade HF and HNO_3 (10 parts HNO_3 to

1 part HF). After rinsing the samples with demineralized water and drying them with high purity acetone, they were weighed on a Mettler type "M" electrical balance and sealed in 7 millimeter diameter quartz vials. Four unknowns and four standards were packaged in aluminum foil and placed in a standard 3/4 inch inside diameter cold-weldable aluminum irradiation can. The assembly was then turned over to the McMaster Reactor Operational Control Committee and it was irradiated in a flux of about 10^{13} neutrons/cm^2-sec for a time long enough to give a measurable activity (usually about twelve hours for copper and one hour for gold). After an irradiation, the canned assembly was kept in storage for about ten hours so that the packaging materials and the silicon matrix could "cool" down.

The standards used were aluminum - 1 weight pct. copper and aluminum - 0.5 weight pct. gold alloys. These elements were diluted with aluminum, a non-interfering matrix, so that sufficient quantities of materials could be weighed accurately and still not produce an undue amount of radio-activity. The alloys were prepared by levitation melting in an argon atmosphere followed by "splat-cooling" between two copper plates. The apparatus for this operation was designed and constructed by Mr. D. W. Gomersall of McMaster University and is described by Carryl and Ward (1967). Standards prepared in this manner are homogeneous because of the rapid quench rate and are also in a convenient thin foil form. Samples weighing between five and ten milligrams were cut from the foil, weighed, and sealed in two millimeter diameter quartz vials to be irradiated along with the unknowns.

After an irradiation assembly was removed from the storage bay, it was transported to a hot lab in the Nuclear Sciences Building where it was opened behind lead bricks. The quartz vials containing the unknowns were broken and the samples were placed in teflon beakers containing about ten milliliters of HF. The beakers were placed in a fume hood, and HNO_3 containing copper carrier was added drop by drop until the silicon samples were dissolved. The solutions were heated until they evaporated to dryness and the beakers and the standards were then moved to another fume hood in the Engineering Building. After dissolving the copper residues in five milliliters of 1 N HCl, the solutions were stored in stoppered test tubes. The copper standards were dissolved in a few milliliters of aqua regia and the solutions were evaporated to dryness. The residues were dissolved in 1 N HCl and transferred to a volumetric flask. A volume was chosen which would give the standard solutions an activity per unit volume approximately equal to those expected in the unknown solutions. After the residues of the gold unknowns were dissolved in ten millilitres of aqua-regia, the solutions were transferred to 25 milliliter volumetric flasks. The gold standards were also dissolved in aqua-regia, evaporated, redissolved, and placed in volumetric flasks.

For counting purposes, three milliliters of sample solution were pipetted into a wide mouth counting vessel which was then placed in the well crystal of the scintillation detector. The same vessel was used for counting all the samples, so after each measurement it was dipped in aqua-regia, washed with soap and water, and dried. All of the counting was carried out using a photomultiplier voltage of approximately 1200 volts and an attenuation setting of either 64 or 128 on the linear amplifier. Slight adjustments were made to obtain a flat countrate - voltage characteristic and a welldefined photopeak. Before each set of analyses the pulse height analyser was set to a narrow window width and the complete spectrum was scanned by varying the amplitude setting. A typical scan of the copper-64 spectrum is shown in Figure 5.10. In this way, the characteristic photopeak position could be accurately positioned. The window was then positioned over the photopeak for sample counting. Copper and gold activities were measured by counting the 0.51 MeV and the 0.412 MeV photopeaks, respectively. Counting times were preset on the electronic timer which would allow a total count of at least 10^4 disintegrations. If the count rate was less than five disintegrations per second,however, the maximum time allowed for a reading was 2×10^3 seconds. The counting sequence was clockwise (or anticlockwise) around the sample configuration shown in Figure 5.11. The concentration of U1 (unknown number one) say, was then determined by a comparison with S4 and S1, i.e.

$$N_{U1} = \frac{C_{U1}}{C_{S1} + C_{S2}} \cdot \frac{(W_{S1} + W_{S4})f}{W_{U1}} \cdot \frac{V_{U1}}{V_{S1,S4}} \cdot \frac{A}{M} \cdot \rho \qquad (5.2)$$

where N_{U1} is the impurity concentration (atoms per cm^3) of the unknown, the C's are corrected counting rates, the W's are the weights of the samples, the V's are the volumes of the solutions, A is Avogadro's number, M is the gram molecular weight of the unknown element, ρ is the density of the semiconductor, and f is the weight pct. of unknown in the standard alloys.

The corrected count rates were calculated by subtracting from the total count rate of a sample the background countrate which arises mainly from cosmic and matrix radiation. The cosmic radiation contribution was determined by two counts with an empty counting vessel - one before the sample counting sequence and the other afterwards. It was assumed that the decay curve was linear over the counting time for two standards and an unknown, and no activity correction *per se* was made for decay. Background from the matrix materials (Si,Al) was determined by conducting blank runs with solute-free semiconductor material and pure aluminum. The amount of activity from a one milligram aluminum sample was found to be negligible and unknown matrix background effects were significant only for very low solute concentrations. In addition, the half-lives of the standards were determined by measuring their activities as a function of time. These results are shown in Figure 5.12 and the good agreement with reported values indicates that the prepared standards were radio-chemically "pure". The actual compositions of the standards were determined by wet chemical analysis to an accuracy of ± 2 pct. of the amount present. (Cu - 1.01 wt. pct.; Au - 0.52 wt. pct.)

(b) Radio-Tracer Analysis of Copper and Gold in Germanium

For each solubility determination, two quartz vials, each containing about five milligrams of pure copper or gold, were irradiated for five minutes. The samples were dissolved (copper in HNO_3 and gold in aqua-regia) and the solutions were evaporated. One of the residues was dissolved in five milliliters of 1 N HCl acid. A few drops of HF were added and the solution was then used as a displacement plating bath. The other residue was also dissolved but was stored for later use as a standard. After the plated semiconductor slices were diffused, the analysis procedures were practically identical to those for the silicon samples.

(c) Errors

The principal sources of errors in radio-activity measurement are self-absorption, scattering, geometric errors, background, radio-active decay, and instrumental errors. Instrumental errors are usually due to a lack of proportionality between decay rate and measured counting rate. This effect can usually be minimized by using unknowns and standards which contain about the same concentration of radio-active isotope. Decay problems can be overcome by a direct calculation of the decay rate of the isotope but it can often be assumed linear over the time in which a counting sequence is conducted. The other errors can usually be circumvented by comparison methods of counting in which homogeneous samples of the same size are used with reproducible positioning in a well-shielded counter. Errors in chemical separation may arise because two main considerations are not met. These are: 1) The carrier must exchange completely with the radio-active isotope or must be in the same chemical form, and, 2) the separated isotope must be radio-chemically pure. The latter condition can usually be checked by determining the half-life of a sample and by conducting blank runs.

Activation errors arise because of transmutation and flux variation effects. Possible matrix transmutation effects can also be checked with blank runs. Neutron flux variations across an irradiation package are caused by neutron attenuation by the samples and packaging materials and by inhomogeneity of the unperturbed flux. Self-absorption by dilute samples can be avoided if the matrix materials have low neutron capture cross sections. Often unknowns and standards of the same material and size may also be used. The samples should be contained in capsules of the same material and wall thickness because of packaging material attenuation. Overall inhomogeneity of the flux across an irradiation unit may usually be circumvented by judicious positioning of the unknowns and the standards. The best way to overcome this problem is to map out the flux of a particular irradiation position by a standardization experiment (Plumb and Lewis, 1955), but this is often impractical if a large number of irradiations are to be conducted over a long period of time.

In the present work, random chemical analysis errors arose from the counting, weighing, diluting, and pipetting steps. The counting error for a given sample was determined by the usual formula

$$\sigma = \pm \frac{(C + 2B)}{C}^{1/2}$$

where B and C are the counts from the background and the sample, respectively. The percentage errors for the standards were converted to counts (a,b) and the total counting error, σ_C, for an unknown, U1 say, was determined from the expression

$$\sigma_C = \pm \left(\sigma_{U1} + \frac{a + b}{C_{S4} + C_{S1}} \right)$$

where C_{S4} and C_{S1} are the counts for the standards (almost identical in magnitude) and σ_{U1} is the error in the unknown count.

The solutions were pipetted into the counting flask in 3.00 ± 0.01 milliliter aliquots. Since the operation was conducted for both unknowns and standards, the pipetting volume error was ± 0.67 pct. For the particular counting arrangement used, however, Slater (1960) has shown that the actual counting error arising from the volume error is about one third of the latter. The pipetting error was therefore estimated to be ± 0.25 pct. The standards were usually diluted in 100.00 ± 0.16 milliliter volumetric flasks and therefore contributed an error of ± 0.16 pct. to the analysis. The residues of the copper and gold unknowns were dissolved in 5.00 ± 0.01 milliliter (± 0.20 pct.) and

25.00 ± 0.06 milliliter (± 0.26 pct.) solutions, respectively. Errors in weighing the unknowns were negligible since samples of no less than 0.1 grams were weighed to better than ± 50 micrograms. The standards were weighed to ± 10 micrograms, or an accuracy of ± 2.0 pct. (0.5 mgm. sample) to ± 1.0 pct. (1.0 mgm. sample). The random analysis errors for a single determination were calculated by summing the relevant contributions discussed above. For an average standard weight of 0.75 milligrams, the percentage error in a determination was approximately ± (σ_C + 2) pct.

Systematic errors, which affect the accuracy of a particular determination, were also present. The most important of these was the error in the composition of the standards (± 2 pct.). Systematic weighing errors were probably small because differences instead of absolute values were measured. Pipetting errors were also small since the unknowns and standards were treated by the same procedure. Chemical yield differences between the unknowns and the standards also probably introduced a systematic error in the anlysis, but an attempt was made to minimize this problem by treating them as similarly as possible. An accurate determination of the chemical yield of the unknowns was not possible since copper and gold doped materials of accurately known composition are not available. Experiments in which pure semiconductor and a known amount of bulk radio-active copper or gold were analyzed showed no observable chemical yield effect. In any case, systematic errors influence in the same manner the absolute magnitudes of all the concentrations in a particular system, and hence do not affect to any significant extent the measured dependence of the solubility limit on temperature and defect concentration.

5.C.3 Cu_3Si Preparation

The copper silicide compound was prepared by melting together copper and silicon in the apparatus described in Section 5.B.2. Relative amounts of each component were chosen which yielded a nominal composition of 17 weight pct. silicon. According to the copper-silicon phase diagram, a liquid solution of this composition should solidify as a two phase mixture of non-stoichiometric silicon saturated Cu_3Si and a small amount of copper saturated silicon.

The two elements were heated inductively in an alumina crucible after the system was purged with purified argon for about thirty minutes. After the silicon melted, the temperature was held at approximately 1000°C for a few minutes and the power was then turned off and the liquid solution was allowed to solidify in the crucible. The Cu_3Si ingot was removed and crushed after immersion in liquid nitrogen.

A small portion of the ingot was mounted in cold setting resin for metallographic observation and for chemical analysis with an Acton (Cameca) electron probe micro-analyser. After microscopic examination, the polished surface was coated with a thin film of evaporated carbon in order to ensure that the sample would be electrically conducting for the probe analysis. The standards used in the analysis were high purity copper and silicon.

5.C.4 Identification of Interface Precipitates.

Light microscopy was used to observe the precipitation characteristics of Cu_3Si between interdiffusing layers of copper and silicon below 802°C. Copper plated silicon slices were annealed for various times at 700°C and 750°C, quenched, and mounted in cold setting resin. Taper sections were taken on most samples by mounting the plane of the interface at an angle of ten degrees to the polishing plane. This procedure greatly magnified features normal to the interface and made observations of precipitate particles much easier than was possible with the standard perpendicular mounting method. After the samples were mounted they were lapped on 600 mesh silicon carbide paper and then automatically polished with 0.3 micron alumina powder on a Syntron vibratory polisher. The unetched interface region was then examined with a Reichert metallograph.

Since more than one phase may form in a diffusion couple between silicon and copper, it was necessary to identify the observed interface precipitates. An X-ray diffractometry and micro-analysis study was therefore conducted. Crystallographic information about Cu_3Si was not found in the ASTM X-ray spectra card index so a powder sample of this compound was scanned with a Philips X-ray diffractometer. Silicon slices which had been copper plated and annealed at 810°C and 750°C were also scanned and the lines observed were compared to those found for Cu_3Si and those reported for other copper silicides. The precipitates in the 750°C sample were also analyzed with the electron probe microanalyser.

5.C.5. Low Temperature Precipitation Study

Single crystal silicon slices one millimeter thick were cut from a Czochralski grown ingot which had a dislocation density of 4×10^4 cm./cm.^{3} and contained a carrier (n-type) concentration of 1×10^{13} atoms/cm.^{3}. The samples were plated with copper and saturated in an argon atmosphere at temperatures ranging from 700°C to 1000°C. They were quenched in water to room temperature and the external phase was removed with 600 mesh silicon carbide paper. The samples were placed in the resistance monitoring apparatus within two minutes of the quench and the circuit current was measured as a function of time. The lapped surface of the specimens ensured that a non-rectifying ohmic contact was obtained for these measurements (Sittner, 1956). The temperature was maintained at 30°C for precipitation from solutions saturated at 700, 800, 900 and 1000°C. Four other samples which were saturated at 900°C were treated at temperatures between 40°C and 70°C in order to obtain an activation energy for the precipitation reaction.

5.C.6 Copper Segregation During Device Heat Treatment

A 1.5 millimeter thick slice of phosphorus doped silicon (7×10^{17} atoms/cm^3) was saturated with copper at 900°C. The sample was quenched to room temperature and after the external phase was removed it was chemically polished to a thickness of one millimeter with CP-8.* The slice was then encapsulated in quartz under vacuum (10^{-4} mm. Hg) with about one gram of boron nitride powder which served as a diffusion source for boron. To the author's knowledge this compound has not been previously employed for diffusion doping of silicon. Phosphorus nitride has been used, however, (LaChapelle and Heller, 1964) and it was found to give a clean surface in contrast to most commonly used oxide diffusion sources which produce a liquid

---

* The recipe for CP-8 is 25 m. HNO_3, 15 ml. HF, and 15 ml. acetic acid.

slag on the semiconductor surface. These slags act as getters for many fast diffusing impurities (Ing et al, 1964), an effect that was necessary to avoid in the present study.

The diffusion doping operation was conducted at 1300°C for a period of 24 hours, after which the quartz capsule was quenched in water. The silicon slice was then re-encapsulated and annealed at 975°C for two hours. After the anneal one portion of the slice was mounted in cold setting resin for a metallographic determination of the p-n junction depth. The junction was delineated by etching with a solution of twenty parts of HNO_3 to one part of HF (Wong, 1965). From a determination of the junction depth, x, and a knowledge of the boron concentration at the junction, $N(x,t) = 7 \times 10^{17}$ atoms/cm^3 , and the boron diffusion coefficient at 1300°C, D, the boron concentration at the surface, N°, was estimated from the equation for diffusion into a semi-infinite medium

$$N(x,t) = N^\circ \left(1 - \text{erf} \frac{x}{2\sqrt{Dt}}\right) \quad . \qquad (5.3)$$

It must be assumed that the diffusion coefficient is independent of concentration for the above equation to be correctly applied to the problem at hand.

The remaining portion of the slice was divided into two parts for chemical analysis. One section was analysed for an over-all average copper concentration after etching lightly in high purity HNO_3 to which a few drops of HF had been added. The other was chemically dissolved to a thickness of 0.5 millimeters before analysis in order that the copper concentration in the interior of the sample could be compared with the total concentration to give a qualitative picture of possible copper segregation to heavily doped regions of a device during heat treatment operations.

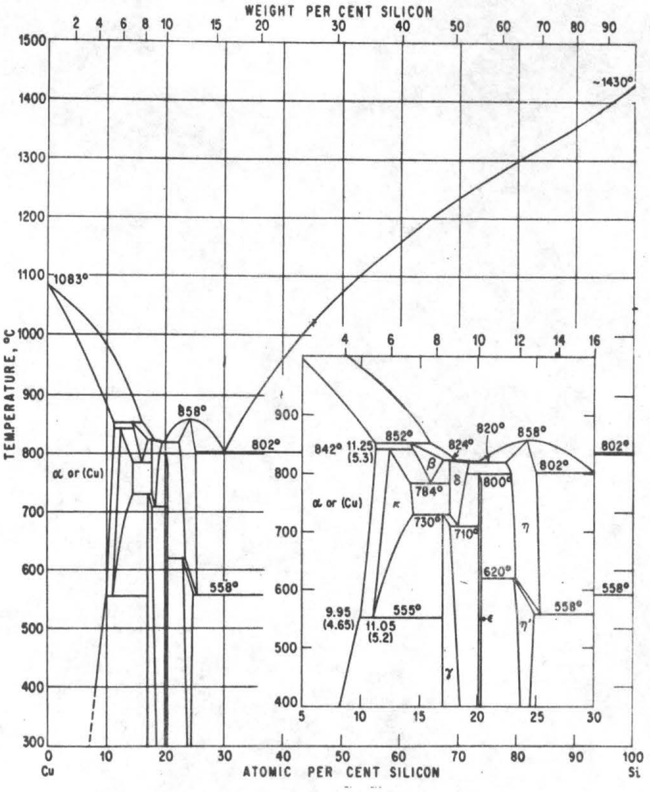

Figure 5.1. Phase diagram of the copper-silicon system. After Hansen, (1958)

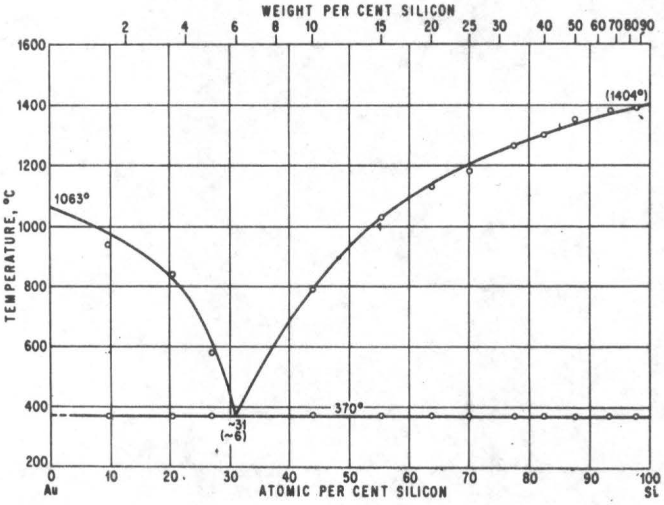

Figure 5.2. Phase diagram of the gold-silicon system. After Hansen, (1958)

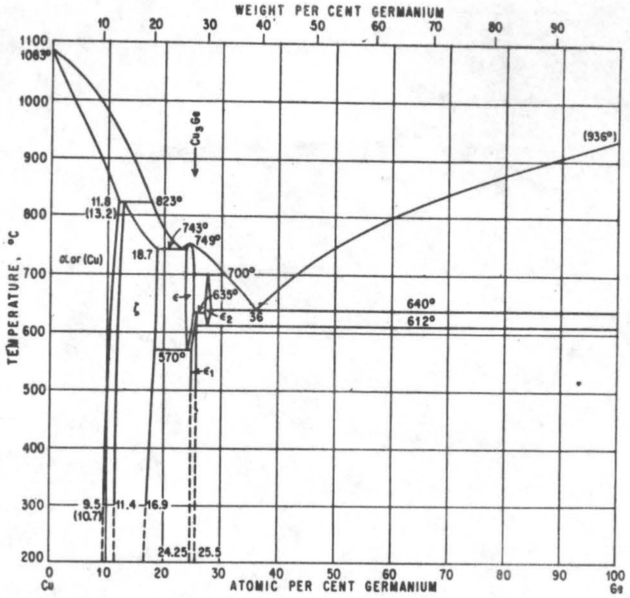

Figure 5.3. Phase diagram of the copper-germanium system. After Hansen, (1958)

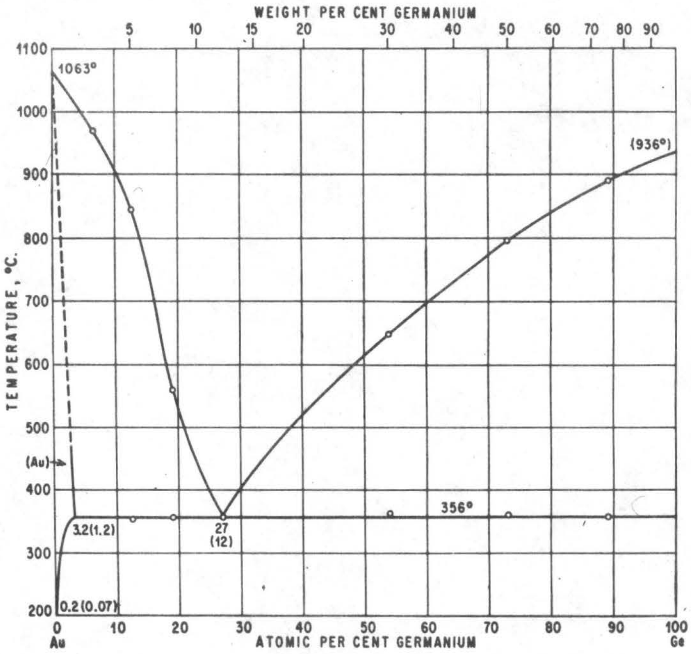

Figure 5.4. Phase diagram of the gold-germanium system. After Hansen, (1958)

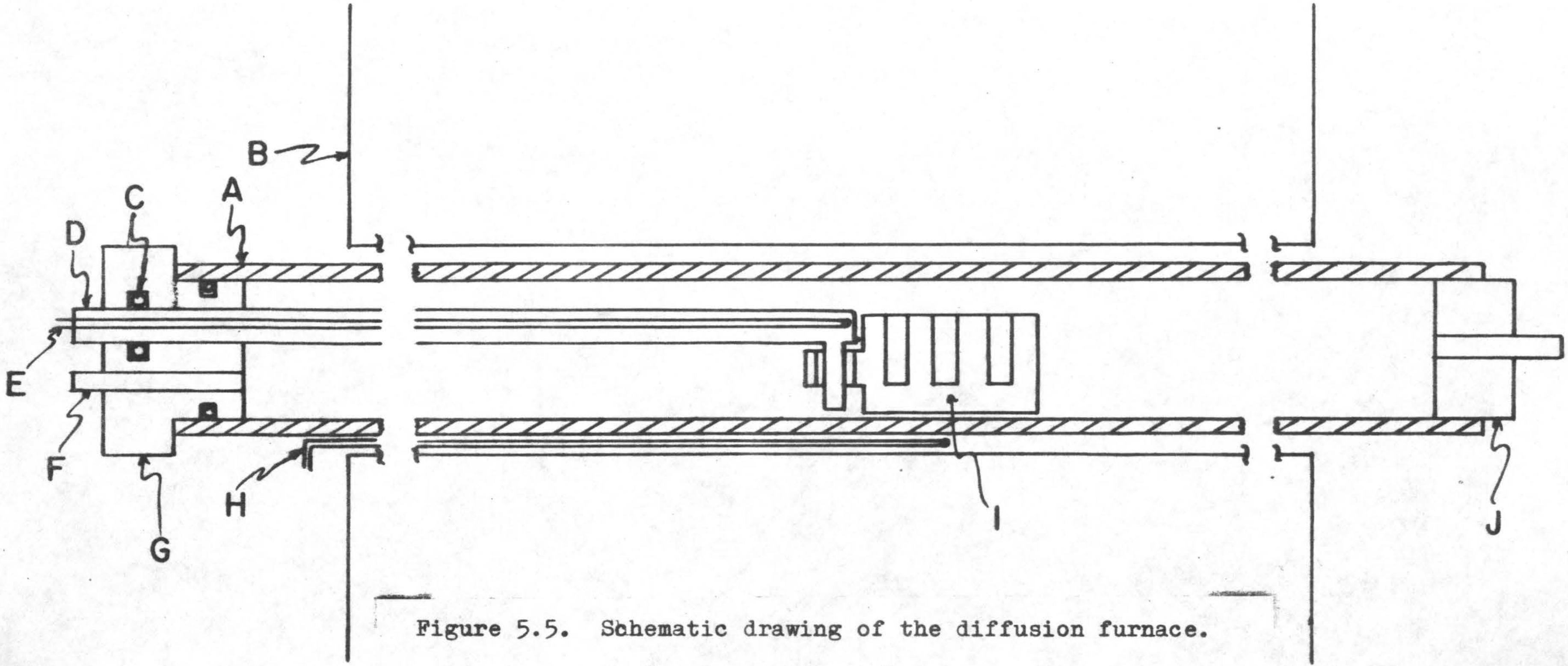

Figure 5.5. Schematic drawing of the diffusion furnace.

A	Quartz working tube
B	Electrical resistance furnace
C	"O" ring seals
D	Quartz control tube
E	Thermocouple
F	Argon inlet
G	Brass end plug
H	Control thermocouple
I	Sample boat
J	Rubber plug with argon outlet

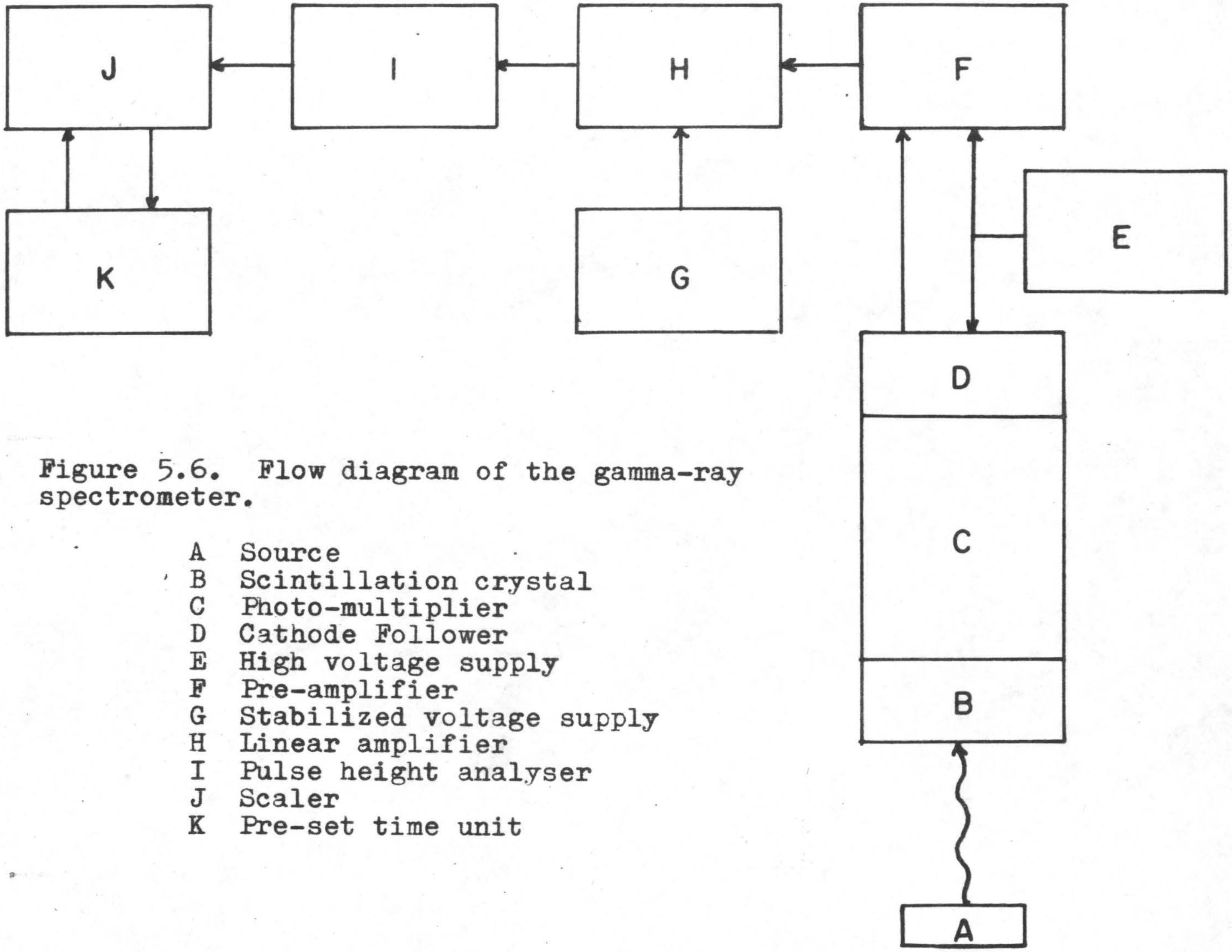

Figure 5.6. Flow diagram of the gamma-ray spectrometer.

A	Source
B	Scintillation crystal
C	Photo-multiplier
D	Cathode Follower
E	High voltage supply
F	Pre-amplifier
G	Stabilized voltage supply
H	Linear amplifier
I	Pulse height analyser
J	Scaler
K	Pre-set time unit

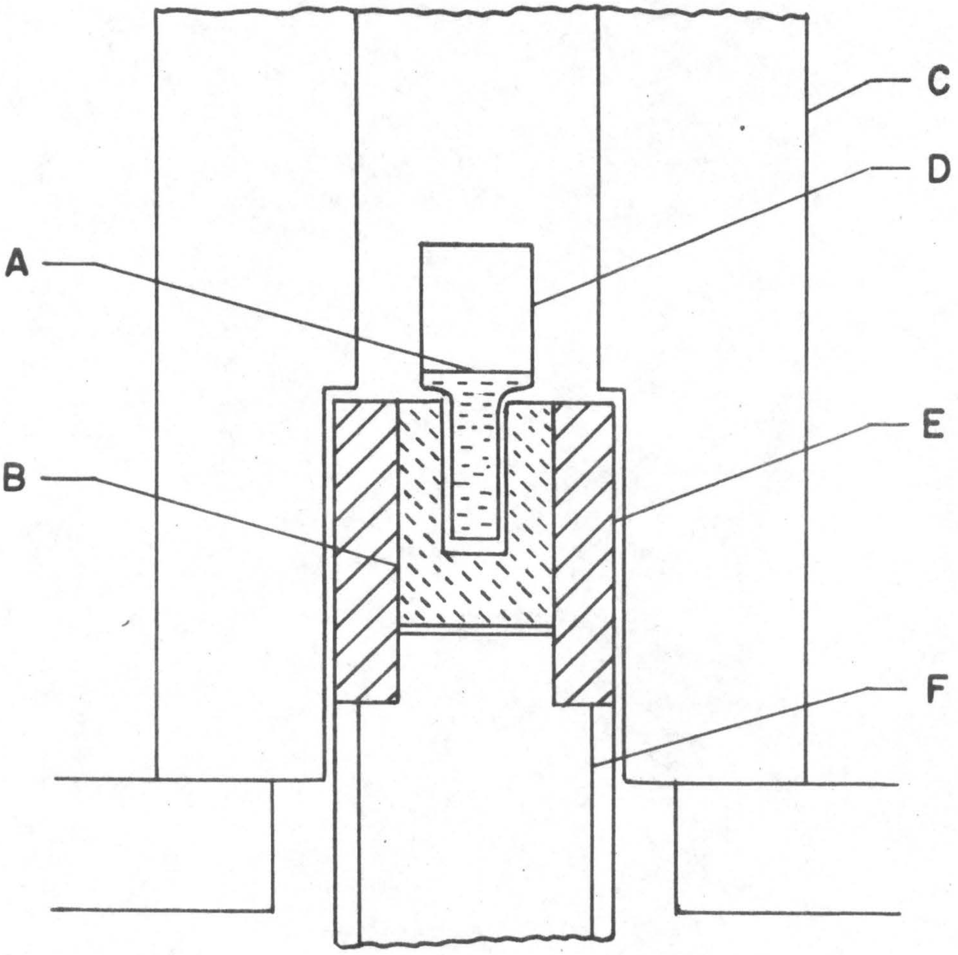

Figure 5.7. Sectional diagram of the crystal-source configuration used to measure the radio-activities of liquid solutions.

A	Sample Solution	D	Glass Counting Vessel
B	NaI(Tl) Well Crystal	E	Lead Shielding
C	Lead Castle	F	Photo-multiplier

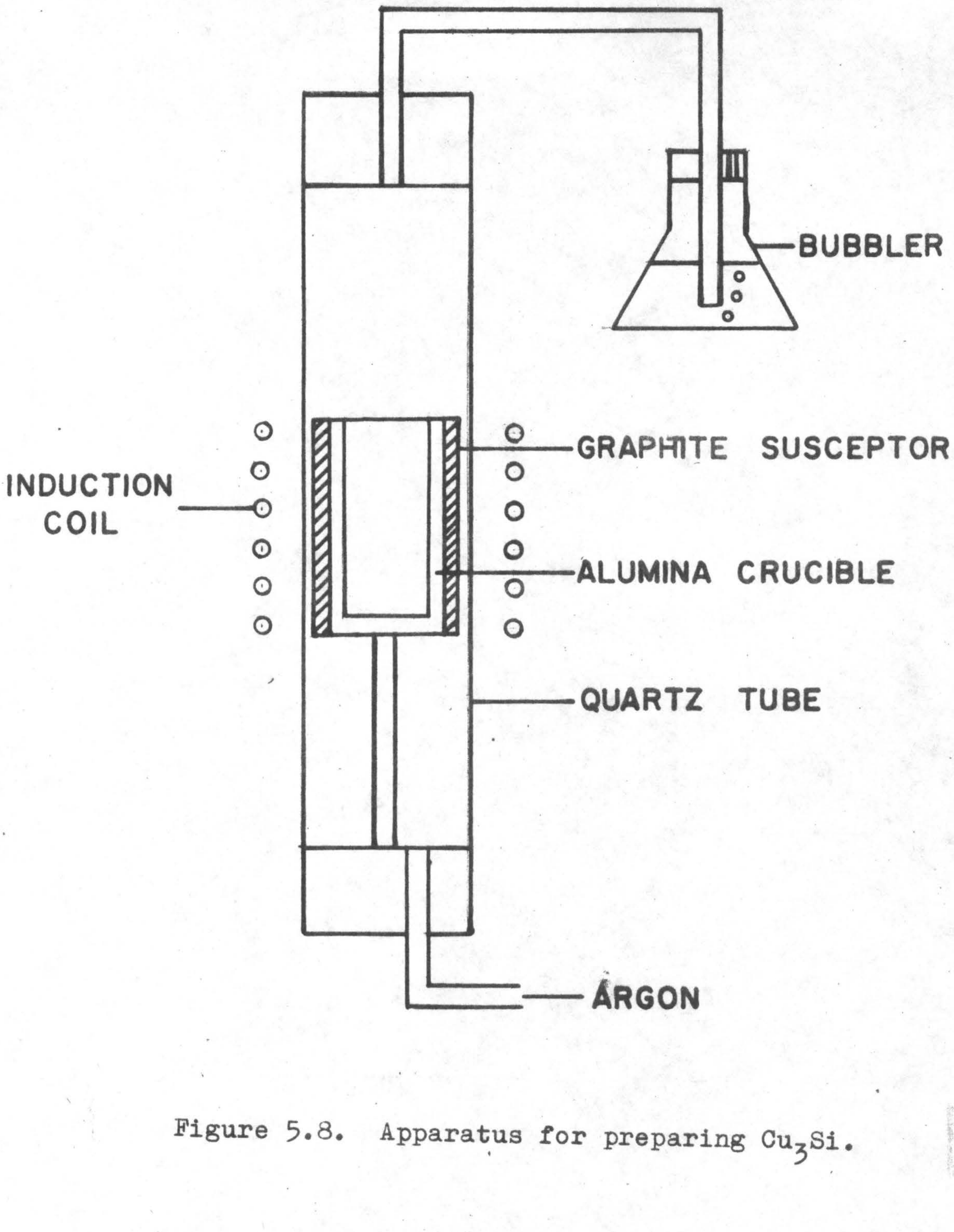

Figure 5.8. Apparatus for preparing Cu_3Si.

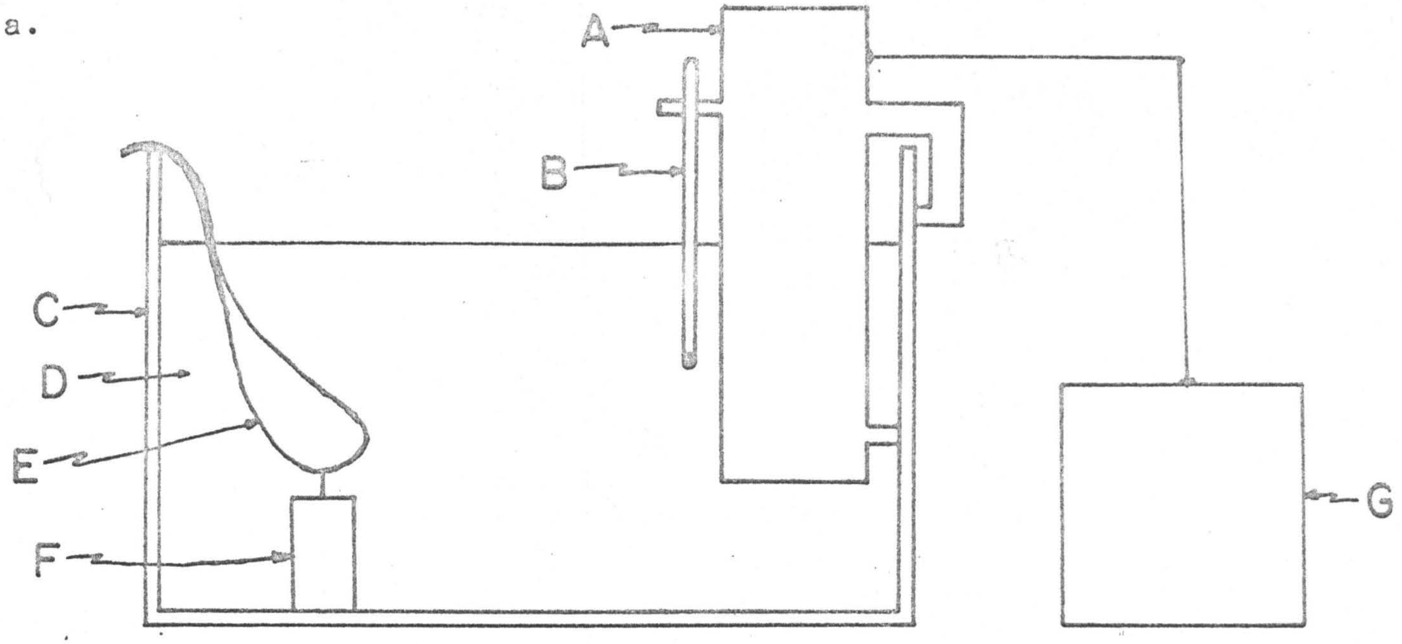

A	Heater and stirrer
B	Thermometer
C	Glass container
D	Water
E	Rubber envelope
F	Immersion weight
G	Temperature control unit
H	Insulating hinge
I	Electrical probes
J	Sample
K	Constant tension device

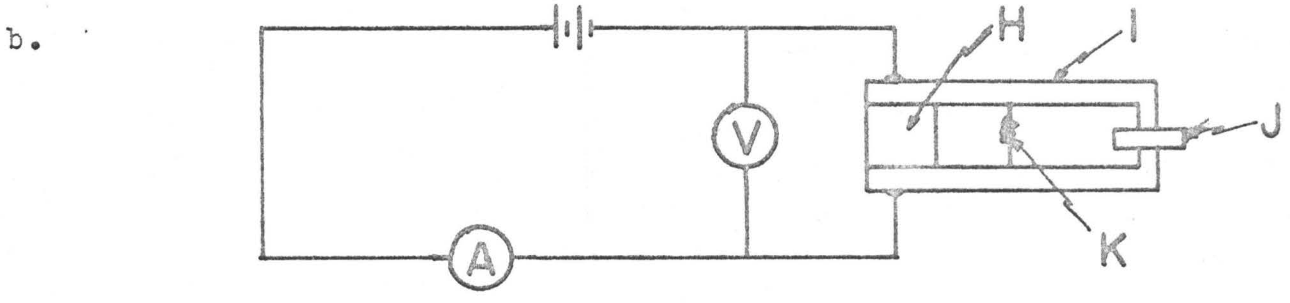

Figure 5.9. Schematic drawings of the resistance measuring apparatus: (a) constant temperature bath (b) sample holder.

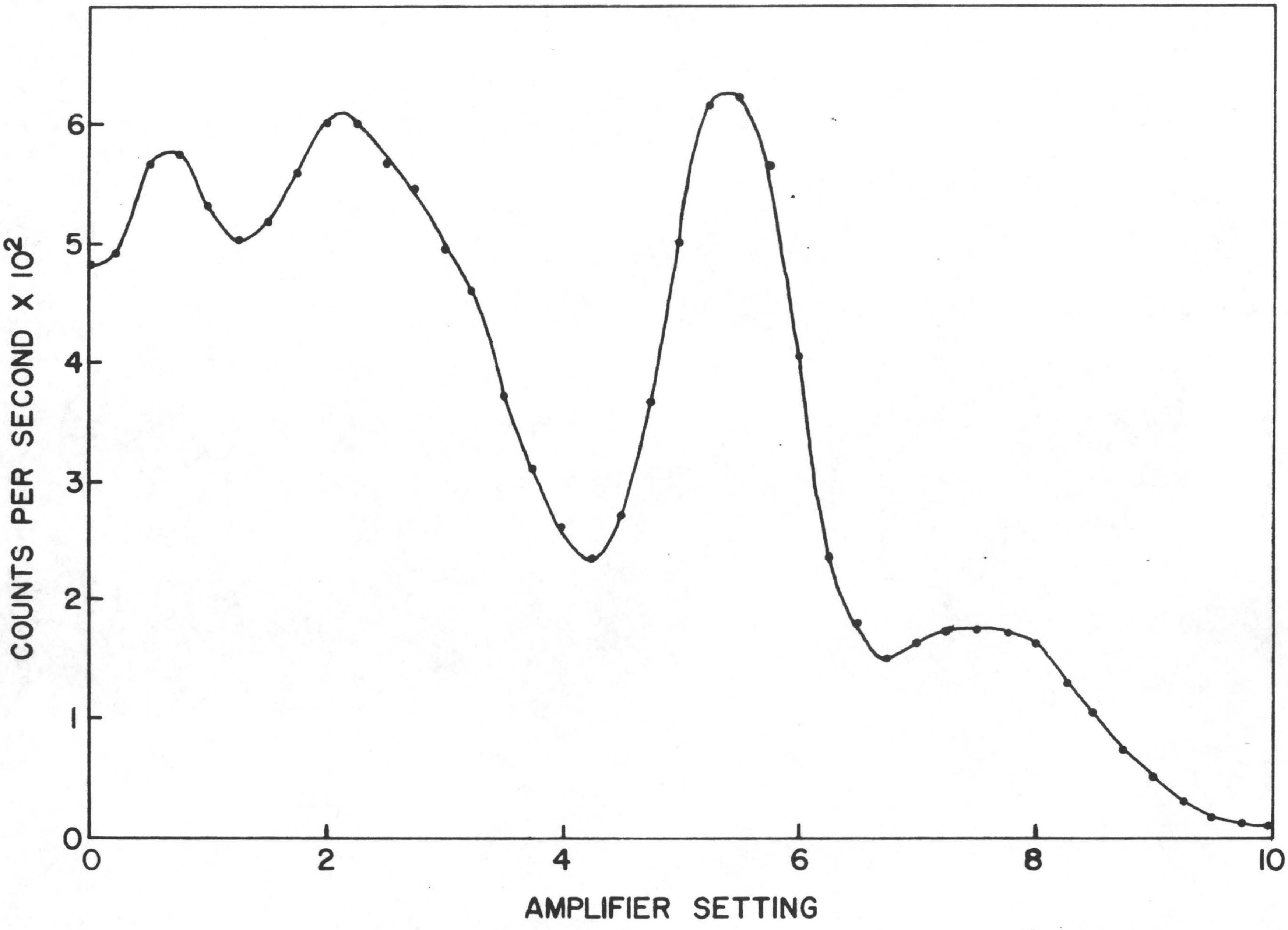

Figure 5.10. Spectrometer scan of the Cu-64 spectrum.

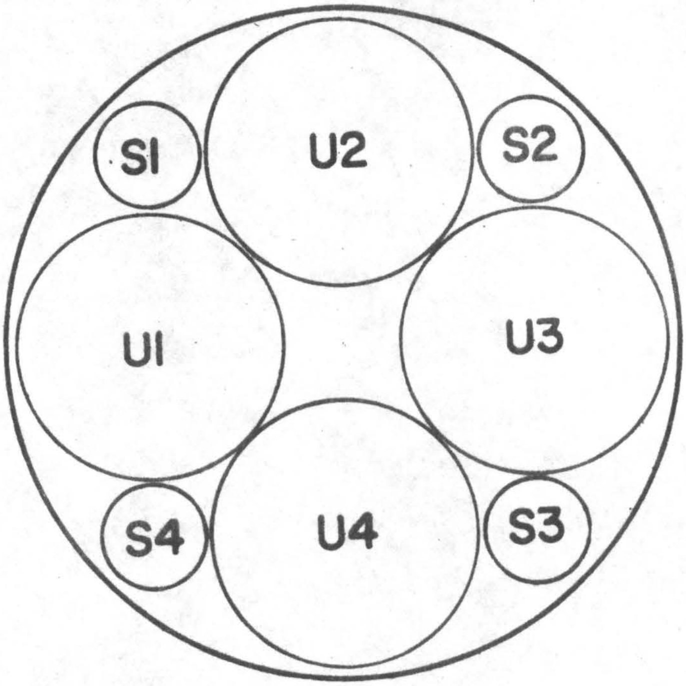

Figure 5.11. Schematic representation of the irradiation assembly. U (unknown), S (standard)

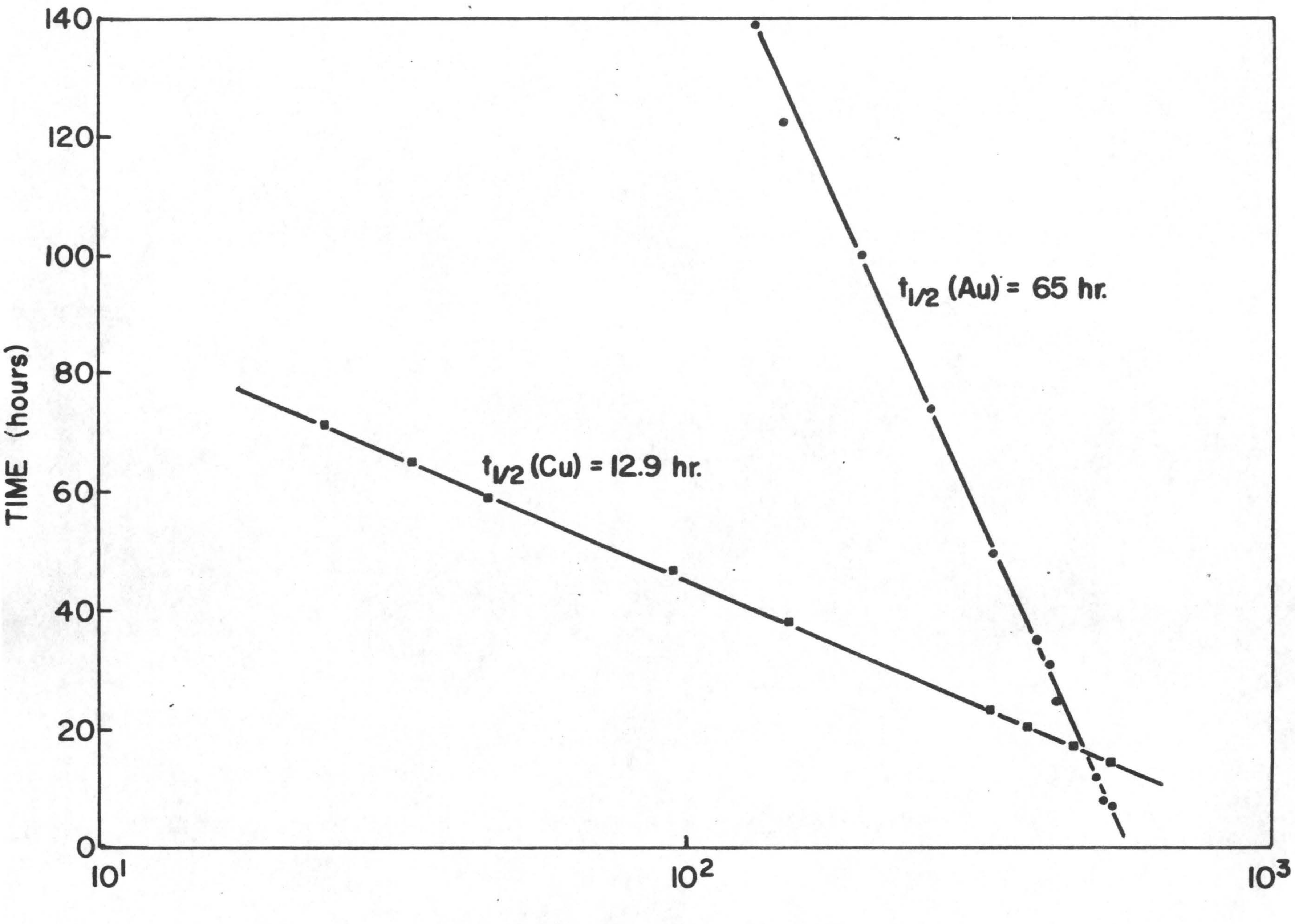

Figure 5.12. Decay curves for the copper and gold standards.

CHAPTER 6

RESULTS

6.A Solubility Measurements

Most of the results in this section are presented on graphs. Appendix B contains the results of all the solubility and precipitation measurements in tabular form.

6.A.1 Copper in Silicon

The results of the "solubility" vs. time experiments designed to investigate the nucleation and growth characteristics of Cu_3Si in copper-silicon diffusion couples are shown in Figures 6.1 and 6.2 for temperatures of 750°C and 700°C, respectively. The solubilities depicted by crosses are those determined by equilibration with Cu_3Si via the vapor phase. Two determinations of the true solubility were conducted at 700°C by equilibration for different times in order to ensure that a rate limitation was not influencing the results. Micrographs of prepared Cu_3Si and the interfaces of various couples are shown in Figures 6.3 to 6.6.

Electron micro-probe analysis of the prepared Cu_3Si yielded a relative copper intensity, I/I_o, of 0.824 ± 0.017 using pure copper as a standard (see Table 6.1). The theoretical value for the relative copper intensity from silicon saturated Cu_3Si is 0.810 as calculated by the method of Lifshin and Hanneman (1965). A number of precipitate particles in the interface region of copper-silicon couple reacted at 750°C for 48 hours were also analysed by this method and they were found to be of the same composition as the prepared copper silicide

($I/I_o = 0.806 \pm 0.018$). The nearest copper silicide to Cu_3Si on the phase diagram ($Cu_{15}Si_4$) has a theoretical relative copper intensity of 0.838. An X-ray diffractometer scan of powdered Cu_3Si was conducted and the region of the most intense peaks is reproduced in Figure 6.7. Figure 6.8 shows diffractometer traces from the interface regions of couples reacted at 810°C for two hours and at 750°C for 48 hours. Crystallographic data for Cu_3Si is not available from the ASTM card index and information available from the literature is inconsistent so the observed lines and approximate relative intensities are shown in Table 6.2 together with those for copper, silicon, and the other copper silicides.

The solubility of copper in pure single crystal silicon over the temperature range 650°C to 1100°C is shown as a partial phase diagram in Figure 6.9. The high "solubility" points below the eutectic temperature, which were determined by the plate-and-anneal method for short diffusion times, are included for comparison. No difference in solubility was observed between Czochralski and float-zoned crystals. Figure 6.10 is a comparison of previously determined data with the present work. A plot of $\ln k^e$ vs. $1/T$ is shown in Figure 6.11. The equilibrium distribution coefficients at the melting points of the solvents for all the systems studied were taken from the review paper by Trumbore (1960). The dashed line of Figure 6.11 represents $\ln(k^e/\gamma^1)$ where γ^1 was determined from Equation 4.3 with the data of Thurmond and Kowalchik (1960), in which they give a =-11,910 cal./mole and b =-7.19 cal./mole -°K. The relative partial molar enthalpy of copper in silicon was calculated from a computerized least squares analysis of the $\ln(k^e/\gamma^1)$

vs. 1/T plot as 37.3 ± 0.5 Kcal./mole. From the intercept of this graph the relative partial molar excess entropy of copper in silicon was determined to be 7.1 ± 0.4 cal./mole - °K. The errors quoted are probable errors based on the least squares analysis (Worthing and Geffner, 1943). In the above calculations the enthalpy and entropy of fusion of pure copper were taken as 3.11 Kcal./mole and 2.30 cal./mole-°K respectively (Smithells, 1962). The enthalpy and entropy of solution of copper in silicon <u>with respect to</u> Cu_3Si were calculated in a similar manner as 40.2 ± 0.5 Kcal./mole* and 9.7 ± 0.5 cal./mole - °K respectively.

The solubility of copper in pure polycrystalline silicon is shown in Figure 6.12. The dot-dashed line is assumed to represent the solubility (on a bulk sample basis) of copper in the grain boundaries. The heat of solution of copper in silicon grain boundaries (with respect to Cu_3Si) was calculated from the slope of this plot to be 6.3 ± 0.4 Kcal./mole. An assumption inherent in the above calculation is that the heat of solution is concentration independent over the composition range considered. The binding energy as given by Equation 3.32 is then 33.9 ± 0.9 Kcal./mole or 1.47 ∓ 0.04 eV/atom. Substitution of this value into Equation 3.31 gives a grain boundary concentration of $X^{g.b.} = 0.43 \pm 0.10$ at 700°C. Micrographs of the vapor grown polycrystalline silicon are shown in Figures 6.13 and 6.14.

Figure 6.16 shows the solubility of copper in silicon doped with boron to a level of 5 X 10^{18} atoms/cm.^{3}. Assuming complete

---

* Gram-atom of copper.

ionization of the dopants and non-degenerate conditions, the theoretical dot-dashed line was calculated from Equation 3.4 with $(E_f^\circ - E_f)$ given by Equations 2.11 and 2.12, in which n_i^2 was taken from a curve of n_i vs. 1/T by Hall and Racette (1964). These values are included in Table B.2.

6.A.2 Copper in Germanium.

The solubility of copper in pure single crystal germanium over the temperature range 650-900°C is shown in Figure 6.17. A plot of $\ln k^e$ vs. 1/T is shown in Figure 6.18. The dashed line in this figure represents $\ln(k^e/\gamma^1)$, where γ^1 has been calculated from Equation 4.3 with a = -7,360 cal./mole and b = -7.67 cal./mole-°K (Thurmond and Kowalchik, 1960). The partial molar excess entropy and enthalpy of solution were calculated to be 10.3 ± 0.6 cal./mole-°K and 41.3 ± 0.7 Kcal./mole, respectively. The open circles in Figure 6.17 represent the solubility of copper in germanium doped with arsenic to a level of 7×10^{17} atoms/cm.^{3}. The curve drawn through these points is based on Equation 3.10 with $\Delta H_b = 1.0$ eV, $\Delta S^{th} = 0$, and N_2° equal to the total intrinsic copper solubility. Since copper may exist in three charge states, however, it is quite probable that the only significant interaction is that of arsenic ions and the triply charged copper ions. This problem will be discussed further in the next chapter.

6.A.3 Gold in Silicon

The solubility of gold in pure single crystal germanium over the temperature range 900-1300°C is shown in Figure 6.19. Figure 6.20 is a plot of $\ln(X^\alpha/X^1)$ and $\ln(k^e/\gamma^1)$ vs. 1/T from which the partial molar enthalpy and excess entropy of solution were determined to be 43.8 ± 1.4 Kcal./mole and 6.8 ± 1.0 cal./mole-°K, respectively. The heat and entropy of fusion of gold was taken as 3.06 Kcal./mole and 2.29 cal./mole-°K, respectively (Smithells, 1962). γ^1 was calculated from Equation 4.3 with a = -19,540 cal./mole and b = -10.28 cal./mole-°K (Thurmond and Kowalchik ,1960). It was also observed that a boron doping level of 5 X 10^{18} atoms/cm.^{3} reduced the gold solubility approximately 35 pct. at 900°C and 1000°C.

6.A.4 Gold in Germanium

The solubility of gold in pure single crystal germanium at 850°C was found to be 2.7 X 10^{16} atoms/cm.^{3} . Figure 6.21 is a plot of ln k^e vs. 1/T as determined from a combination of the present result and other data obtained from solidification experiments. The equilibrium distribution coefficient, as shown, may be represented by the equation

$$k^e = 4.0 \times 10^2 \exp \frac{-42{,}000}{RT} \quad .$$

No attempt was made to calculate accurately the enthalpies and entropies of solution in this system because of the lack of experimental data. Arsenic doping (5 X 10^{17} atoms/cm.^{3}) did not alter the solubility of gold in germanium to an observable extent at 850°C.

6.B Redistribution of Copper in Diffusion Doped Silicon

Chemical analysis of the complete sample yielded a concentration of 3.3 x 10^{16} atoms/cm.^{3} compared to a value of 1.5 x 10^{16} atoms/cm.^{3} for the inner region. Chemical etching of the p-n junction region showed a junction depth of (5 ± 0.1) x 10^{-3} cm. (see Figure 6.15) Solution of Equation 5.3 with $N(x,t) = 7 \times 10^{17}$ atoms/cm.^{3} (± 10 pct.), t = 8.64 x x 10^4 seconds, $x = 5 \times 10^{-3}$ cm. (± 2 pct.), and $D = 2 \times 10^{-11}$ cm.^{2}/sec. at 1300°C (Fuller and Ditzenberger, 1956) gave a value of N°, the surface boron concentration, equal to $(9.7 \pm 2.3) \times 10^{19}$ atoms/cm.^{3}.

6.C Precipitation of Copper in Silicon

A $\ln (N_0/N(t))$ vs. $t^{2/3}$ plot for copper precipitation at 30°C from samples saturated in the temperature range 700-1000°C is shown in Figure 6.22. Concentration changes were related to conductivity measurements by the relation

$$\frac{N_0}{N(t)} = \frac{I_0 - I_f}{I(t) - I_f}$$

where I_0 is the initial sample current, I_f is the current after the reaction was completed, and $I(t)$ is the current at time, t. A least squares analysis of the data for the complete reaction yielded a correlation coefficient of 0.9870. Figure 6.23 shows precipitation curves for samples saturated at 900°C and aged at 30°C, 40°C, and 50°C. The correlation coefficients for these plots are 0.9983, 0.9985, and 0.9951, respectively.

The activation energy for the reaction was determined from the plots of $\ln t_f$ vs. $1/T$ in Figure 6.24. The solid line represents the time to 100 pct. completion (observable) and the dashed line gives the time to 50 pct. completion. A least squares analysis of the former line gave an activation energy of 1.10 ± 0.05 eV for the precipitation reaction. Table 6.3 shows the dependence of the initial copper concentration at zero time on the saturation temperature. Figure 6.25 is a plot of $\ln(\ln(N_0/N(t)))$ vs. $\ln t$ for precipitation at 30°C in four samples saturated in the temperature range 700 to 1000°C. The time exponent for the reaction (the slope of the plot) was determined from a least squares analysis of the data to be 0.687 ± 0.043 using 95 pct. confidence limits.

Blank runs which were conducted with annealed copper-free samples did not reveal any observable conductivity changes when aged near room temperature. The sign of the Hall voltages for a number of the samples was measured after completion of the precipitation reaction and it was observed that they remained n-type for all saturation temperatures. Within experimental error, the conductivities of all the samples also returned to their original values when the precipitation reaction was completed.

The error in each current measurement was estimated to be not greater than ±2 pct. In view of the large conductivity changes involved, this degree of precision is quite sufficient to obtain meaningful kinetic curves. Representative error bars which include the systematic error in in $(I_o - I_f)$ are indicated in Figure 6.23.

Table 6.1. Results of the electron micro-probe analysis of prepared Cu_3Si and interface precipitates of a Cu-Si diffusion couple which was reacted for 48 hours at 750°C.

Prepared Cu_3Si	Standard	Precipitates	Standard
1720	2020	2170	2520
1750	2060	1960	2570
1610	2020	2080	2460
1620	2000	1950	2590
1730	2070	2200	2500
1630	2110	2130	2540
1740	1960	1920	2460
1740	2030	2030	2560
1630	1960	1930	2510
1640	2130	1880	2460
1680 ± 19	2040 ± 19	2030 ± 33	2520 ± 16
I/I_o = .824 .017		I/I_o = .806 .018	

Table 6.2. X-ray data (2θ and relative intensities) for copper, silicon and copper silicides. (Cu K_α radiation)

Cu_4Si	Cu_5Si	$Cu_{15}Si_4$	Cu	Si	Cu_3Si
43.1 (100)	43.7 (100)	43.7 (100)	43.3 (100)	28.4 (100)	44.4 (100)
46.1 (31)	46.1 (80)	34.5 (80)	50.4 (46)	47.4 (60)	45.0 (40)
79.2 (31)	48.4 (80)	47.6 (80)	69.1 (20)	56.1 (35)	37.0 (20)

Table 6.3. Initial copper concentration after quenching as a function of the saturation temperature (assuming complete ionization of the copper centers at room temperature).

	Saturation Temperature (°C)				
	600	700	800	900	1000
N_o X 10^{13} (atoms/cm.^{3})	-	1.0	2.8	5.2	13.0

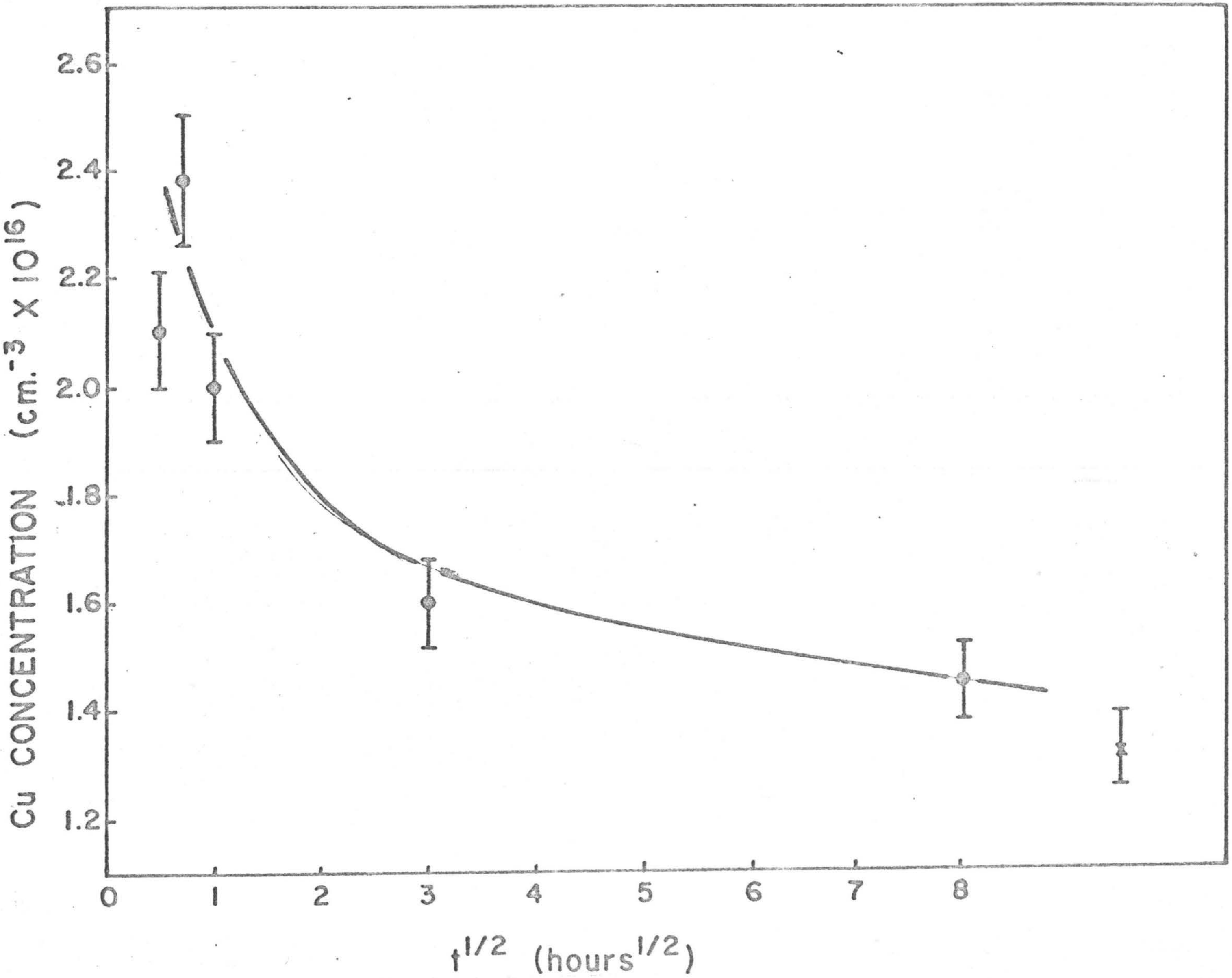

Figure 6.1. Solubility vs. time for copper in silicon at 750 C. The point represented by a cross indicates the true equilibrium solubility found by equilibration with Cu_3Si.

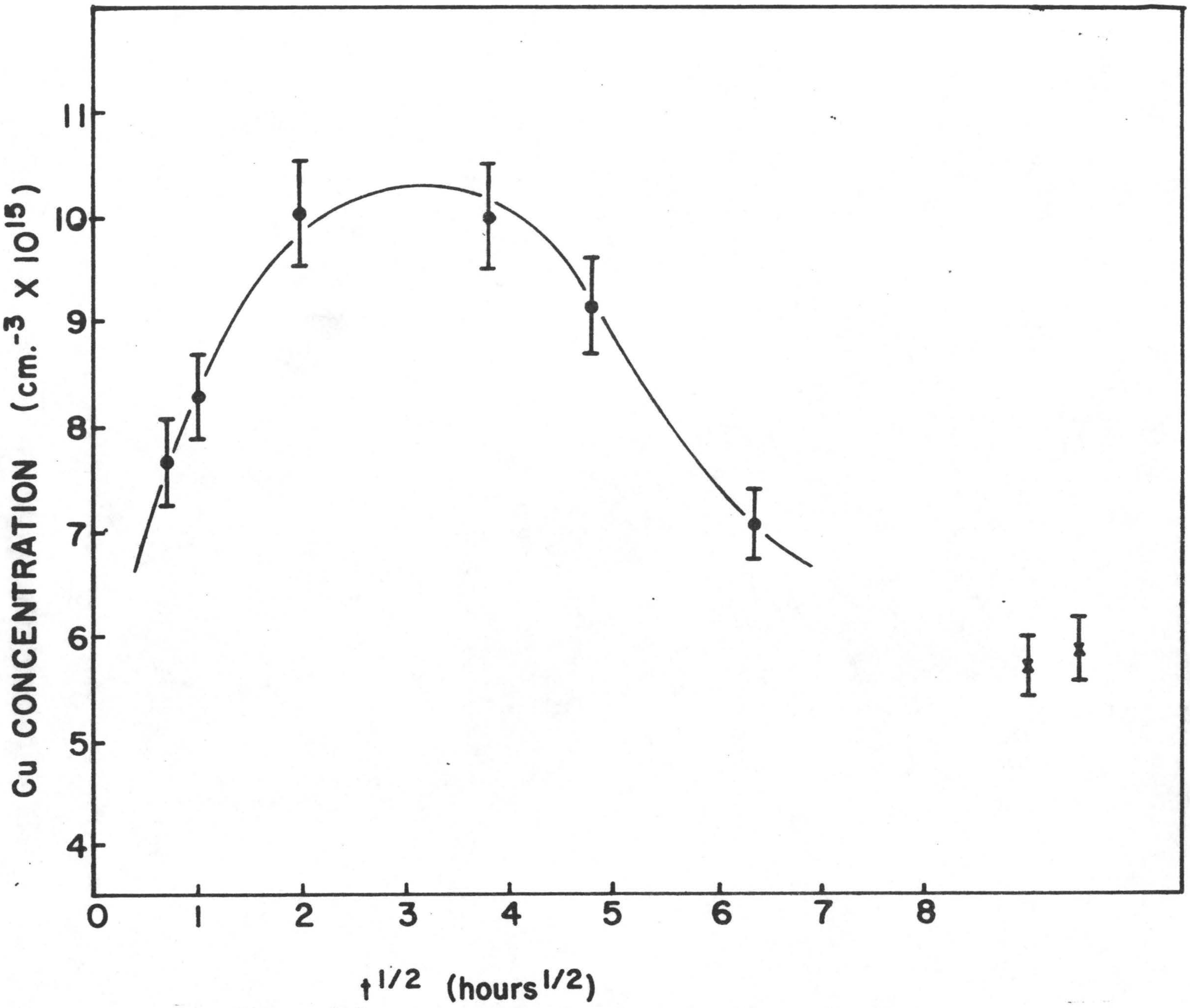

Figure 6.2. Solubility Vs. time for copper in silicon at 700 C. The points represented by crosses indicate the true equilibrium solubility.

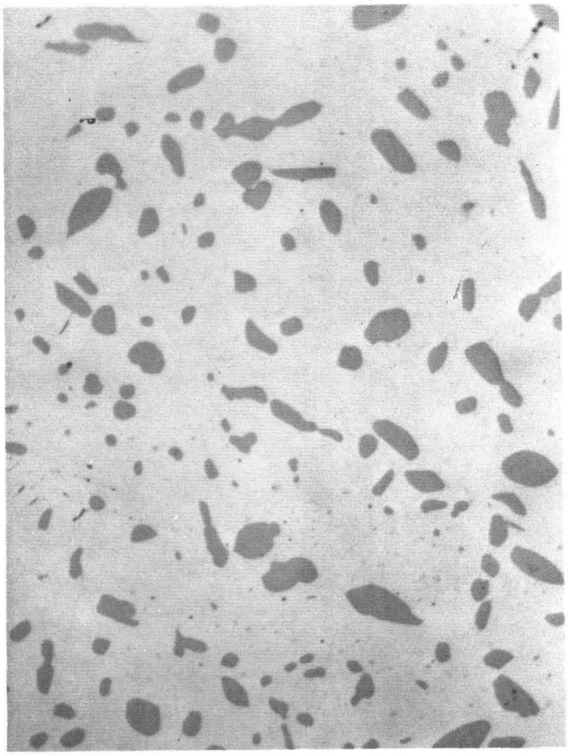

Figure 6.3. Prepared Cu_3Si containing Si (dark areas) X165, unetched.

Figure 6.4. As-plated Cu-Si interface X750, taper section, unetched.

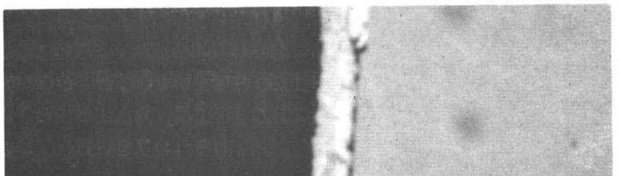

Figure 6.5. Cu-Si couple reacted 24 hrs. X1800, perpendicular section, unetched. T = 750°C.

Figure 6.6. Cu-Si couple reacted 2 hrs. X750, taper section, unetched. T = 750°C.

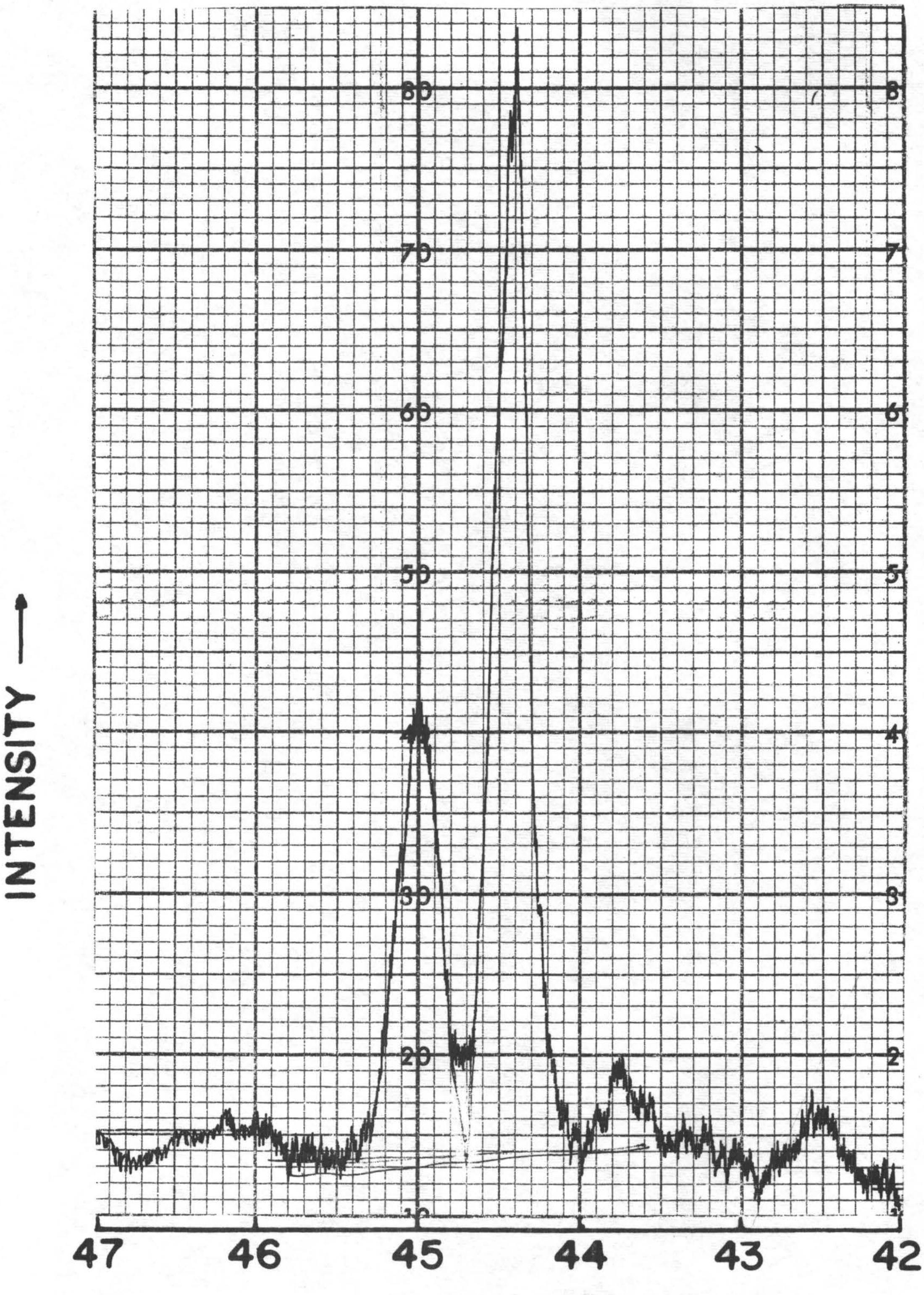

Figure 6.7. X-ray diffractometer scan of prepared Cu_3Si. (Cu K_α radiation)

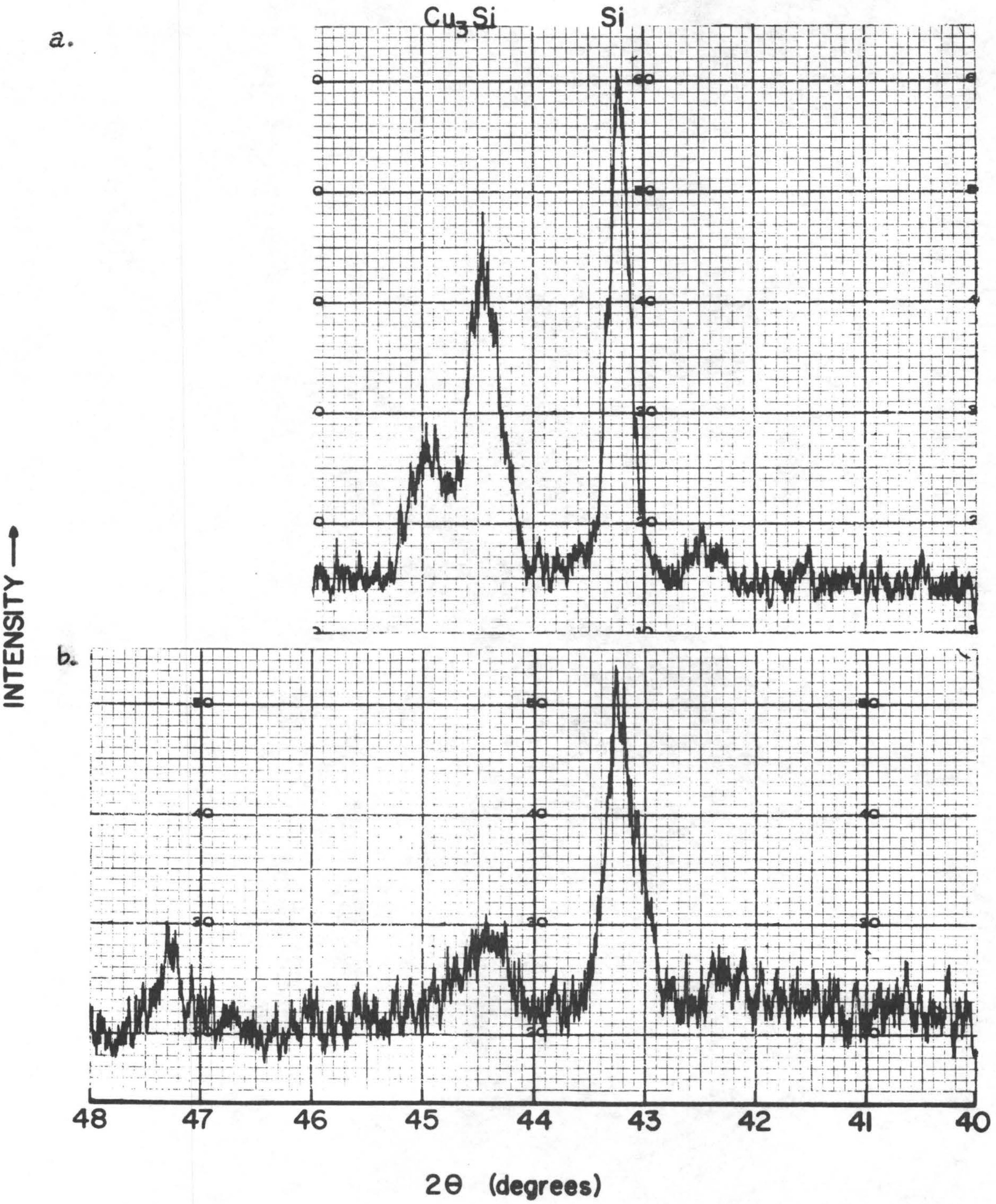

Figure 6.8. X-ray diffractometer scan for precipitates in interface regions of Cu-Si couples reacted for (a) 2 hours at 810°C, and (b) 48 hours at 750°C. (Cu K_α radiation)

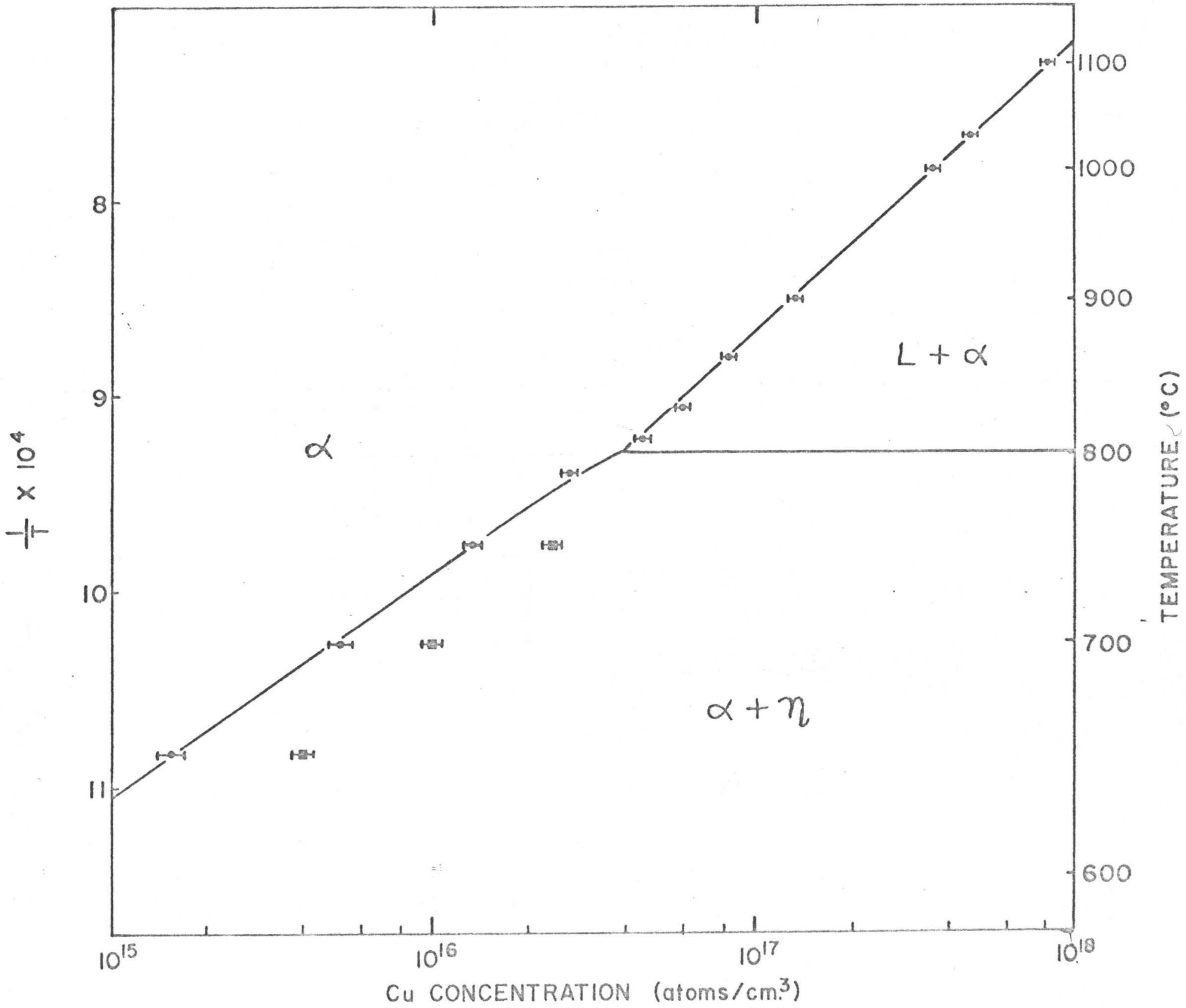

FIGURE 6.9. SOLUBILITY OF COPPER IN PURE SINGLE CRYSTAL SILICON (CIRCLES). THE SQUARES REPRESENT "SOLUBILITIES" DETERMINED BY THE PLATE - AND - ANNEAL METHOD.

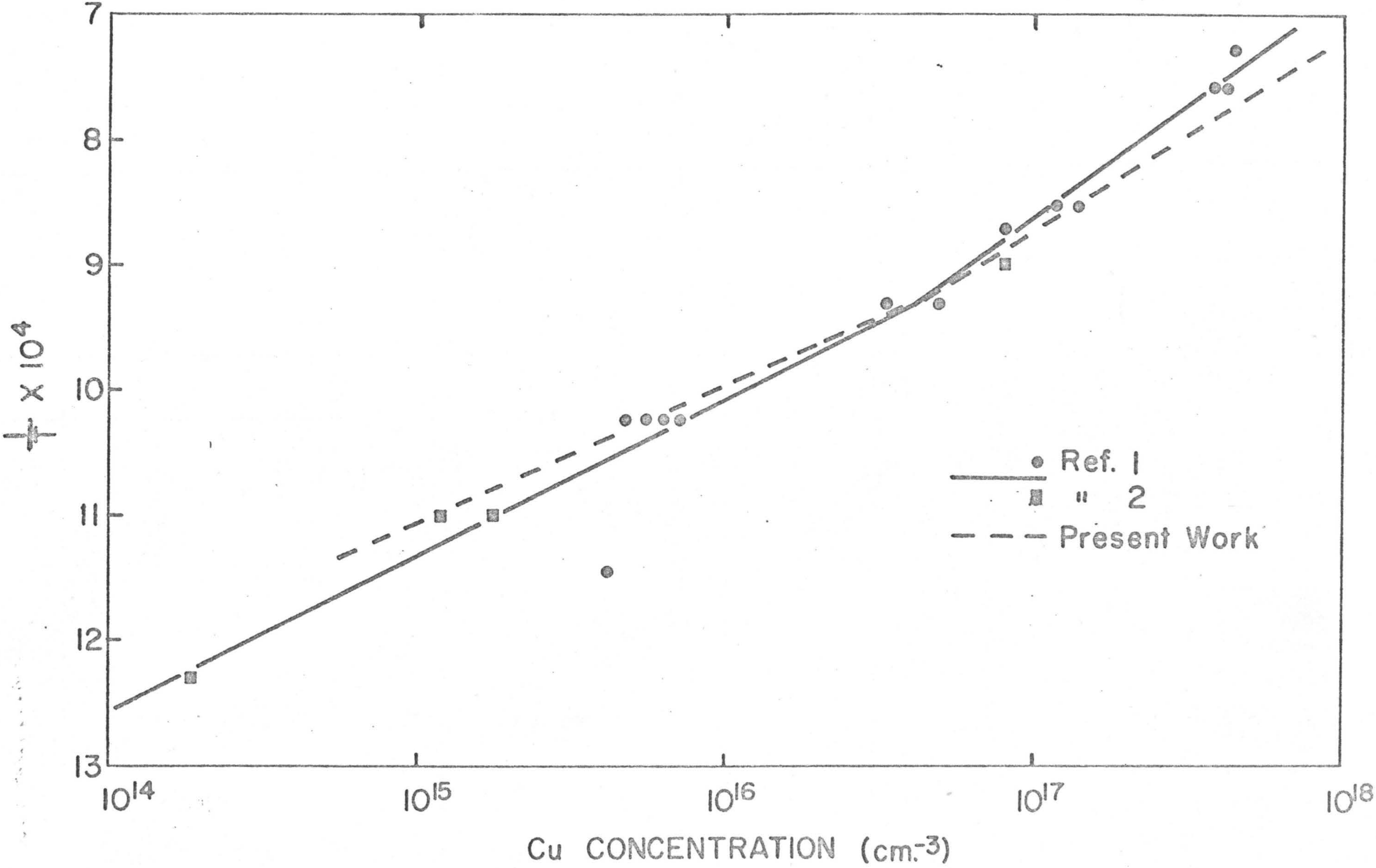

Figure 6.10. Comparison of previously reported solubility data with the present work on the Cu-Si system.
(1) Thurmond and Struthers (1953)
(2) Hall and Racette (1964)

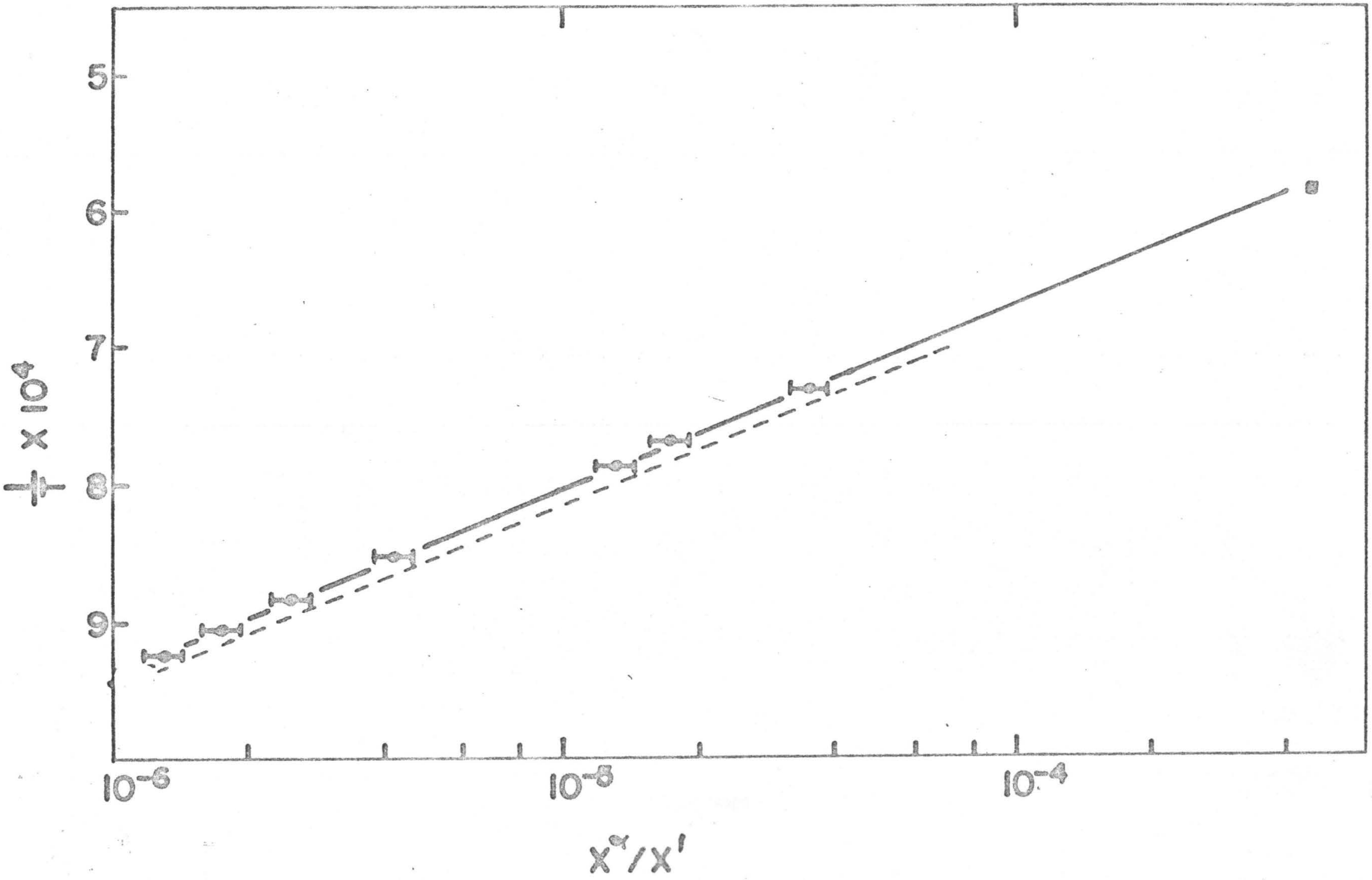

Figure 6.11. Plot of $\ln(X^{\alpha}/X^{1})$ vs. 1/T for copper in silicon. The dashed line represents $\ln(k^{e}/\gamma^{1})$ and the square point represents k_{m}^{e} reported by Trumbore (1960).

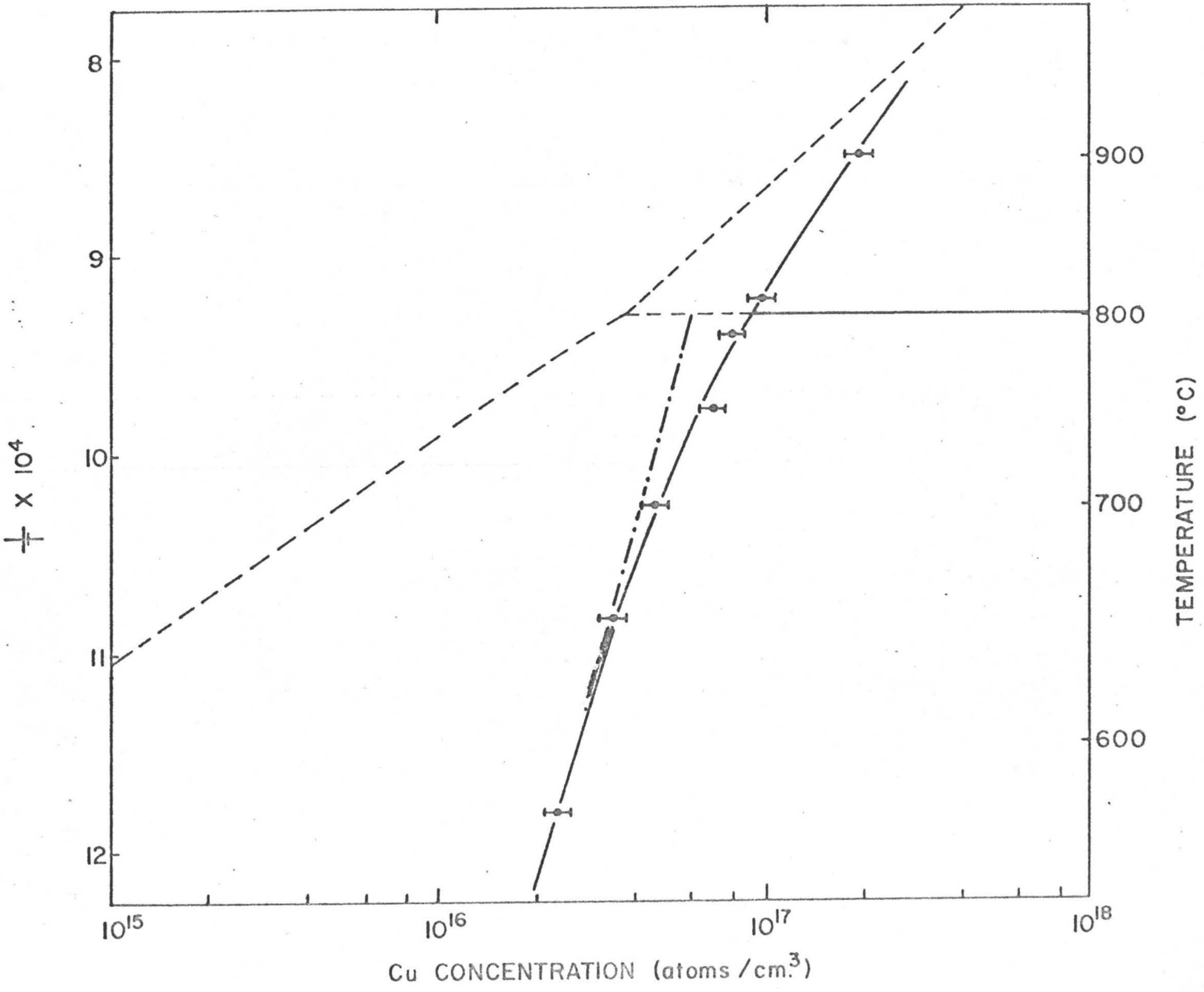

FIGURE 6.12. SOLUBILITY OF COPPER IN PURE POLYCRYSTALLINE SILICON. THE DASHED LINE REPRESENTS THE SINGLE CRYSTAL RESULTS AND THE DOT - DASHED LINE GIVES THE GRAIN BOUNDARY SOLUBILITY (ON A BULK SAMPLE BASIS).

Figure 6.13. Micrograph of polycrystalline Si X200, CP-4 etch. (perpendicular to growth direction)

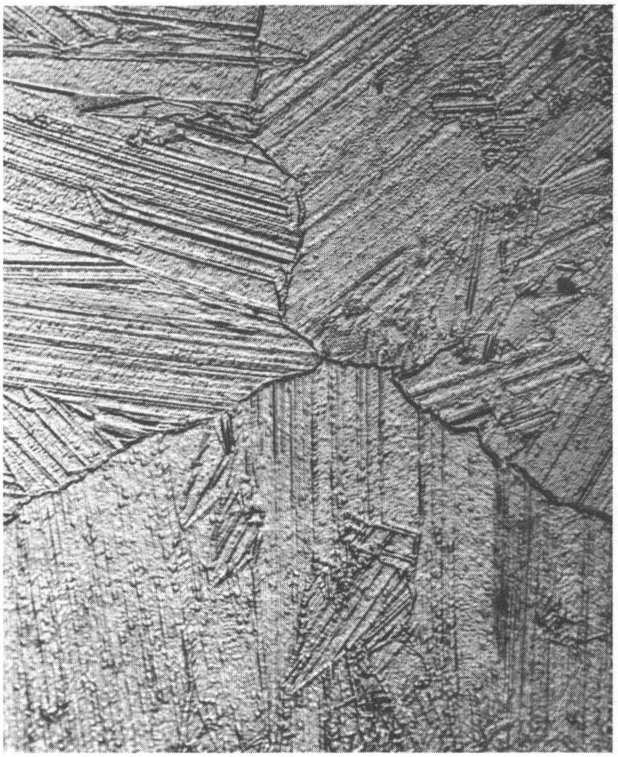

Figure 6.14. Micrograph of polycrystalline Si X625, CP-4 etch. (perpendicular to growth direction)

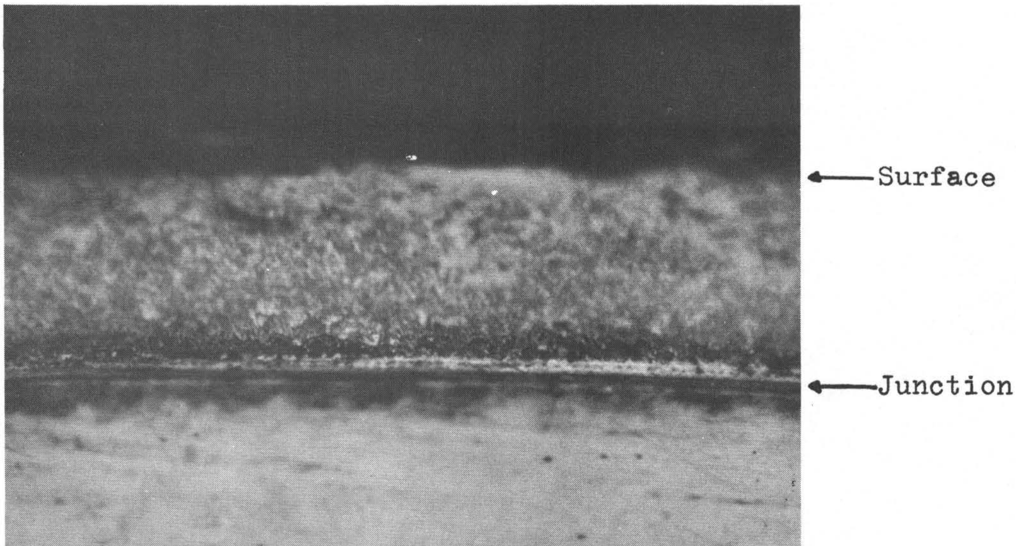

Figure 6.15. Micrograph of a p-n junction X565.

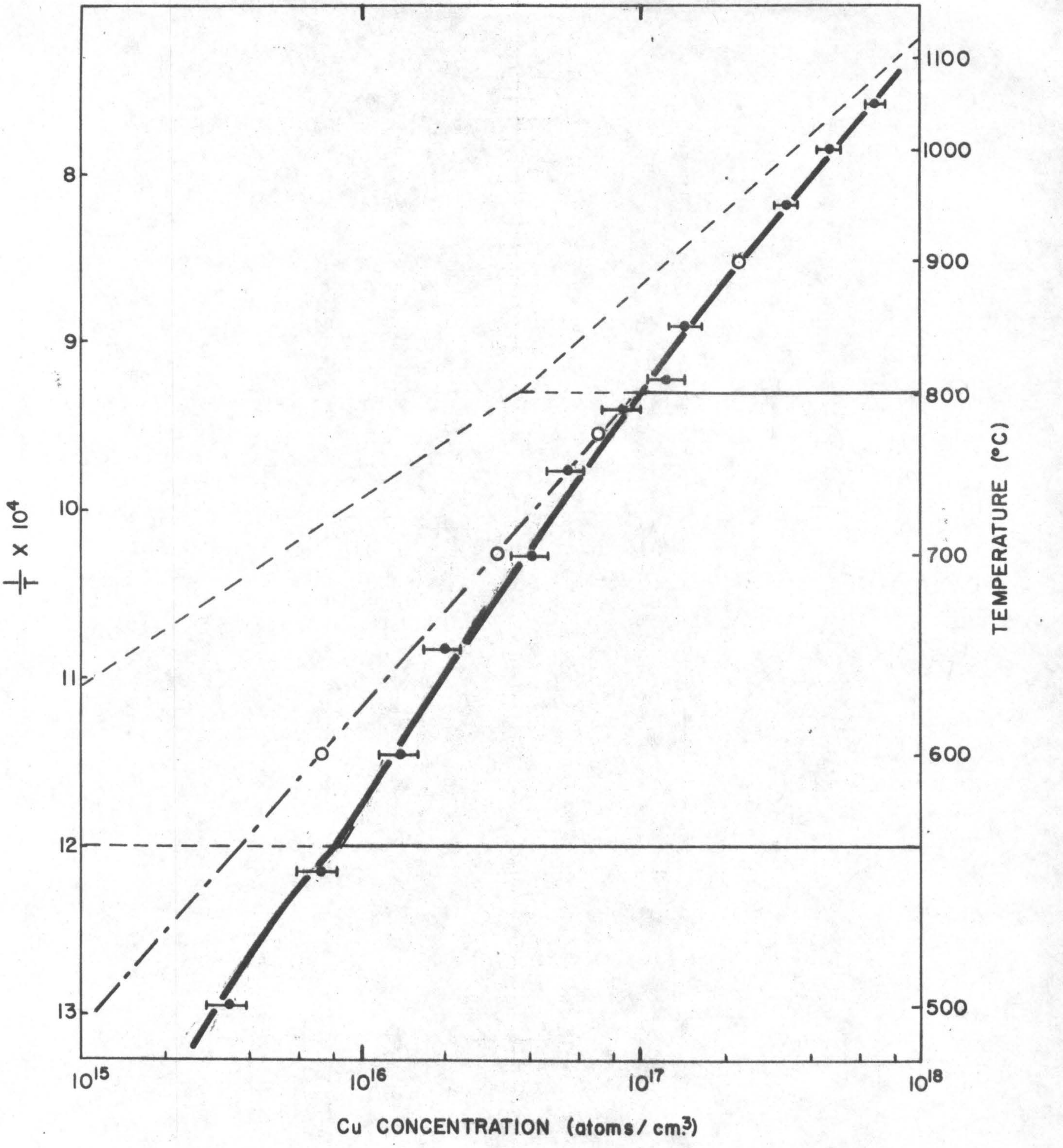

FIGURE 6.16. SOLUBILITY OF COPPER IN BORON DOPED SILICON (5 X 10^{18} ATOMS/CM^3).
THE DOT - DASHED LINE REPRESENTS THE THEORETICAL SOLUBILITY.

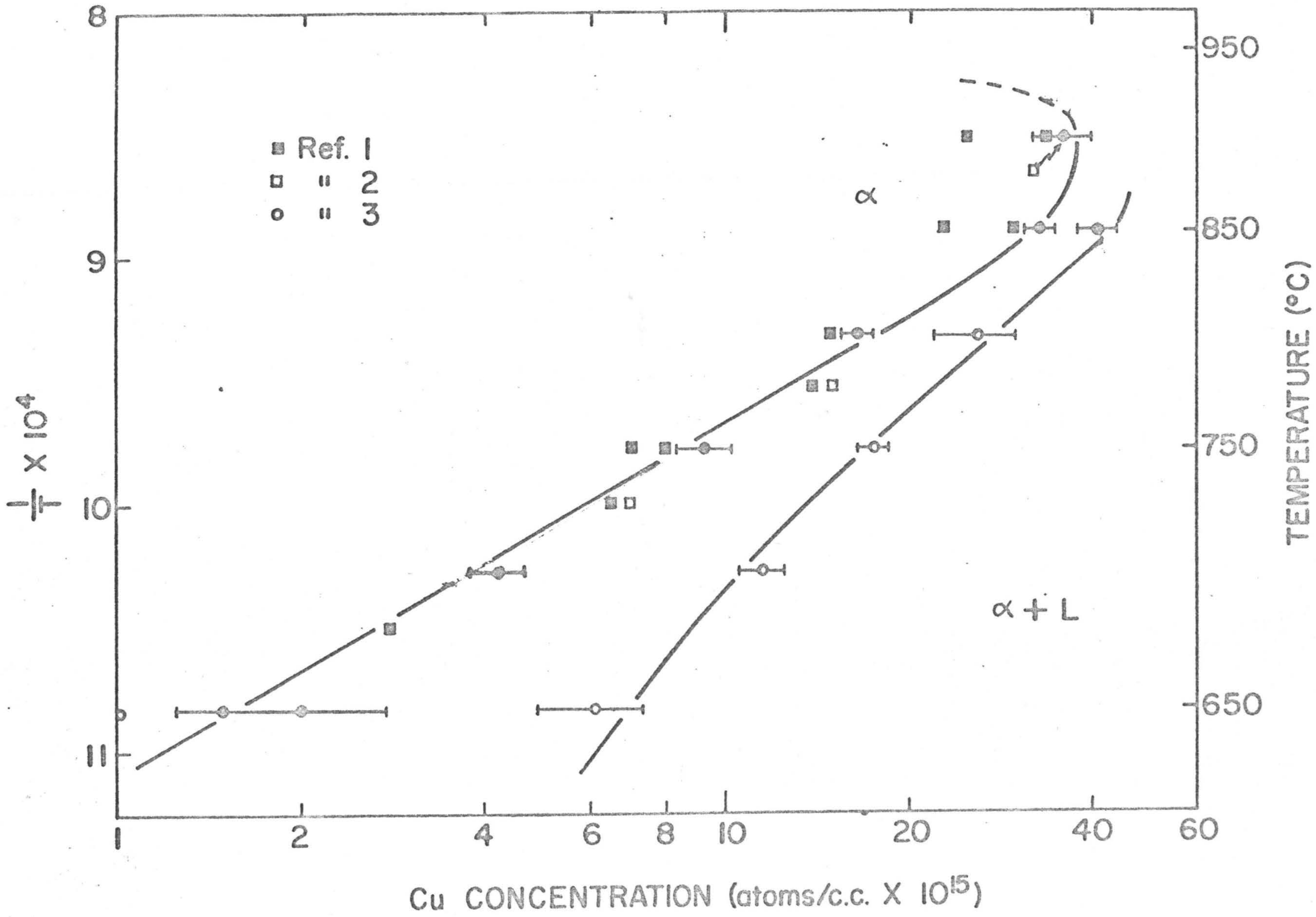

Figure 6.17. Solubility of copper in pure (solid circles) and in arsenic doped (open circles) germanium. Previously determined data for pure germanium is included for comparison. (1) Tyler (1959); (2) Burton et al (1953b); (3) Hall and Racette (1964).

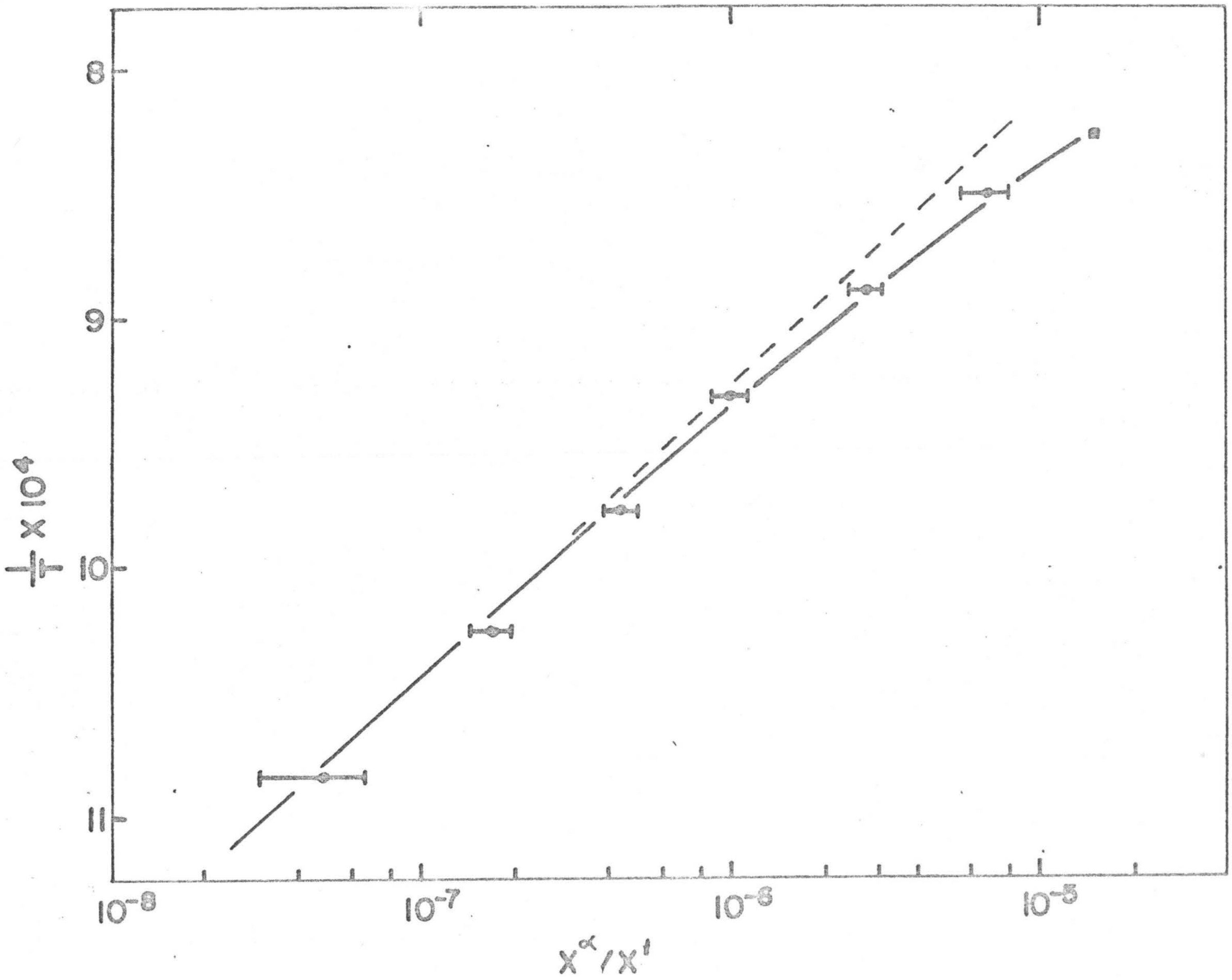

Figure 6.18. Plot of $\ln(X^{\alpha}/X^{l})$ vs. $1/T$ for copper in germanium. The dashed line represents $\ln(k^{e}/\gamma^{l})$ and the square point represents k_{m}^{e} reported by Trumbore (1960).

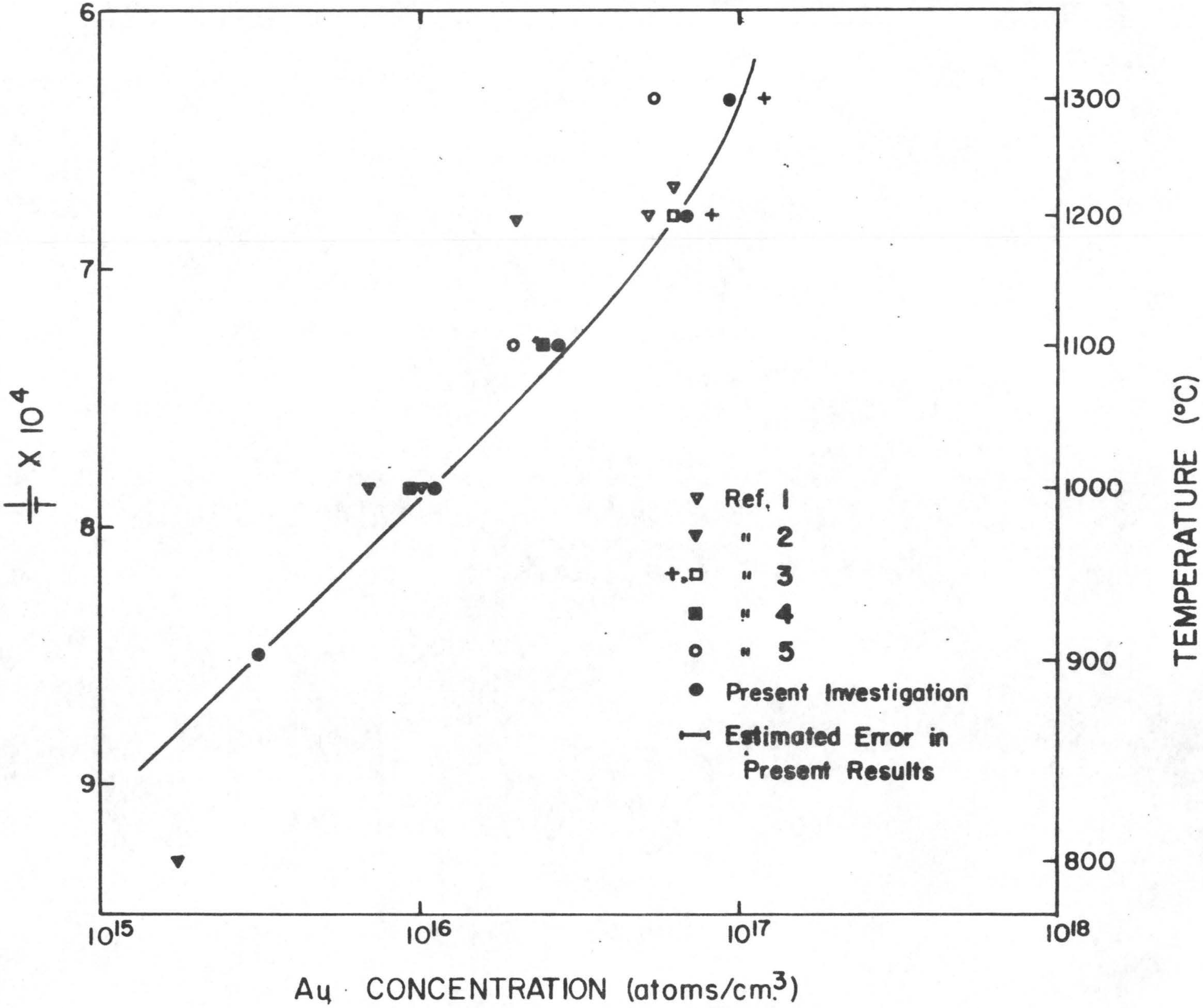

Figure 6.19. Solubility of gold in pure single crystal silicon. The previously determined data are from: (1) Struthers by private communication to Trumbore (1960); (2) Struthers (1956); (3) Collins et al (1957); (4) Sprokel and Fairfield (1965); and (5) Boltaks et al (1960-61).

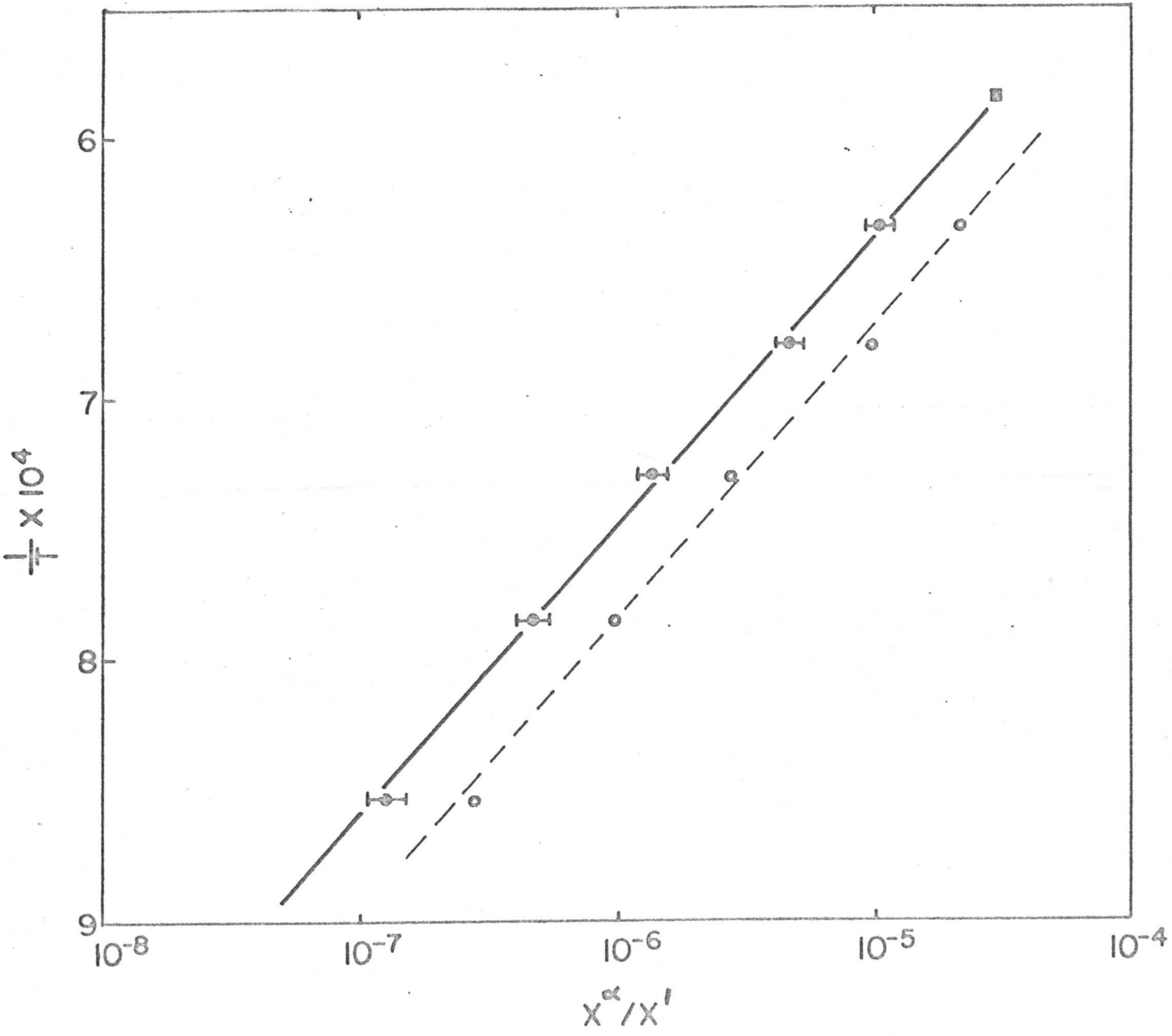

Figure 6.20. Plot of $\ln(X^{\alpha}/X^{l})$ vs. $1/T$ for gold in silicon. The dashed line represents $\ln(k^{e}/\gamma^{l})$ and the square point represents k_{m}^{e} reported by Trumbore (1960).

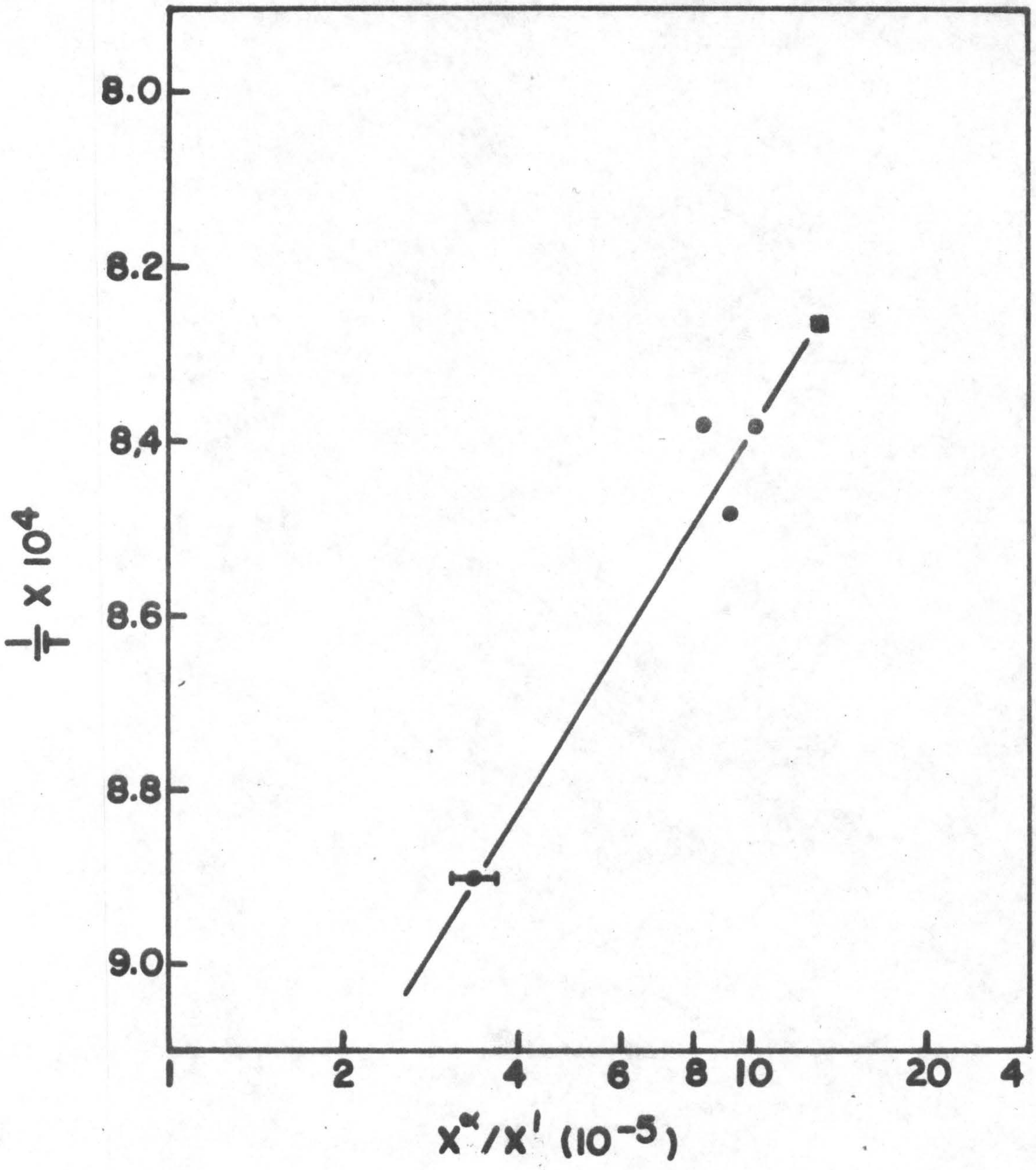

Figure 6.21. Plot of ln(X /X^{1}) vs. 1/T for gold in germanium. Square point (Trumbore, 1960), open circles (Tyler, 1959), solid circle (Syed, 1964).

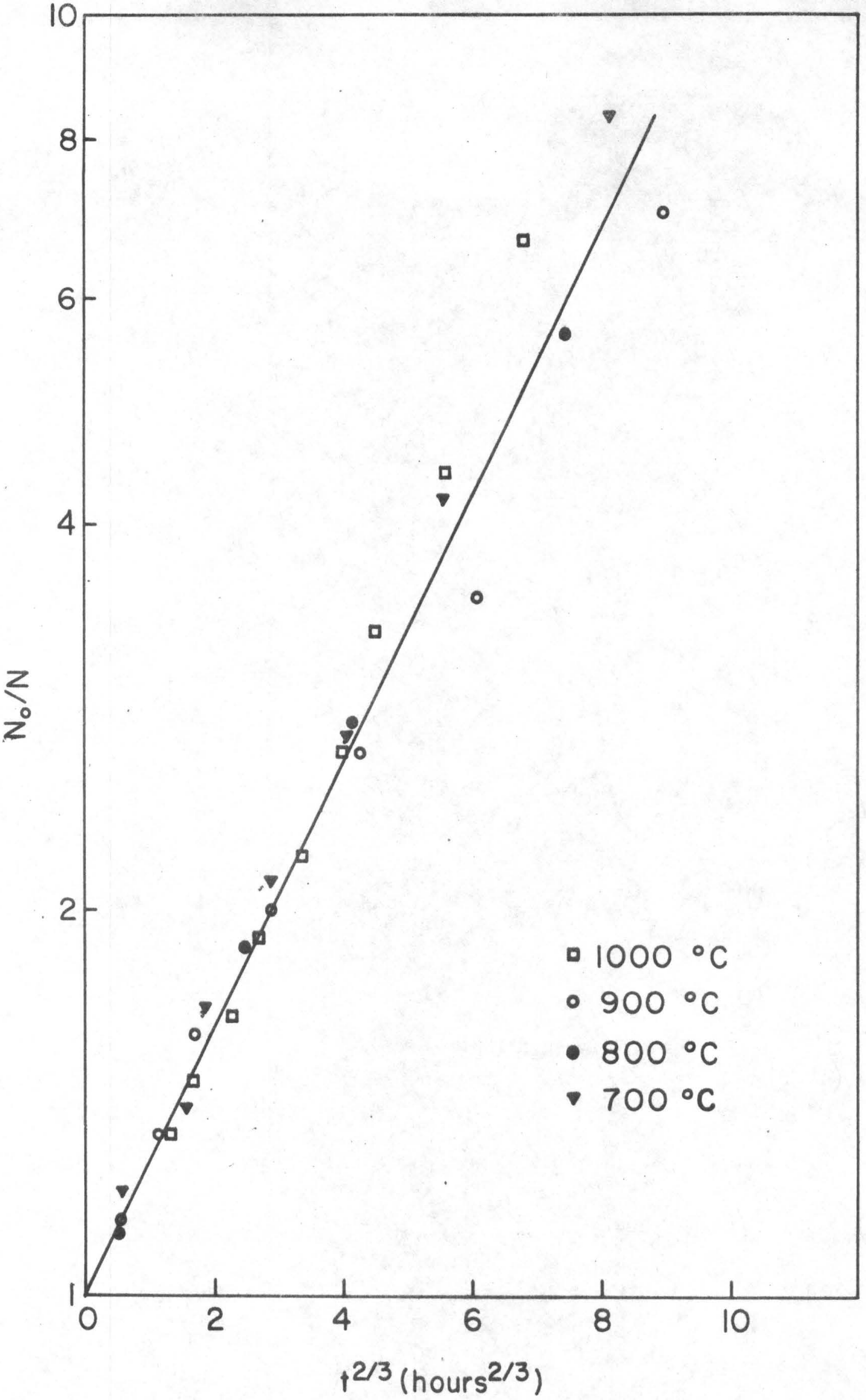

Figure 6.22. Plot of $\ln(N_o/N(t))$ vs. $(\text{time})^{2/3}$ for copper precipitation in silicon at 30°C. The various symbols represent different saturation temperatures.

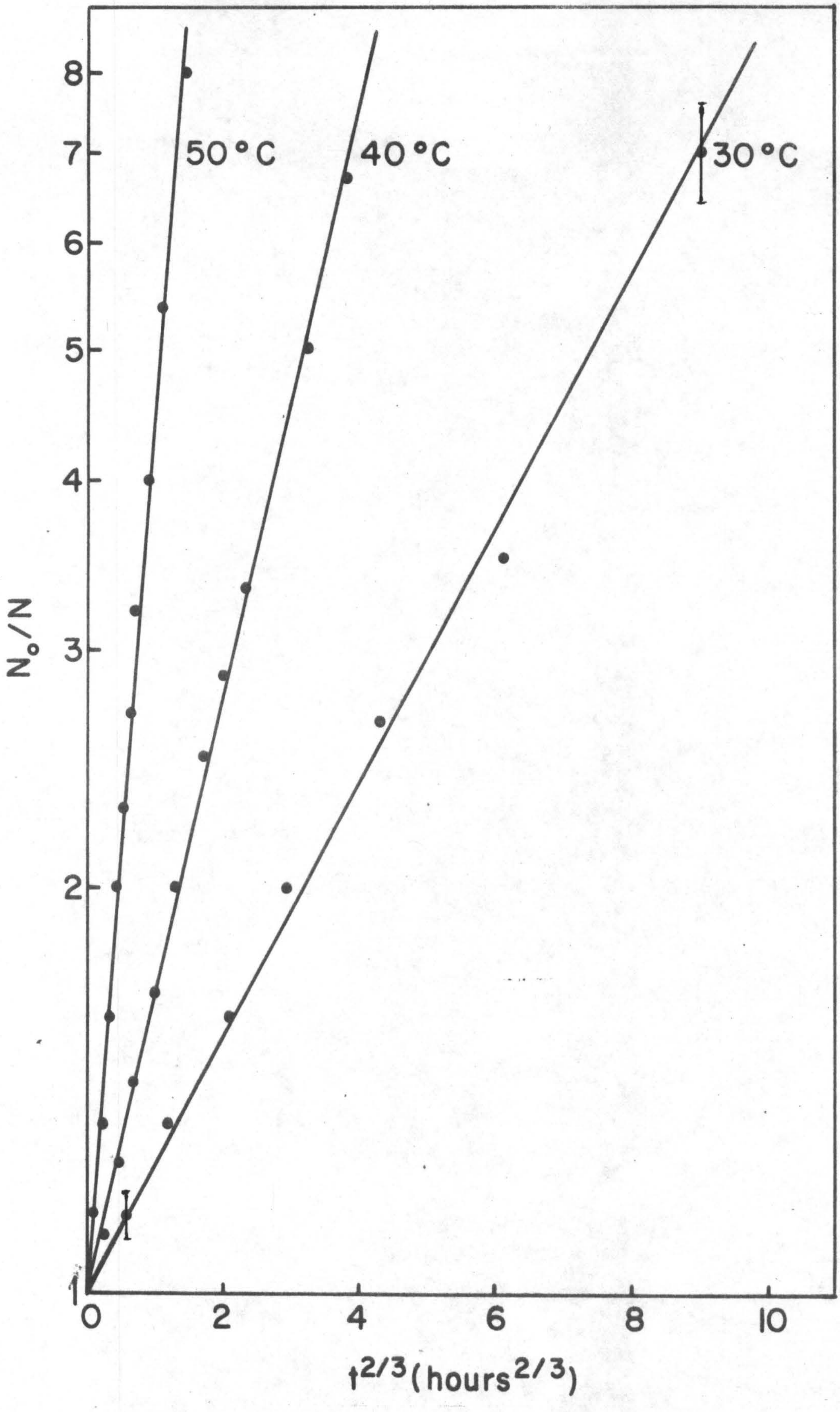

Figure 6.23. Precipitation curves for copper in silicon near room temperature. All samples were saturated at 900°C.

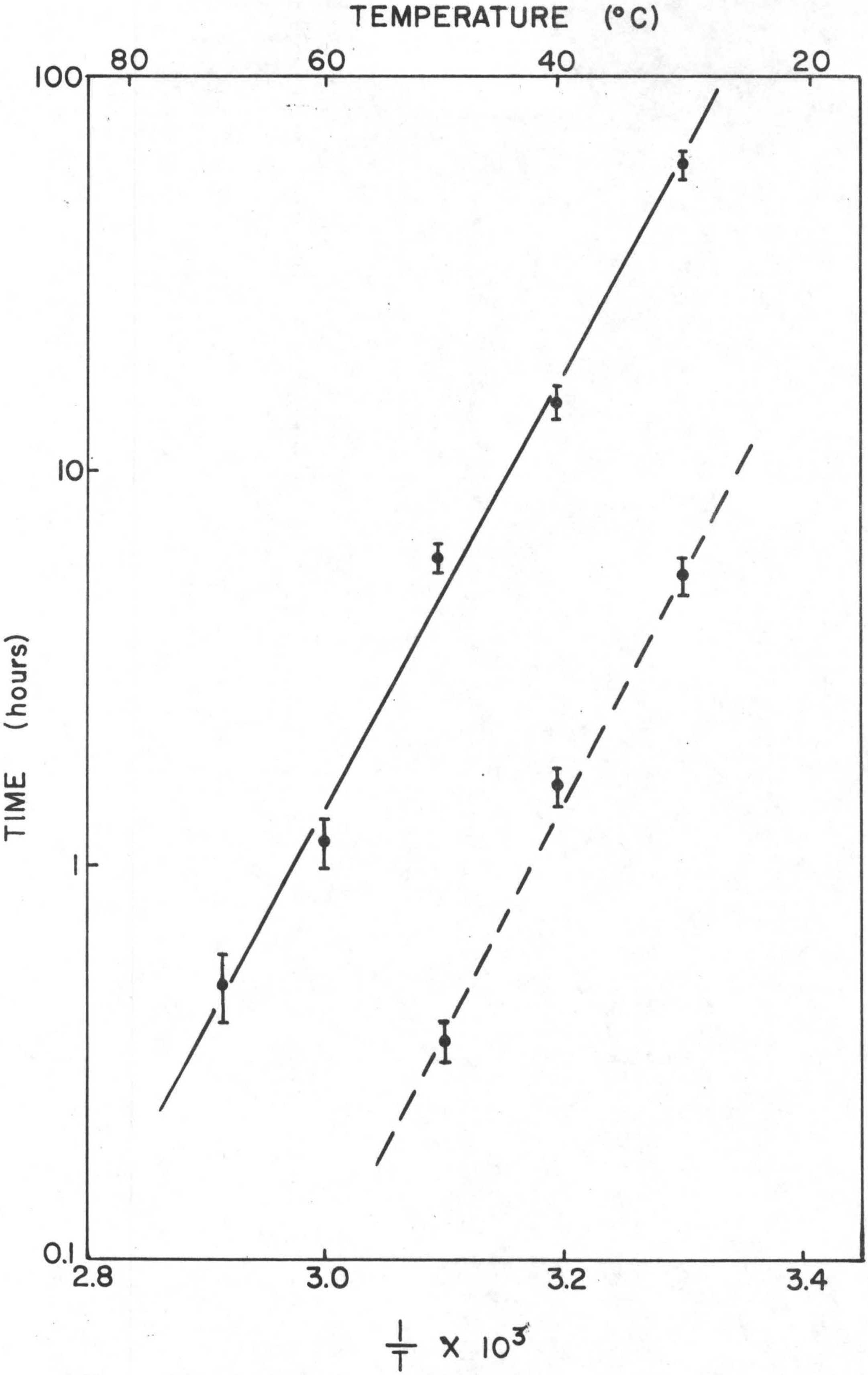

Figure 6.24. Plot of t_f vs. 1/T for copper precipitation in silicon. The solid line represents the time to 100 pct. completion and the dashed line represents 50 pct. completion. The former gives an activation energy of 1.10 ± 0.05 eV and the latter gives approximately 1.15 eV.

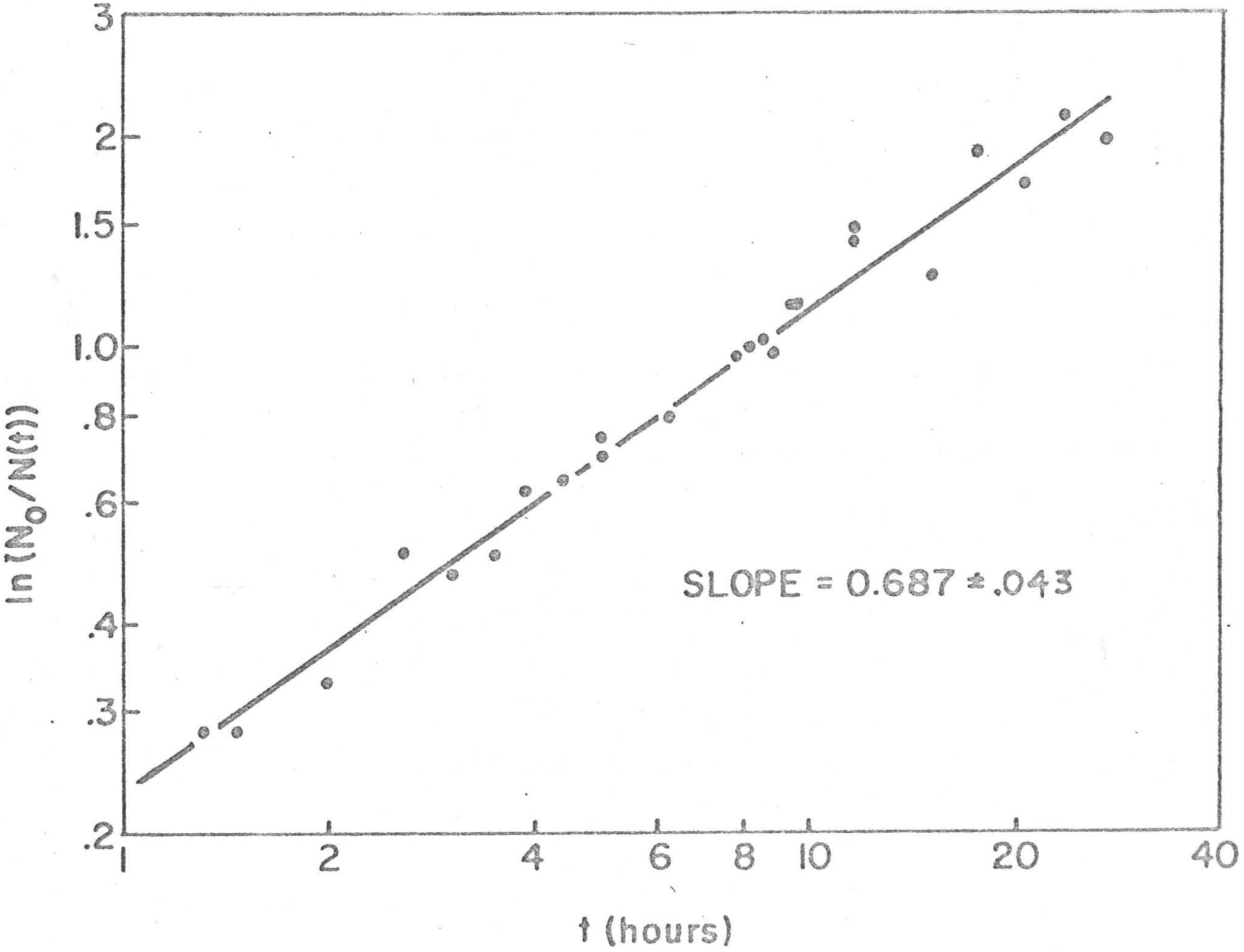

Figure 6.25. Plot of $\ln(\ln(N_0/N(t)))$ vs. $\ln(t)$ for precipitation of copper in silicon at 30°C.

CHAPTER 7

DISCUSSION OF RESULTS

7.A Binary Solution Thermodynamics

7.A.1 The Copper-Silicon System

The relative partial molar enthalpy and excess entropy of copper in silicon (37.3 ± 0.5 Kcal./mole and 7.1 ± 0.4 cal./mole - °K respectively) were determined from Equation 4.1 after calculating the activity coefficient of copper in the liquidus alloy by methods outlined in Chapter 4. Calculations to determine the effect of neglecting the heat capacity difference between pure solid and pure liquid copper at the various temperatures were conducted (see Appendix C) and the results show good justification for neglecting this term. It was also assumed that the partial molar enthalpy of solution was independent of temperature over the ranges considered, and this can really be justified only by experimental evidence in a broad range of systems. Experiments in which solubility measurements are made in simple two phase systems of low mutual miscibility, where complicating effects due to non-ideality of the solute in equilibration phases are absent, usually yield linear ln X vs. 1/T plots.

The error in the assumption of the temperature independence of ΔH can be roughly estimated by the following iterative procedure.

Equation 4.1 may be written as

$$\ln \frac{k_2^e}{\overset{T}{\gamma}_2} = \frac{\Delta H_2^f\,(T') - \Delta\overline{H}_2^{\alpha}\,(T')}{RT} + \frac{\Delta\overline{S}_2^{ex,\alpha}\,(T') - \Delta S_2^f\,(T')}{R}$$

$$+ f_1\,(T) + f_2\,(T),$$

where T' is an arbitrarily specified temperature within the range considered, f_1 (T) is described in Appendix C, and

$$f_2\,(T) = \frac{\Delta\overline{C}_2^{\alpha}}{R}\,(\ln \frac{T}{T'} - \frac{T - T'}{T}). \tag{7.1}$$

$\Delta\overline{C}_2^{\alpha}$ is the relative partial molar heat capacity of the solute and is assumed to be temperature independent over the range of interest. An alternative procedure frequently encountered assumes that

$$\Delta S = \text{Constant}$$

and

$$\Delta H = \Delta H^{\circ}\,(1 + \theta T),$$

where ($\Delta H^{\circ}\theta$) is a temperature independent heat capacity factor. In our treatment, however, the entropy term is not considered independent of temperature so that the thermodynamic relationship

$$(\frac{\partial(\Delta S)}{\partial T})_P = \frac{1}{T}\,(\frac{\partial(\Delta H)}{\partial T})_P$$

is obeyed, as it must be.

Our procedure goes as follows. The relative partial molar excess entropy of a solute may be expressed by

$$\Delta\overline{S}_2^{ex,\alpha} = \int_0^T \frac{\Delta\overline{C}_2^{\alpha}}{T}\,dT\,.$$

It is conceivable that a first value of $\Delta\bar{C}_2^{\alpha}$ can be estimated from experimental determinations of $\Delta\bar{S}_2^{ex}$ (assuming $f_2(T)$ to be zero) and an empirical correlation of heat capacity and absolute entropy values for a number of metals at temperatures of interest. Such an estimate at 1300°K indicates that $\Delta\bar{C}_2^{\alpha} \approx 1.5$ cal./mole-°K (conservatively large) for $\Delta\bar{S}_2^{ex} = 10$ cal./mole-°K.(a reasonable value based on the present work). Further iteration seems unnecessary since $f_2(T)$ evaluated at 1100°K for T' = 1300°K is only 0.01. The above treatment is undoubtedly subject to question; however, in view of the observed linearity of the present experimental solubility curves it is not inconsistent with the fact that $\Delta\bar{C}_2^{\alpha}$ should be small, viz.

$$\frac{\partial(\Delta\bar{H}_2^{\alpha})}{\partial T} = \Delta\bar{C}_2^{\alpha} .$$

The value of the extrapolated equilibrium distribution coefficient at the melting point of silicon (4×10^{-4}) agrees very well with that reported by Trumbore (1960) as determined by solidification experiments. Other values of the solubility parameters have been reported by Hall (1957) and by Thurmond and Struthers (1953). Hall gives $\Delta\bar{H} = 37$ Kcal./mole or $\Delta\bar{S}^{ex} = 5.9$ cal./mole - °K (not interpreted as an excess entropy factor by Hall), and $k^e = 2.5 \times 10^{-4}$. Thurmond and Struthers determined $\Delta\bar{H} = 35.7$ Kcal./mole and $K^e = 3.2 \times 10^{-4}$. Neither of these investigations took into account non-ideality of the liquid phase but this effect is not really significant in this system. The present data yields values of $\Delta\bar{H} = 36.9$ Kcal./mole and

$\Delta\overline{S}^{ex}$ = 6.7 cal./mole - °K when the corrections are neglected, as compared to the values given on page 124.

Below the eutectic temperature where equilibration was conducted with Cu_3Si, the partial molar enthalpy and excess entropy were determined to be 40.5 Kcal./mole and 9.7 cal./mole - °K respectively (with respect to Cu_3Si). If account is taken of the fact that Cu_3Si is probably ordered, the excess entropy term is 9.1 cal./mole - °K, ie. $R \ln X_{Cu}^{\eta} \approx - 0.6$. It is seen that the excess entropy is greater when evaluated with respect to the intermediate compound than with respect to the pure metal. Freedman and Nowick (1958) suggested the possibility of this behavior because of tight binding of intermediate compounds, but they could not prove the hypothesis from their tests on various binary metallic alloys in which compensating near-neighbor interactions are believed to occur (see Section 4.B.2).

The absolute entropies of copper and silicon at 1300°K are 17.44 and 13.08 cal./mole - °K, respectively (Stull and Sinke, 1956). The entropy change relative to the pure silicon lattice (specific thermal entropy) is therefore 11.5 ± 0.5 cal./mole - °K (cf. Equation 3.20). Zener's qualitative approach to the determination of the thermal entropy cannot be applied to this system because theoretical predictions indicate that interstitial copper does not strain the silicon lattice (Weiser, 1962). Attention instead must be focussed on near neighbour chemical interactions. Since copper in silicon is an interstitial impurity and its atoms probably do not share covalent bonds with the host atoms (loosely bound), the near neighbor vibrational interactions which Freedman and Nowick considered should be small, ie. $\nu_{12} < (\nu_1\nu_2)^{1/2}$. A low vibrational frequency of the copper ions (also influenced by their relatively large mass) therefore favors a large positive thermal entropy.

The polarization entropy obviously does not contribute significantly to the excess entropy since it amounts to only 1 cal./mole - °K. (see Section 3.D). Other factors which have not been considered may also play a role in the lattice dynamics of this interstitial solution. The solute atoms may possibly reduce the bond energies or increase the effective masses of the surrounding silicon atoms. With "looser" bonds and/or larger atomic masses, the lattice would have lower vibrational frequencies and a higher thermal entropy. Weiser's assumption that the solvent atoms retain their equilibrium positions in the presence of copper ions may also be incorrect, and in this case strain energy considerations should be taken into account. If such is the case, a negative contribution to the thermal entropy would also arise because the restoring forces between the host atoms are increased (Huntington et al, 1955).

7.A.2 The Gold-Silicon System

The partial molar enthalpy and excess entropy of solution of gold in silicon were calculated in the same way as for the copper-silicon system to be 43.8 ± 1.4 Kcal./mole and 6.8 ± 1.0 cal./mole - °K, respectively. Neglecting non-ideality of the liquid phase in this system does not alter the heat of solution but does result in a low excess entropy. Appendix C shows that the heat capacity difference between liquid and solid gold can be disregarded in this system. The extrapolated value of the equilibrium distribution coefficient at the melting point of silicon (3×10^{-5}) agrees well with Trumbore's (1960) value of 2.5×10^{-5}.

Calculations by Hall (1957) and by Wackwitz (Bullis, 1966) based on the experimental results of Collins et al (1957) gave the enthalpy of solution as 51.1 and 51.8 Kcal./mole, respectively. The author also analyzed these results and obtained a solution enthalpy of 49.1 Kcal./mole and an equilibrium distribution coefficient of 4×10^{-5}. The discrepancy between the two calculations is probably due to the fact that Hall used ideal liquidus compositions rather than the values depicted by the phase diagram for the system. Wackwitz's method is not known since his result was reported as unpublished work by Bullis. The present solubility data are believed to give more accurate solubility parameters because measurements were conducted over a wider temperature range and the equilibrium distribution coefficient is nearer to the value obtained from solidification experiments.

The thermal entropy change relative to the silicon lattice is 14.6 ± 1.0 cal./mole - °K (using $S^\circ_{A\mu}$ at 1300°K as 20.9 cal./mole - °K). This is seen to be substantially larger than the thermal entropy of copper in silicon. Part of this difference probably arises because of the relatively heavy mass of a gold atom. It is hardly valid to compare the thermal entropies of solution of gold and copper in any case because of their differences in lattice position. Gold is a substitutional impurity and has a large tetrahedral covalent radius compared to that of silicon (1.50 A° and 1.18 A°, respectively). A large portion of the excess entropy therefore may be explained by Zener's predictions concerning strain energy effects. Tending to counteract this contribution will be an effect arising from atom crowding in the vicinity of the gold ions. Another factor favoring a positive excess entropy in this system is the fact that gold and silicon do not form any intermediate compounds suggesting that strong chemical bonding does not take place between the solvent and solute atoms.

7.A.3 The Copper-Germanium System

The relative partial molar enthalpy and excess entropy of copper in germanium were determined to be 41.3 ± 0.7 Kcal./mole and 10.3 ± 0.6 cal./mole - °K, respectively. It was discovered that the effect of non-ideality of the liquid phase on the distribution coefficient is quite significant in this system, especially near the melting point of germanium. If a smooth curve is drawn through the $\ln(X^{\alpha}/X^{1})$ values and the equilibrium distribution coefficient at 937°C reported by Trumbore (1960) it is seen that the curvature in the $\ln k^{e}$ vs. $1/T$ plot is quite marked (Figure 6.18).

Previous experimental determinations of these parameters are given by Hall (1957) as $\Delta\bar{H} = 44$ Kcal./mole and $\Delta\bar{S}^{ex} = 12$ cal./mole - °K. Thurmond and Struthers calculated the heat of solution as 45.2 Kcal./mole. An ideal liquidus was assumed in both of these investigations, however, and this probably accounts for the discrepancy since the present solubility data agree quite well with the determinations of Thurmond and Struthers.

The thermal entropy of copper in germanium relative to the germanium lattice is 8.7 ± 0.6 cal./mole - °K.* This is much lower than the thermal entropy of gold in silicon, and probably one of the most important factors contributing to this variation is the difference in relative masses of the atoms in these systems. As was discussed previously, strain energy effects must be taken into account for substitutional solutes. Copper in germanium does not result in as much misfit as does gold in silicon (r_{Cu} = 1.35 A° and r_{Ge} = 1.22 A°), but Equation 3.20 shows that the thermal entropy arising from strain effects is proportional to - $(\partial\mu/\partial T)$. McSkimin (1953) has shown that this factor is approximately 1.5 times as large for germanium than for silicon so strain effects are more significant in germanium for given differences in atomic size. If it is assumed that the strain free energy is proportional to $R_1(\delta R)^2$ (Freedman and Nowick, 1958), where R_1 is the radius of a solute atom and δR is the difference in the radii of the solvent and solute atoms, then the strain contribution to the thermal entropy of the gold-silicon system is four times that of the copper-germanium system.

It is questionable, however, whether a normal tetrahedral covalent radius can be assigned to these impurities because their covalent bonds with surrounding solvent atoms are not complete unless they are triply charged. Gold in silicon only has one acceptor level

---

[*] Evaluated from data given by Smithells (1962).

in the band gap at room temperature so it is doubtful whether more than two bonds are complete in this system. The acceptor levels of copper in germanium on the other hand are nearer the valence band so its covalent bondage will be relatively more complete. Consequently, the difference in strain free energy between the two systems is probably not as great as originally estimated here.

Another factor which has not been considered is that of nearest neighbor chemical interactions. Since intermediate compounds are formed between copper and germanium, it may be expected that because of tighter bonding, this system will also tend to have a lower thermal entropy than the gold-silicon system due to high vibrational frequences in the neighborhood of a solute atom.

7.A.4 The Gold-Germanium System

Figure 6.21 shows fairly good agreement between the solubility determined at 850°C by diffusion methods and other measurements conducted by solidification experiments. The thermodynamic properties of the system were not determined because the experimental data are insufficient to justify such calculations. Further experimentation on this system was not conducted because long diffusion times are required to saturate samples of a reasonable size for accurate chemical analysis. On the basis of the available results, however, the equilibrium distribution coefficient was estimated to be represented by the relation

$$k^e = 4.0 \times 10^2 \exp\left(\frac{-42{,}000}{RT}\right) .$$

Since the activity coefficient of gold in liquid germanium is less than unity and decreases with decreasing concentration (cf. Equation 4.3 and the liquidus data of Thurmond and Kowalchik, (1960)), it would appear from the above relation that the partial molar enthalpy and the specific thermal entropy of solution are not less than 45 Kcal./mole and 16 cal./mole - °K, respectively.

7.B Meta-stable Copper-Silicon Equilibrium

Fairly conclusive evidence has been found for retardation in the nucleation of intermediate compounds in copper-silicon diffusion couples. Figures 6.1 and 6.2 show how the "solubility" of copper in silicon obtained from such couples varies with time. The silicon wafers used for these studies were one millimeter thick and since the diffusion coefficient of copper in silicon is large, the time required for saturation was short. High initial solubilities for short times indicate meta-stable equilibrium (see Figure 2.7) which can only occur in the absence of Cu_3Si. In other words, the silicon is initially in meta-stable equilibrium with either copper or a copper silicide other than Cu_3Si.

A number of couples were reacted in the temperature range 650°C to 800°C for various times and the interface regions were observed with an optical microscope. This method of observation must be treated with reservations because the nuclei may be too small to be visible at early times; however, it is often useful for supplementing other measurements. Interface precipitates were not observed until the samples had been reacted for at least one hour. Figure 6.6 shows the interface region of a sample reacted at 750°C for two hours and it reveals two small precipitate particles. Another sample reacted for 24 hours at 750°C (Figure 6.5) showed only about 25 per cent interface coverage. In all cases only one type of precipitate was observed by metallographic means, thus indicating the continuing absence of three other copper silicides which should appear at these temperatures. This suggests that meta-stable equilibrium occurs between copper and silicon.

The interface precipitates were analyzed by electron microprobe analysis using pure copper as a standard and a relative intensity of 0.806 ± 0.018 was obtained. Similar analysis of prepared Cu_3Si yielded a relative intensity of 0.824 ± 0.017. The theoretical value for Cu_3Si was calculated to be 0.810. These results indicate that the interface precipitate is Cu_3Si, however, another copper silicide ($Cu_{15}Si_4$) has a theoretical relative intensity of 0.838 so it was decided to conduct X-ray diffraction tests for further identification. These data (Figures 6.7 and 6.8 and Table 6.2) show quite conclusively that the interface precipitate is in fact Cu_3Si. It is also interesting to note that the X-ray diffraction experiment did not reveal the presence of any other copper silicides thus giving further support to the suggestion that the high solubility at early times indicates meta-stable equilibrium between copper and silicon.

Another sample which was reacted at 810°C (above the eutectic temperature) for two hours was also observed metallographically and tested by X-ray analysis in order to ensure that equilibrium was attained with the liquidus. According to the phase diagram a liquidus alloy at this temperature should solidify to Cu_3Si plus a small amount of silicon. Precipitates of this type were observed and the X-ray analysis identified the major precipitate as Cu_3Si.

The requirement for nucleation of a second phase in a diffusion couple between two elements is that the free energy of the system be lowered by such a process. The free energy associated with the formation of a second phase is generally composed of three terms: a chemical or volume component which is negative, a surface component which is positive, and a positive strain component which arises if volume changes are significant. Quite often the system chooses a configuration which minimizes the last two terms. If normal surface energies are high the precipitate - matrix interface may be coherent, i.e. atomic bonding is maintained across the interface, at the expense of strain energy. The shape of the precipitates is also often subject to conditions which tend to minimize the free energy. Spherical particles, for example, have the lowest surface energy per unit volume of chemical free energy. Precipitates often form as disks or needles, however, to lower the strain energy of the system.

In most practical cases the formation of a new phase occurs at defects present in the system (heterogeneous nucleation). In this way the energy required to form a new surface may be reduced by nucleation on inclusions and grain boundaries. In the same way strain energy may be reduced by nucleation at dislocations. It could be expected that nucleation of a second phase in a diffusion couple should occur at the interface between the two materials since the degree of supersaturation is greatest at this region and also because a surface is present. Dislocations may also play an important role near the interface if the diffusion process generates these defects (Jaccodine, 1964) or if they were introduced during sample surface preparation.

An important parameter in the present problem is the nucleation rate, ie. the number of nuclei that appear per unit area of interface per unit time. The nature of heterogeneous nucleation is very complex and since little or nothing is known about the surface, volume, and strain contributions to the free energy of formation of intermediate phases in the copper-silicon system, the discussion will be limited to a qualitative description.

The number of critical nuclei, n, present in a system is given by (Burke, 1965)[b]

$$n = N \exp\left(- \frac{\Delta F}{kT}\right),$$

where N is the number of available nucleation sites and ΔF is the free energy required to form a critical nucleus. A critical nucleus is one which may lower its free energy by growing in size by an infinitesimal amount. The free energy of formation as discussed previously is composed of volume, strain, and surface terms. A critical nucleus becomes a stable nucleus when it gains one or more atoms, so if the jump process across the precipitate-matrix interface is governed by an activation energy, U, the frequency with which critical nuclei become stable is $n_s.p.\nu.\exp(-U/kT)$, where n_s is the number of atoms in the matrix at the surface of the critical nucleus, ν is the frequency of vibration of these atoms, and p is the probability that a vibration is in the direction of the nucleus times a factor which expresses the fact that attachment of atoms may occur preferentially at certain points on the surface. Under steady state conditions the nucleation rate, I, is then

$$I = N.n_s.p.\nu.\exp\left(-\frac{U + \Delta F}{kT}\right) .$$

Probably the most important factor in this expression is the free energy of formation of a critical nucleus. If the strain and surface terms are large compared to the volume component of the free energy, the nucleation rate will be slow and could, in fact, be negligible.

Of interest also is the rate at which the stable nuclei grow in the interface region once they have formed. This is governed partially by the diffusion coefficients of the two elements in the intermediate phase. If the diffusion coefficients are low, then the precipitate naturally grows slowly.

It should also be mentioned that certain criteria pertaining to the growth of the precipitates also must be satisfied in order to maintain a stable precipitate layer at an interface between two interdiffusing elements. A critical nucleus has a critical size as well as a critical free energy of formation. If a nucleus forms in the interface region of a diffusion couple and its kinetically predicted thickness calculated from time zero is less than its critical size, then a stable growing precipitate layer would not be expected to form (Cox, 1965).

The results and theory discussed above show that care must be taken when determining the solubility of one element in another by placing them in intimate contact and allowing them to interdiffuse. If intermediate phases exist in the system, these phases must nucleate and grow in the reaction zone between the two materials in order that a true equilibrium solubility can be obtained. If nucleation problems are present, long diffusion times must be employed to ensure that true equilibrium is attained. The present results obtained in this manner agree quite well with the solubility determined by vapor equilibration with Cu_3Si.

7.C Grain Boundary Solubility of Copper in Silicon

It was found that the solubility of copper in polycrystalline silicon is greatly enhanced as compared to single crystal material. The enthalpy of solution is also much less ($\bar{H} - \bar{H}^{g.b.} = 33.9 \pm 0.9$ Kcal./mole) and this quantity may be regarded as a binding energy of copper ions in grain boundary regions. This is much larger than binding energies in metals which have been estimated to be a few tenths of an electron volt. Van Bueren (1960)[b] has suggested that strong chemical bonds may form between unpaired electrons at dislocations in homopolar crystals. It appears reasonable that similar effects may occur at grain boundaries since they are probably regions of broken covalent bonds.

In calculating the binding energy it was assumed that the enthalpy of solution is independent of concentration and the linearity of the ln $X^{g.b.}$ vs. 1/T plot tends to support this assumption. A calculation of the grain boundary solubility from Equation 3.31 (a mole fraction of 0.43 ± 0.10) would seem to make this calculation less accurate, however, since Henry's law is usually obeyed only up to a maximum concentration of about one or two atomic per cent in normal non-ideal solutions.

An attempt was made to estimate the grain boundary area by metallographic studies. Figures 6.13 and 6.14 show that the grain structure of vapor grown silicon is very complex and consequently a quantitative determination was impossible. The polycrystalline ingots have a major structure of columnar grains about 0.5 millimeters in diameter. These major grains contain a dense sub-structure which appears to be composed of twinned regions separated by low angle grain boundaries. The high angle grain boundary area contributed by the columnar grains is about 40 cm^2/cm^3. Since approximately 10^{15} atoms/cm^2. constitute a monolayer, the maximum concentration of solute in a polycrystalline sample which can be ascribed to the high angle grain boundaries is about 4×10^{16} atoms/cm^3. This value is very close to the solubility limit obtained in this investigation, indicating that the grain boundaries are almost saturated to the maximum extent. It is quite possible, however, that a large portion of the excess copper is actually situated in the interior of the columnar grains, and the maximum allowable solubility quoted above is consequently too low.

Another factor which should be considered is that of thermal entropy which was disregarded in the calculation of the expected grain boundary solubility. Reference to Equation 3.33 shows that a negative entropy change lowers the solubility from that determined on the basis of enthalpy effects alone. If strong chemical bonding is involved with the segregation of solute atoms to grain boundaries, it could be expected that the tight binding would result in lower vibrational entropies (high frequencies) and hence tend to counteract solubility enhancement. It should be remembered that interstitial copper in silicon has a large positive intrinsic thermal entropy, and in Section 7.A.1 a large part of this effect was ascribed to the absence of chemical bonding. If copper in grain boundaries is tightly bound, on the other hand, it would be expected that a large negative thermal entropy change should accompany the transfer of an atom from an interstitial position in a single crystal region to a grain boundary area.

Entropy changes of the grain boundary itself may also influence the degree of grain boundary segregation. As was mentioned in Section 3.F solute atoms often act as pinning points for grain boundaries and the situation may be subject to the theory of Bauer (1966) on the binding entropy of solute atoms to dislocations. Bauer has shown that a negative contribution to the binding entropy arises from a change in the vibrational entropy of a dislocation when pinning points form on it. The quantitative treatment of this problem is quite complex and is undoubtedly even more difficult for grain boundaries.

In summary, the grain boundary solubility is probably less than that estimated above, but it was not possible to quantitatively determine the actual concentration. If the grain boundary solubility is of the order of one to ten atomic per cent, this represents a difference of five or six orders of magnitude between the copper concentration in single crystal and in grain boundary regions over the temperature range 600°C to 800°C.

7.D Complex Formation and the Solubility of Copper in Arsenic Doped Germanium

As was indicated in the previous chapter the interaction energy of 1.0 eV between copper and arsenic was determined by assuming that all the copper ions interacted on an equal basis with the arsenic ions. This is undoubtedly a poor assumption, however, since copper introduces three acceptor levels into the band gap of germanium and may therefore exist in four different charge states ($r = 0, -1, -2, -3$). If the interactions are coulombic in nature, one would expect the triply charged species to play a major role in complexing reactions since Equation 3.10 shows that the number of pairs is exponentially proportional to the binding energy.

A serious complication arises when attempting to calculate the extent of complexing of a multiply charged deep level impurity. The charge statistics of the dopant must be calculated but it is not known if the energy levels are dependent on temperature or if they remain fixed with respect to one of the band edges. It has been suggested that they should be scaled in proportion to the energy gap

(Shockley and Moll, 1960); however, experimental studies on the effect of pressure on the ionization energies of deep level impurities indicate that their energy levels are fixed much more securely to the valence band than to the conduction band (Paul and Brooks, 1963).

The charge statistics of copper in germanium have been determined by the methods outlined in Section 2.B.2 for: (a) scaled energy levels, and (b) energy levels fixed with respect to the valence band. It was also assumed that the degeneracy factors, β_r, are the same for all states. The Fermi energy of intrinsic germanium was calculated from Equations 2.3 and 2.4 and the condition for electrical neutrality with $N_c = 1.995 \times 10^{16}\ T^{3/2}$ and $N_v = 1.035 \times 10^{16}\ T^{3/2}$ (Geballe, 1959). The energy gap in electron volts was calculated from the relation (Morin and Maita, 1954)

$$E_g = 0.76 - 4.4 \times 10^{-4}\ T.$$

The results of these calculations are given in Tables 7.1 and 7.2 It can be seen that the occupation statistics for these two cases are radically different and calculations of the binding energy required to produce the observed amount of complexing with the triply charged species give

(a) $\Delta H_b = 1.09$ eV

and (b) $\Delta H_b = 1.49$ eV.

These values can be compared with the binding energy predicted by Equation 3.16 between singly and triply charged ions. Substitution of a_o = 2.35 A° (the interatomic distance of germanium) and κ = 12 gives $\Delta H_b \approx 1.2$ eV. However, it is rather doubtful if this comparison has any meaning because of the limitations in using Equation 3.16 to calculate interaction energies between nearest neighbours in the solid state. Another limitation in this comparison arises because the binding energies were calculated from Equation 3.10 by neglecting the ΔS^{th} term. If the complex involves tight binding it is quite possible that this factor is negative, and consequently the calculated binding energies may be lower than the actual value.

The present results may be combined with the data obtained by Hall and Racette (1964) at 650°C on the solubility of copper in germanium doped with higher arsenic concentrations than those employed in the present study. These supplementary solubility data are given in Table 7.3

The procedure involves a combination of the effects of complex formation and electronic interactions. It is therefore necessary to examine the energy level characteristics of copper in n-type germanium. The energy level data for copper in non-degenerate germanium doped to different concentrations of arsenic are given in Tables 7.4 and 7.5 for the two cases discussed previously. The Fermi energy was calculated from Equations 2.9 and 2.10.

Again assuming complexing of the triply charged species, the solubility, N', for the various arsenic doping levels, N_3, is given by

$$N' = N^i \frac{\Sigma N_r'/N_o}{\Sigma N_r^i/N_o} + \frac{N_3}{5 \times 10^{17}} \cdot \frac{N_{-3}'/N_o}{N_{-3}/N_o} \cdot N_c \ , \qquad (7.1)$$

where N^i is the copper solubility in intrinsic material, and N_{-3}/N_o and N_c are the relative ratio of the triply charged species and the concentration of complexes, respectively, in material doped with 5×10^{17} arsenic atoms/cm^3. The first term on the right hand side of this equation is an electronic interaction term and the other is due to complexing. The calculations based on this equation with $N_c = 5.5 \times 10^{15}$/cm^3 are given in Table 7.6 for fixed and proportionally varying energy levels. These results are also plotted as the solid line in Figure 7.1 together with the experimental results. The dashed line was calculated assuming that all the copper atoms take part in the complexing reaction with equal probability.

Unfortunately both energy level conditions predict the same behavior so the analysis is useless for purposes of investigating the energy level - temperature relations. As seen in Figure 7.1 surprisingly good agreement is obtained with the results of Hall and Racette if the triply charged species is assumed to interact with the arsenic ions. The calculations are probably somewhat in error at the high copper concentrations ($\approx 1 \times 10^{18}$ atoms/cm^3), however, because the Fermi energy was assumed to be controlled only by the arsenic doping. The acceptor levels introduced by the copper atoms will tend to lower the Fermi energy and hence negate slightly the solubility enhancement effect. The results should not be altered significantly if the degeneracy factors of the energy levels are included because the major contribution to the solubility enhancement is due to complexing, and for the model proposed this depends only on ratios of the concentration of triply charged states at different arsenic doping levels.

7.E Electronic Interactions and the Solubility of Copper and Gold in p-type Silicon

7.E.1 Copper

Figure 6.16 shows that the solubility of copper in p-type silicon is accurately predicted by the electronic interaction theory except at low temperatures where the enhancement is greater than expected. It was initially suspected that the discrepancy might be due to complexing between copper and boron ions. A calculation of the binding energy at 600°C based on Equation 3.15a (neglecting ΔS^{th}) gave a value of $\Delta H_b \approx 0.75$ eV. For coulombic interactions, Equation 3.16 predicts an interaction energy of approximately 0.7 eV if the copper and boron radii are taken as 0.96A° and 0.88A°, respectively. It is seen, therefore, that the theoretical binding energy predicts the observed solubility enhancement. It must be remembered, however, that Equation 3.16 is probably a poor approximation for binding energies between nearest neighbors in the solid state and that thermal entropy changes due to complexing were neglected when calculating the interaction energy from experimental results.

Work by Hall and Racette (1964) on the diffusion of copper in highly boron doped (5×10^{20} atoms/cm^3) silicon has shown that boron and copper do not form complexes since the diffusion coefficients they obtained were in the range 3×10^{-6} to 3×10^{-5} cm^2/sec at 400°C and 680°C, respectively. These values compare quite well with the diffusion coefficient obtained by Struthers (1956) at 900°C in intrinsic silicon, so complexing must not occur in this system (cf. Equation 3.18), at least not for the boron concentration employed in the present study. It may be wondered why complexing does not occur at a boron concentration of 5×10^{20} atoms/cm^3, and the explanation is probably concerned with the thermal entropy change involved. The high intrinsic thermal entropy of interstitial copper in silicon was partially ascribed to loose chemical bonding. If a copper ion forms a complex with another ion, tight chemical bonding is involved which results in a lower binding free energy than would be expected on the basis of enthalpy considerations alone.

It remains to investigate the possible causes of the discrepancy between theory and experiment at low temperatures. In the theoretical calculations of the solubility enhancement it was assumed that the semi-conductor remains non-degenerate at all temperatures. If the semi-conductor contains a degenerate concentration of electrons, however, the rate at which the Fermi energy changes with carrier concentration becomes more rapid and the present method of calculation is no longer valid. Hall and Racette (1964) have determined correction factors for degeneracy and showed that Equation 2.12 may be written as

$$\frac{p\varepsilon}{n_i} = \exp\left(\frac{E_f^\circ - E_f}{kT}\right) ,$$

where $\varepsilon = \varepsilon(p/N_v)$. According to the present results ε should be approximately 2 at 600°C if degenerate conditions are influencing the copper solubility. Geballe (1959) gives $N_v = 2.22 \times 10^{15}\ T^{3/2}$ (or 5.78×10^{19} at 600°C) for silicon. Hall and Racette give $\varepsilon \approx 1$ for $p/N_v = 0.1$. This cannot account for the observed results unless the density of states of the valence band reported by Geballe is about one order of magnitude too large ($\varepsilon = 1.5$ for $p/N_v = 1$).

Despite the fact that densities of states cannot be accurately extrapolated to high temperatures (Blakemore, 1962)[a], the discrepancy is of such a magnitude that it is doubtful if the degeneracy effect can account for the observed difference between the theoretical and the experimental solubility. Shrinkage of the band gap due to heavy doping cannot explain the results either because this phenomenon has the opposite effect from that observed (Hall and Racette, 1964).

It may also be possible that the substitutional (acceptor) contribution to the total copper solubility is significant at high temperatures and thus affect the results in the manner observed. This is doubtful, however, because Hall and Racette (1964) have shown quite conclusively from determinations of the copper solubility in n-type silicon that the interstitial/substitutional ratio is about 10^4 at 700°C. A change in this ratio over a temperature range of 300°C drastic enough to cause the present effect is unlikely, and furthermore, would render the heat of solution of copper in silicon rather temperature dependent over the range investigated in the present study.

It was assumed in the theoretical analysis that the boron concentration of the doped silicon crystal was known accurately and that the copper atoms are completely ionized at all temperatures. Judging from unfortunate personal experiences with suppliers, it is quite likely that the boron concentration was higher than that which was quoted (say 1×10^{19} atoms/cm^3). The associated error would make the theoretical solubility at high temperatures greater than that which was observed experimentally.

If copper is not completely ionized in slightly p-type silicon (the position of the donor level for interstitial copper is not definitely known) at these temperatures, it may be expected that a larger fraction of the copper centers would exist in a charged state as the temperature decreases and the semiconductor becomes more extrinsic (cf. Equation 2.5). This type of behavior requires that the copper donor level lie near the middle of the band gap at 1000°C. A certain amount of support is given to this hypothesis of incomplete ionization by the work of Gallagher (1957) who estimated from ionic mobility studies that approximately 35 pct. of copper atoms dissolved in silicon migrate as positive ions at 1100°C. If a larger fraction of ionized states exists at low temperatures, the electronic interaction has a larger effect and consequently enhances the solubility to a greater extent than expected when compared to the high temperature results.

7.E.2 Gold

It was observed that the solubility of gold in silicon was reduced by about 35 pct. at 900°C and 1000°C by a boron concentration equal to that used for the study of the solubility of copper in p-type silicon. This result indicates that acceptor states are the predominant gold species at these temperatures since a high donor concentration would result in solubility enhancement.

Collins et al (1957) discovered a donor level and an acceptor level at 0.35 eV and 0.62 eV above the valence band, respectively, below room temperature. Both these levels are believed to be due to substitutional gold since the interstitial/substitutional ratio is about 10^{-1} at 1000°C and decreases with decreasing temperature (Wilcox and La Chapelle, 1964). The present results on the solubility of gold in pure silicon indicate that this ratio may be even lower than 10^{-1} because of the linear ln k^e vs 1/T plot obtained above 900°C. If the ratio were much larger than 10^{-1} above 1000°C a temperature dependent heat of solution would be expected.

Since the ionization energy of the acceptor state is less than that of the donor state near room temperature, the acceptor/donor ratio will be larger than unity in intrinsic material providing the degeneracy factors of the two states are about equal. This property was also observed at 1000°C so one of the following energy level-temperature conditions can satisfy the results:

(a) proportionally scaled energy levels,

(b) acceptor fixed to the valence band and the donor fixed to the conduction band,

(c) acceptor fixed to the conduction band and the donor fixed to the valence band, and

(d) both levels fixed to the conduction band.

As indicated previously pressure studies tend to eliminate the third and fourth possibilities. It is possible that more gold solubility data for higher boron concentrations may yield more information on this problem, but complicating effects of degeneracy and energy gap shrinkage due to heavy doping make data analysis difficult and uncertain.

7.F Electronic Interactions and Segregation in Device Structures

As has been indicated in previous chapters, equilibrium measurements may often be used to predict certain kinetic properties of a system and special consideration was given to diffusion phenomena. One of the easiest experimental tests of this premise is the quasi-steady state diffusion experiment of Kirkaldy and Purdy (1962)[b] in which a fast diffusing solute is allowed to diffuse on a concentration gradient of a second slow diffusing solute and come to a state of transient equilibrium. If the second solute decreases the activity of the first solute, the latter will segregate to regions of high concentration of solute 2. After this state of equilibrium is established, the distribution of the fast component changes slowly in unison with the slow one. From such an experiment one can determine the D_{22}/D_{23} ratio which was shown (with an approximation) in Appendix A to be a thermodynamic parameter obtainable from equilibrium measurements.

It was our original desire to conduct an experiment of this type in semi-conductors with the concentration gradient of the slow diffusing solute established as a step function across a finite diffusion couple. Experimental difficulties intervened (see Chapter 9) so an analytically less tractable experiment was designed in which the concentration gradient of the second solute was established by pre-diffusion (see Section 5.C.6). Although the complexity of the experiment did not allow a comparison of kinetically and thermodynamically determined D_{22}/D_{23} ratios, the results did demonstrate that the segregation of mobile impurities to heavily doped regions of device structures was in order of magnitude agreement with a thermodynamic estimate.

Chemical analysis of a silicon sample initially containing 7×10^{17} atoms/cm^3 of phosphorus and a uniform concentration of copper, which was diffusion doped with boron at 1300°C for 24 hours and then annealed at 975°C for two hours, yielded an average copper concentration of 3.3×10^{16} atoms/cm^3. The inner (boron free) region of the sample contained 1.5×10^{16} copper atoms/cm^3. The copper was therefore segregated to the outer region of the sample which contained a surface boron concentration of about 1×10^{20} atoms/cm^3 (see Section 5.C.6). Figure 7.2 is a schematic representation of the various concentration profiles involved in this experiment. The intrinsic carrier concentration at 975°C is 6×10^{18}/cm^3 so the activity coefficient of copper at the surface of the sample is given by (cf. Equation 3.7)

$$\gamma = \gamma^\circ . \frac{6 \times 10^{18}}{1 \times 10^{20}} = \frac{\gamma^\circ}{16.7} ,$$

where γ° is the activity coefficient in the interior of the crystal.

Since at equilibrium the chemical potential of the copper is everywhere the same, the concentration of copper at the surface should be 16.7 times that of the interior. The depth over which the sample was extrinsic at 975°C may be approximated from Equation 5.3 by setting $N(x,t) = 6 \times 10^{18}$. Calculation gives $x = 3.5 \times 10^{-3}$ cm. If the boron concentration profile is assumed linear, the mean concentration enhancement factor is then 16.7/2 over a depth of about 3.5×10^{-3} cm. on all surfaces of the sample. Neglecting edge effects, the total concentration in a sample 0.1 cm. thick should be approximately $1.5C_o$ where C_o is the concentration in the inner region of the sample. The present experimental result gives $2C_o$ but in view of the approximations involved with this treatment, the order of magnitude agreement is quite good.

An inherent assumption in the above discussion is that the quench time was sufficiently rapid that a concentration distribution representative of conditions at 975°C was obtained. Because of the high mobility of copper, however, it may be possible for it to segregate upon cooling to the surface which becomes more extrinsic as the temperature decreases.

Nevertheless the experiment has demonstrated that mobile impurities may segregate to certain regions of device structures as a result of electron-solute atom interactions and that the effect can be estimated from solubility measurements. In the same way, ionic interactions should result in similar behavior . As Hall and Racette (1964) have pointed out, when trace amounts of mobile impurities concentrate in heavily doped regions of a junction structure, serious consequences may result. Upon cooling, these regions become supersaturated and probably produce precipitates in regions adjoining the junction.

For more exact time dependent descriptions of segregation and other ternary diffusion problems, the equations outlined in Appendix A must be solved. These equations are very complex for the general diffusion problem, but numerical methods could probably be employed without undue difficulty if reasonable assumptions and approximations are made.

7.G The Precipitation Kinetics of Copper in Silicon

It can be seen from Figures 6.22 and 6.23 that the $(\text{time})^{2/3}$ rate law proposed by Harper appears to represent very well the precipitation behaviour of copper in silicon in addition to many other systems (see Section 4.D.1). These results support the preliminary interpretation (by the author) of Hall and Racette's Hall coefficient measurements on silicon supersaturated with copper. Figure 6.25 shows that the time exponent of the rate equation for the present study could actually range from 0.644 to 0.730. As yet no quantitative theory exists for observed kinetics of precipitation at dislocations and the problem can only be approached qualitatively.

In the present work a number of assumptions were made in calculating the $\ln(N_0/N(t))$ vs. $t^{2/3}$ curves. It was assumed that changes in carrier concentration were directly proportional to changes in the electrical conductivity. This means that the dependence of the electrical mobility on the concentration of scattering impurity centers and on the growth of precipitates was neglected. These effects are difficult to assess without accurate Hall coefficient measurements but in any case they have opposite consequences and tend to compensate for each other. Another assumption was that either the copper atoms in solution are completely ionized or a constant ratio of unionized atoms to ions is maintained throughout the period of the precipitation reaction. It was observed that typical carrier concentrations after quenching from a temperature giving a saturation concentration of about 1×10^{17} atoms/cm^3 were only 5×10^{13}/cm^3. This could mean that a great deal of pre-precipitation occured upon quenching or that copper centers are incompletely ionized near room temperature in n-type material. It is almost certain that the first suggestion is true because of the high mobility of copper, but on the basis of the results of the solubility determinations of copper in boron doped silicon, it is also possible that the copper atoms are incompletely ionized. According to Equation 2.3, as the number of charge carriers decreases in n-type material the Fermi energy is lowered. Reference to Equation 2.5 then shows that as the Fermi energy is lowered, the relative number of neutral donor impurities is also decreased. The ratio of ionized copper atoms should therefore increase as the precipitation reaction proceeds. This effect, then, would tend to make the actual time exponent even less than the observed exponent.

The present results show practically identical kinetics for all degrees of supersaturation (Figure 6.22 and Table 6.3), ie. the kinetics are independent of the initial quantity of solute in solution. This also indicates that the number of active precipitation sites is independent of the degree of supersaturation and the amount of pre-precipitation.

Another point which should be mentioned is that the room temperature rate constant found from Hall and Racette's work is much lower (≃1/30) than the rate constant for the present precipitation study. An important factor governing the precipitation rate is the dislocation density. Hall and Racette did not quote a dislocation density but the float zoned silicon which they used probably had a higher dislocation density than the Czochralski grown material used in this study.

It remains to suggest mechanisms whereby a time exponent less than unity is obtained. The activation energy for the process obtained from Figure 6.24 as 1.10 ± 0.05 eV may yield information about the rate controlling step of the reaction. Activation energies for diffusion of copper in silicon have been reported as 0.43 eV between 400°C and 700°C (Hall and Racette, 1964) and 1.0 eV between 800°C and 1000°C (Boltaks, 1963). The results of Hall and Racette compare better with the single value reported by Struthers (1956) at 900°C and with a theoretical activation energy of 0.64 eV calculated by Millea (1966). On the basis of the most recent results it may be concluded that the rate controlling factor is not copper diffusion. A calculation of the precipitation time required for a copper diffusion controlled process was not carried out because the diffusion coefficient of copper at room temperature is not known with sufficient accuracy to justify such a determination.

Another possible rate controlling step is the diffusion of vacancies. Since copper is an interstitial impurity, vacancies probably must be supplied to the precipitation areas in order for the reaction to proceed. A theoretical calculation of the activation energy for vacancy diffusion in silicon gives 1.06 eV (Swalin, 1961), however, recent electron paramagnetic resonance studies by Watkins (1963) indicate that charged vacancies in p-type silicon migrate with an activation energy of 0.33 eV. Swalin's theoretical treatment involved many assumptions, the most important of which concerned relaxation behavior of the atoms surrounding a vacancy. If Watkin's activation energy is applicable to vacancies in general (Watkins stated in a discussion of his paper that changes in activation energy with charge state are not great), simple diffusion of ions or vacancies does not appear to control the rate at which copper precipitates out of solution in silicon. Self-diffusion and/or vacancy formation must not play any significant role either because the activation energies for these processes are very large (3.5 - 4.0 eV). This means that dislocation climb (Rieger, 1964) is not the rate controlling process for room temperature precipitation.

The hypothesis presented by Doremus (1960) whereby subgrain boundaries act as surface sinks also does not appear to apply to the present results unless the conclusion that the kinetics are not diffusion controlled is incorrect. It is possible, however, that the quenching operation could introduce dislocation boundaries (Penning, 1958) and thus provide surface sinks giving rise to a time exponent less than unity (providing the reaction is diffusion controlled).

The above discussion indicates that the precipitation reaction may be controlled by an interface rate limitation. This was predicted by Bullough and Newman (1962) for carbon precipitation in alpha iron. They also proposed a transient rate limitation which increased with time in order to correlate the theory with observed kinetics (see Section 4.D.1). Bullough and Newman reasoned that one might expect the velocity of transfer (K_c in Equation 4.4) across the precipitate-matrix interface to be large in the early stage of precipitation and to decrease gradually as the precipitates grow if there is a local increase in volume on formation of the second phase. It is quite possible that a local increase in volume does occur when interstitial copper precipitates out of solution. Although the composition and crystal structure of the precipitates are not known, they are probably a meta-stable form of Cu_3Si. This hypothesis also supports the observations of Reiger (1964) who found that copper rich precipitates which formed upon cooling were of a fixed size independent of the degree of supersaturation; their number and the volume in which they appear increase with supersaturation. It is possible that once the precipitates reach a certain size, the rate limitation becomes very large and the copper atoms are forced to nucleate elsewhere in the neighbourhood of the dislocations (where the vacancy concentration is high - see Section 4.D.1).

According to Bullough and Newman, the temperature dependence of K_c in Equation 4.4 is dominated by the enthalpy of activation in $K_c°$ since the energy term, $p\Delta V$ (or φ), is probably not much larger than kT. The transient rate limitation theory is therefore not inconsistent with the fact that the activation energy is essentially the same when evaluated for 50 pct. completion and for 100 pct. completion.

It may be wondered why a transient rate limitation appears to generate a unique $(\text{time})^{2/3}$ rate law. This is probably due to inaccuracies in experimental measurement and assumptions involved in correlating measurements with actual concentration changes. Many of the existing experimental data, for example, could undoubtedly be plotted using a $t^{1/2}$ or a $t^{3/4}$ abscissa and still show as good a correlation as obtained with a $t^{2/3}$ plot. The significant point is that the time exponent is less than unity which is inconsistent with simple diffusion controlled precipitation on randomly distributed cylinders.

The present work tends to support the theory of Bullough and Newman in that the activation energy determined for the process does not correspond to a diffusion controlled reaction. A complete picture of the precipitation mechanism remains far from complete, however.

Table 7.1. Energy level data for copper in arsenic doped (5×10^{17} atoms/cm.^{3}) germanium assuming the copper acceptor levels are scaled in proportion to the energy gap. The N_r/N_o values are in the sequence 0 to -3.

Temp. (°C)	E_g(eV)	E_f^o(eV)	ΔE_f(eV)	E_f(eV)	E_r(eV)	N_r/N_o	%N_r/N_o
650	.379	.215	.006	.221	.021	1.0	2.1
					.182	12.4	25.6
					.234	17.8	36.8
						17.2	35.5
750	.335	.196	-	.196	.019	1.0	3.4
					.161	7.5	25.4
					.206	11.1	37.6
						9.9	33.5
850	.291	.177	-	.177	.017	1.0	4.7
					.140	5.2	24.6
					.179	7.6	35.6
						7.5	35.2

Table 7.2. Energy level data for copper in germanium doped as above assuming the copper levels are fixed with respect to the valence band.

Temp. (°C)	E_r(eV)	N_r/N_o	% N_r/N_o
650	.04	1.00	7.5
	.33	9.8	73.5
	.53	2.48	18.6
		0.05	0.375
750	"	1.00	12.8
		5.90	72.0
		1.28	15.6
		0.029	0.354
850	"	1.00	16.7
		4.14	69.0
		0.847	14.1
		0.022	0.360

Table 7.3. Solubility of copper in germanium as a function of arsenic content. The concentrations were taken from a graph by Hall and Racette (1964).

As Concentration (atoms/cm.^{3})	Cu Concentration (atoms/cm.^{3})
1.8×10^{18}	4.8×10^{16}
	5.4×10^{16}
3.5×10^{18}	1.8×10^{17}
7.0×10^{18}	7.0×10^{17}
	1.5×10^{18}

Table 7.4. Energy level data for copper in arsenic doped germanium at 650°C assuming the copper levels are scaled in proportion to the energy gap. F_e is an electronic solubility enhancement factor.

As Content (cm.$^{-3}$)	E_f	N_r/N_o	% N_r/N_o	F_e
Intrinsic	.215	1.0	2.2	-
		11.6	26.0	
		17.8	39.8	
		14.2	31.9	
2×10^{18}	.238	1.0	1.3	1.65
		15.3	19.2	
		31.0	38.7	
		32.5	40.6	
4×10^{18}	.258	1.0	0.7	2.93
		20.0	14.2	
		51.8	36.5	
		69.0	48.6	
7×10^{18}	.283	1.0	0.3	6.25
		27.	8.9	
		96.	31.8	
		178.	59.0	

Table 7.5. Energy level data for copper in arsenic doped germanium at 650°C assuming the copper levels are fixed with respect to the valence band. F_e is an electronic solubility enhancement factor.

As Content ($cm.^{-3}$)	E_f	N_r/N_o	% N_{-3}/N_o	F_e
Intrinsic	.215	1.00		
		9.8		-
		2.48		
		0.05	0.375	
2 X 10^{18}	.238	1.00		
		12.2		1.28
		3.8		
		0.111	0.65	
4 X 10^{18}	.258	1.00		
		15.6		1.69
		6.3		
		0.204	0.88	
8 X 10^{18}	.283	1.00		
		21.5		2.62
		11.8		
		0.532	1.53	

Table 7.6. Calculated copper solubility in germanium as a function of arsenic concentration at 650°C. It was assumed that complexes form between arsenic and triply charged copper ions. All concentrations are in atoms/cm.^{3}

As Concentration	Cu Concentration for Varying Levels	Cu Concentration for Fixed Levels
2 X 10^{18}	4.4 X 10^{16}	5.1 X 10^{16}
4 X 10^{18}	1.8 X 10^{17}	1.8 X 10^{17}
8 X 10^{18}	9.2 X 10^{17}	9.3 X 10^{17}

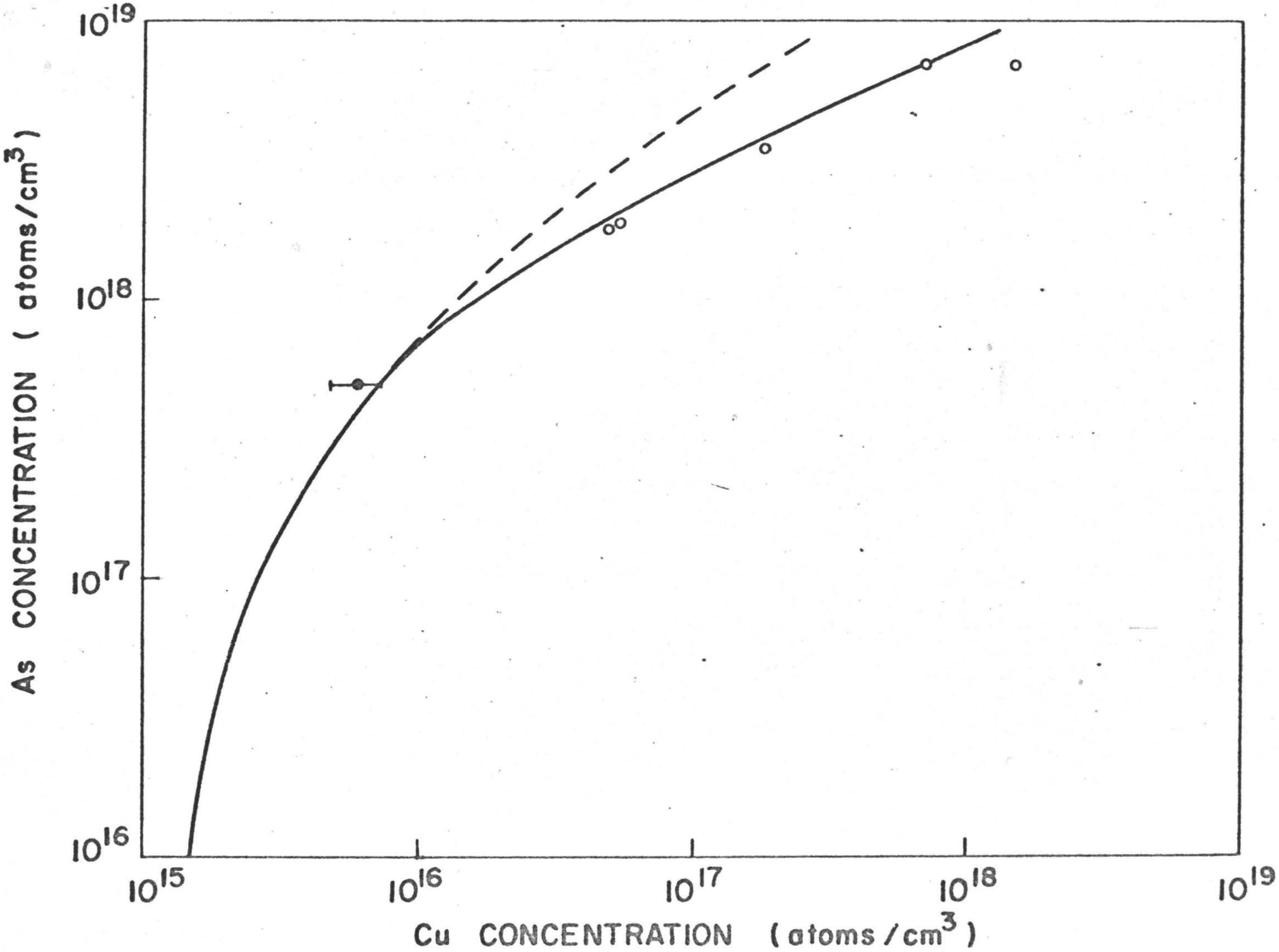

Figure 7.1. Solubility of copper in germanium at 650°C as a function of arsenic content. The points without error bars are data of Hall and Racette (1964). The solid line was calculated from Equation 7.1 assuming complexing of triply charged copper ions. The dashed line was calculated assuming all the copper in solution takes part in the complexing reaction.

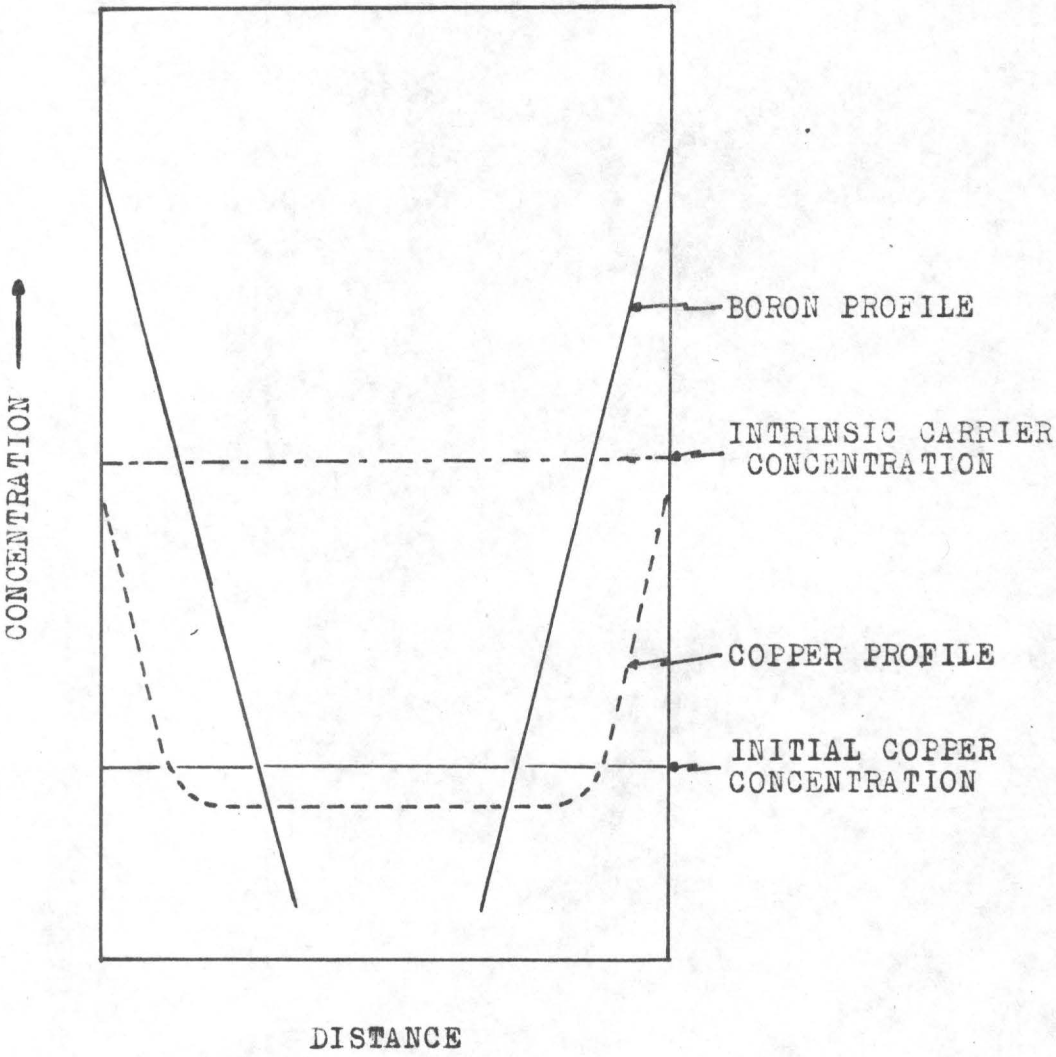

Figure 7.2. Schematic representation of the various concentrations in the boron diffused silicon wafer.

CHAPTER 8

SUMMARY AND CONCLUSIONS

The conclusions and information obtained from this study are summarized in two main categories. These are: (A) Thermodynamic and kinetic properties of defect interactions, and (B) Thermodynamic and physical properties of copper and gold in pure single crystal silicon and germanium. Reference is made to Chapter 6 for a concise summary of numerical determinations of enthalpies and entropies of solution of the various systems studied and the enthalpies of the defect interactions which were investigated. Attention is given here to general conclusions and implications of the investigation.

8.A Defect Interactions

8.A.1 Phonons

(a) Qualitative considerations of chemical bonding, relative ~~atomic~~ masses, and strain energy have been employed to explain the specific thermal entropies of copper and gold in silicon and copper in germanium. Special consideration was given to the fact that near-neighbor interactions must be considered in addition to Zener's strain energy argument. This was especially evidenced by the high thermal entropy of the copper-silicon system in which strain energy effects are absent.

(b) It was found that the partial molar excess entropy of solution of copper in silicon evaluated with respect to Cu_3Si is larger than that evaluated with respect to pure copper.

8.A.2 Grain Boundaries

(a) It has been demonstrated that the solubility of copper in vapor grown polycrystalline silicon is about one order of magnitude greater than in single crystal silicon at 700°C. The ratio of the grain boundary solubility to the single crystal solubility was estimated to be of the order of 5×10^5.

(b) The calculated binding energy (determined by assuming the heat of solution in the grain boundaries is concentration independent) is much larger than expected in metallic systems, and was attributed to chemical bonding. It was also proposed that a large negative thermal entropy change accompanies the formation of this bond.

8.A.3 Other Solute Atoms

(a) The solubility of copper in arsenic doped germanium was quantitatively explained by a theory of complex formation between triply charged copper acceptors and arsenic donors. This theory was found incompatable with the Wagner activity coefficient formalism for dopant concentrations and interaction energies of interest.

(b) The absence of complex formation in the copper-boron-silicon system was attributed to large negative thermal entropy changes accompanying the formation of a tightly bound pair.

(c) It was shown that information obtained from equilibrium solubility determinations could be applied to kinetic problems of ternary diffusion.

8.A.4 Electrons

(a) Solubility studies of copper and gold in p-type silicon demonstrated the dependence of the activity coefficient of ionized solute atoms on the Fermi energy of a solution. It was also indicated that this dependence (in semiconductors) could not be represented by the Wagner formalism.

(b) An experiment was designed to demonstrate the segregation of mobile impurities to highly doped regions of device structures during heat treatment operations.

(c) Generalized diffusion equations were developed which included the effects of electrostatic potentials and complex formation.

8.A.5 Dislocations

(a) The kinetics of copper precipitation at dislocations in silicon were observed to follow a $(\text{time})^n$ rate law where $n = 0.687 \pm .043$.

(b) It was concluded that the reaction is not diffusion controlled, and a transient rate limitation theory was employed to describe the results qualitatively.

8.B Physical and Thermodynamic Properties of Solute Atoms

(a) It was shown that non-ideality of liquidus alloys is an important factor in the determination of solubility parameters of semiconductor (rich)-metal solutions from data obtained above eutectic (or peritectic) temperatures.

(b) Evidence found for meta-stable copper-silicon equilibrium demonstrated that care must be taken when determining solubilities by diffusion methods.

(c) The solubility study of copper in p-type silicon indicated that copper is incompletely ionized at 1000°C and its donor level is located near the middle of the band gap at this temperature.

(d) The acceptor/donor ratio of substitutional gold in silicon was found to be greater than unity at elevated temperatures (900 - 1000°C).

CHAPTER 9

SUGGESTIONS FOR FURTHER WORK

9.A Grain Boundary Solubility Studies

An accurate determination of the grain boundary solubility of copper in silicon was not conducted in the present study because of the complex structure of vapor grown material. If polycrystalline silicon with a reasonable grain structure could be prepared, the overall solubility and the grain boundary area could be compared to obtain a fairly accurate evaluation of the actual concentration of solute in the grain boundaries. It would also be possible, then, to evaluate the thermal entropy change which accompanies the formation of a solute atom-grain boundary bond.

Silicon and germanium with a simple grain structure could possibly be manufactured by a melting and casting procedure, but problems associated with maintaining super-purity would have to be overcome.

Autoradiography may also be useful in complimenting solubility measurements providing a solute is chosen which does not readily precipitate out of solution upon cooling.

A test of the assumption of a concentration independent heat of solution could be accomplished by equilibrating polycrystalline material with a range of chemical potentials of the solute element. Any deviation from linearity in an activity vs. concentration curve would reveal non-Henrian behavior.

9.B Effect of Dislocations and Grain Boundaries on Interstitial Diffusion in Silicon and Germanium

Dislocations and grain boundaries generally constitute high-diffusivity paths in metallic systems. Dislocations also increase the apparent diffusion coefficients of substitutional impurities in silicon and germanium because of their role as vacancy sources. An interesting experimental program would be an investigation of the effect of dislocations and grain boundaries on the diffusion of interstitial impurities in these materials since vacancies are not essential for the migration of this type of impurity. The high binding energy of an interstitial to a grain boundary obtained from the present work on copper in polycrystalline silicon may indicate that these defects could inhibit the diffusion of interstitial solutes. This implication is rather naive, however, and more thought should be given to a comparison of the activation processes and mechanisms involved with diffusion in single crystal and in grain boundary regions.

9.C Ternary Diffusion Studies

Experimental studies of ternary diffusion in semiconductors are of great practical significance to the device industry. There are difficult technical and theoretical problems associated with such investigations however. As indicated in Appendix A, analytical solutions of the diffusion equations are quite complex.

Conventional diffusion couples are difficult to fabricate because of welding problems. It may be possible, however, to pressure weld couples at temperatures near the melting point of the semiconductor, provided pressure is applied only above the temperature at which plastic flow occurs. The working system must also be kept extremely free of impurities at these temperatures.

If couples can be fabricated, the quasi-steady state diffusion experiment (Kirkaldy and Purdy, 1962) should not be difficult to perform. A system must be chosen, however, such that one solute has a much higher diffusion coefficient than the other. This requirement is not too difficult to meet for germanium since the diffusion coefficients of Group III acceptors are one or two orders of magnitude lower than those of Group V donors. The diffusion coefficients of arsenic and antimony in silicon are also at least one order of magnitude less than Group III acceptors. The difficulty which arises from using these impurities for this particular experiment is that extremely long times are required to achieve transient equilibrium in reasonably sized samples. The fast diffusing dopants are difficult to treat theoretically because most of them exist in multivalent states (except lithium in silicon and germanium), the statistics of which are unknown for practical diffusion temperatures. These impurities are also not as interesting from a technical viewpoint as are the common Group III and V dopants.

Another possible experiment is an analysis of diffusion of an impurity from an external source into a semiconductor containing a concentration gradient of a third component. The problem here is to establish a concentration gradient which can be treated with reasonable analytical ease. Possibly the easiest experimental method would be to prediffuse the third component. An exact analysis of the results would be complex but could possibly be conducted by numerical methods. If slow diffusing dopants are employed for this study, an experimental problem of determining concentration profiles arises. Electrical methods are often difficult when more than one dopant is present (compensation), and radio-chemical analysis requires the use of suitable dopants and accurate sectioning techniques.

Of interest also are theoretical considerations of ternary diffusion in semiconductors. Analytical solutions of the diffusion equations outlined in Appendix A would be a valuable contribution. In many practical cases the temperatures of diffusion are high enough that complex formation between singly charged dopants has a negligible effect and only the electrostatic interaction need be considered. It would also be desirable to extend the equations to degenerate conditions but the problems associated with this effect make solutions even more difficult.

APPENDIX A

TERNARY DIFFUSION IN SEMICONDUCTORS

The presence of a third component affects the diffusion of a solute in a normal dilute semiconductor solution in two ways. One is complex formation which has been discussed for a special case in Section 3.C.3. The other is through electrostatic potentials arising as a consequence of the requirement that the Fermi energy be equal throughout a system. In the present treatment it will be assumed that space charge regions are absent and that the semiconductor is non-degenerate.

To simplify the situation, let us consider first the case where electrostatic potentials are absent, i.e. $n_i >> N_2, N_3$. In the absence of electrical forces, a diffusion flux can be expanded as a linear function of all the chemical potential gradients, ∇u_k, in a three-component system, viz., (Onsager, 1945-46).

$$J_i = - \sum_{k=1}^{3} L_{ik} \nabla u_k , \tag{A.1}$$

where L_{ik} satisfies the equalities

$$L_{ik} = L_{ki}$$

$$\sum_i L_{ik} = \sum_k L_{ik} = 0$$

and the inequalities

$$L_{ii} > 0; L_{ii} L_{kk} - L_{ik} L_{ki} > 0 .$$

Equation A.1 may be shown to be identical to

$$J_i = - \sum_{k=1}^{2} D_{ik} \nabla C_k \qquad \text{(A.2)}$$

with the aid of the transformation relationship (Kirkaldy and Brown, 1963)

$$D_{ik} = \sum_{j=1}^{3} L_{ij} \frac{\partial u_j}{\partial N_k} \; . \qquad \text{(A.3)}$$

Combination of the Gibbs-Duhem equation,

$$N_1 \partial u_1 + N_2 \partial u_2 + N_3 \partial u_3 = 0,$$

with Equation A.3 gives

$$D_{22} = \left(L_{22} - \frac{N_2}{N_1} L_{21}\right) \frac{\partial u_2}{\partial N_2} + \left(L_{23} - \frac{N_3}{N_1} L_{21}\right) \frac{\partial u_3}{\partial N_2}$$

and

$$D_{23} = \left(L_{22} - \frac{N_2}{N_1} L_{21}\right) \frac{\partial u_2}{\partial N_3} + \left(L_{23} - \frac{N_3}{N_1} L_{21}\right) \frac{\partial u_3}{\partial N_3} \; .$$

If L_{23} is small compared with L_{22}, and if the solute concentrations are dilute, then the approximation*

$$\frac{D_{23}}{D_{22}} \cong \frac{\partial u_2/\partial N_3}{\partial u_2/\partial N_2} \qquad \text{(A.4)}$$

is obtained. It is seen that this ratio of diffusion coefficients is thermodynamic and can be obtained from equilibrium measurements.

---

* For a more complete discussion of the approximations involved with this operation, see Kirkaldy et al (1965). In actual fact, expressions for $\partial u_2/\partial N_2$ etc. should be inserted before the ratio is taken and the extra terms are neglected.

With the use of Equation 3.14a, the chemical potential of component 2 is given by

$$u_2 = u_2^\circ + kT \ln \gamma_2^\circ + kT \ln N_2 - kT \ln (1 + \Omega N_3 - \Omega N_c). \quad (A.5)$$

In order to differentiate this expression with respect to N_2 and N_3, N_c must be represented as a function of these quantities. The solution of Equation 3.10 for N_c is (Reiss et al, 1956)

$$N_c = \frac{N_2}{2}\left(1 + \frac{1}{\Omega N_2} - \frac{N_3}{N_2}\right) - N_2 \left[\frac{1}{4}\left(1 + \frac{1}{\Omega N_2} + \frac{N_3}{N_2}\right)^2 - \frac{N_3}{N_2}\right]^{1/2} . \quad (A.6)$$

Fick's first law may be written as

$$J_2 = - D_{22}\frac{\partial N_2}{\partial x} - D_{22}\,\frac{\partial u_2/\partial N_3}{\partial u_2/\partial N_2}\,\frac{\partial N_3}{\partial x} .$$

As was indicated in Section 3.C.3, D_{22} is given by

$$D_{22} = \frac{\overset{\circ}{D}_{22}}{2}\left[1 + \frac{\frac{1}{2}\left(N_2 - N_3 + \frac{1}{\Omega}\right)}{\left(\frac{1}{4}\left(N_2 - N_3 - \frac{1}{\Omega}\right)^2 + \frac{N_2}{\Omega}\right)^{1/2}}\right] , \quad (A.7)$$

where $\overset{\circ}{D}_{22}$ is the diffusion coefficient of component 2 in the absence of the third component. Expressions similar to the above equations may also be written for component 3.

Fick's second law may be written for each component as

$$\frac{\partial N_2}{\partial t} = \frac{\partial}{\partial x}\, D_{22}\,\frac{\partial N_2}{\partial x} + \frac{\partial}{\partial x}\, D_{23}\,\frac{\partial N_3}{\partial x}$$

and

$$\frac{\partial N_3}{\partial t} = \frac{\partial}{\partial x} D_{33} \frac{\partial N_3}{\partial x} + \frac{\partial}{\partial x} D_{32} \frac{\partial N_2}{\partial x} \quad ,$$

where the D's are of the form

$$D = D\,(N_2,\ N_3, \Omega) \quad .$$

The solutions of these equations are complex and will not be attempted here, although in principle, they should be tractable by numerical methods.

It may be useful to consider the special case where $N_3 >> N_2$. Equations A.4 and A.5 yield

$$\frac{D_{23}}{D_{22}} = - \frac{N_2 \Omega}{1 + \Omega N_3} \qquad (A.8)$$

and Equation A.7 simplifies to

$$D_{22} = \frac{D_{22}^{\circ}}{1 + \Omega N_3} \quad . \qquad (A.7a)$$

Fick's first law now becomes

$$J_2 = - \frac{D_{22}^{\circ}}{1 + \Omega N_3} \frac{\partial N_2}{\partial x} + \frac{D_{22}^{\circ} N_2}{(1 + \Omega N_3)^2} \frac{\partial N_3}{\partial x} \quad .$$

This special equation has been given by Reiss and Fuller (1959) but a derivation was not presented.

If an electrostatic potential, Φ, exists, the flux equation may be written as

$$J_2 = - D_{22} \frac{\partial N_2}{\partial x} - D_{23} \frac{\partial N_3}{\partial x} + M_2 N_2 \frac{\partial \Phi}{\partial x} \quad , \qquad (A.9)$$

where M_2 is the mobility of component 2. The electrostatic potential may be related to the electron concentration, n, by Equation 2.9, i.e.

$$\frac{n}{n_i} = \exp\left(\frac{e\Phi}{kT}\right) .$$

Then,

$$\frac{\partial\Phi}{\partial x} = \frac{1}{n}\frac{kT}{e}\frac{\partial n}{\partial x} .$$

The electron concentration may be expressed in terms of the dopant concentrations by (cf. Equation 2.10).

$$n = \frac{1}{2}\left[N + (N^2 + 4n_i^2)^{1/2} \right] , \qquad (A.10)$$

where N is equal to the number of donors minus the number of acceptors, providing the dopants are completely ionized and are singly charged. From the above relation we get

$$\frac{\partial n}{\partial x} = \frac{1}{2}\left[1 + \frac{N}{(N^2 + 4n_i^2)^{1/2}} \right]\frac{\partial N}{\partial x} .$$

If, for the sake of argument, component 3 is a donor and component 2 is an acceptor, then

$$N = N_3 - N_2 . \qquad (A.11)$$

The flux equation may now be written as

$$J_2 = - D_{22}\frac{\partial N_2}{\partial x} - D_{23}\frac{\partial N_3}{\partial x} + \frac{D_{22}\,N_2}{2n}\left[1 + \frac{N}{(N^2 + 4n_i^2)^{1/2}} \right]\frac{\partial N}{\partial x} , \qquad (A.12)$$

where n and N are given by Equations A.10 and A.11, respectively, and

M_2 has been replaced by the Einstein relation

$$M_2 = \frac{D_{22}\ e}{kT} \quad .$$

Analytical solutions for the conditions of complex formation and electrostatic potentials are even more complex than for the previously discussed case. Consider instead the following special cases:

(1) $N_3 >> N_2, n_i ; \Omega \neq 0$

The flux equation is

$$J_2 = - D_{22} \frac{\partial N_2}{\partial x} - D_{23} \frac{\partial N_3}{\partial x} + D_{22} \frac{N_2}{N_3} \frac{\partial N_3}{\partial x} \quad .$$

Substitution of Equations A.8 and A.7a gives

$$J_2 = - \frac{D_{22}^{\circ}}{1 + N_3} \frac{\partial N_2}{\partial x} + \frac{D_{22}^{\circ} N_2 (1 + 2\Omega N_3)}{N_3 (1 + \Omega N_3)^2} \frac{\partial N_3}{\partial x} \quad . \qquad \text{(A.13)}$$

It is seen from the above relation that the Fick formalism can be retained to describe ternary diffusion in the presence of electrostatic potentials if

$$D_{23} \equiv \frac{D_{22}^{\circ} N_2 (1 + 2\Omega N_3)}{N_3 (1 + \Omega N_3)^2} \quad . \qquad \text{(A.14)}$$

(2) $N_3 >> N_2, n_i ; \Omega = 0$

Equation A.13 simplies to

$$J_2 = - D_{22} \frac{\partial N_2}{\partial x} + D_{22} \frac{N_2}{N_3} \frac{\partial N_3}{\partial x} \quad ,$$

where $D_{22} = D_{22}^{\circ}$. It may also be shown that this result is identical with that determined by thermodynamic methods. According to Equation 3.7 the activity coefficient of component 2 may be expressed by

$$\ln \gamma_2 = \ln \gamma_2^{\circ} + \ln \frac{N_3}{n_i} \quad .$$

Thus,

$$u_2 = u_2^{\circ} + kT \ln \gamma_2^{\circ} + kT \ln N_2 + kT \ln \frac{N_3}{n_i} \quad .$$

From this equation, we get the thermodynamic relation

$$\frac{D_{23}}{D_{22}} = \frac{\partial u_2/\partial N_3}{\partial u_2/\partial N_2} = \frac{N_2}{N_3} \quad ,$$

which is identical to Equation A.14 with $\Omega = 0$.

(3) $N_2 >> N_3, n_i$

Equation A.12 reduces to the well known "self-field" diffusion relation (Smits, 1958)

$$J_2 = - 2 D_{22}^{\circ} \frac{\partial N_2}{\partial x} \quad .$$

APPENDIX B

TABLES OF RESULTS

Table B.1. "Solubility" of copper in silicon as a function of diffusion time as determined by the plate-and-anneal method.

Time (hours)	"Solubility" (atoms/cm.^{3} X 10^{15})	
	700°C	750°C
0.25		21.0
0.50	7.65	23.8
1.0	8.30	20.0
4.0	10.05	
9.0		16.0
14.5	10.0	
22	9.15	
40	7.05	
64		14.5
Equilibrium Solubility	5.20	13.2

Table B.2. Equilibrium solubility of copper in pure single crystal silicon. The distribution coefficients were calculated from the liquidus compositions given by Hansen (1958). The activity coefficient of solute in the liquid was determined form Equation 4.3 and the data of Thurmond and Kowalchik (1960).

Temperature ($^\circ$C)	Solubility (cm.^{-3} X 10^{16})	X^{α}/X^{l} (X 10^{-6})	γ^{l}
1100	82.	35.	0.807
1025	47.	17.2	
1000	36.	13.1	0.818
900	13.4	4.2	0.826
860	7.3	2.5	
825	6.0	1.75	
810	4.5	1.30	0.837
790	2.9		
785	2.7		
785	2.9		
750	1.35		
700	0.52		
700	0.54		
650	0.155		

Table B.3. Equilibrium solubility of copper in pure polycrystalline and boron doped (5×10^{18} atoms/cm.^{3}) silicon. A tabulation of the intrinsic carrier concentration is also included.

Temperature (°C)	Poly-crystal Silicon (cm.$^{-3} \times 10^{16}$)	Boron Doped Silicon (cm.$^{-3} \times 10^{16}$)	n_i (cm.$^{-3} \times 10^{16}$)
1050		68.	
1000		47.	70.
900	20.	33.	39.
850		14.4	
810	9.8	12.5	21.
785	8.0	8.6	
750	7.0	5.5	
700	4.6	4.1	8.0
650	3.4	2.0	
600		1.50	2.5
575	2.6		
550		0.70	1.25
500		0.31	

Table B.4. Solubility of copper in pure single crystal and arsenic doped (5 X 10^{17} atoms/cm.^{3}) germanium. The distribution and activity coefficients were calculated in the same way as for the copper-silicon system.

Temperature (^{o}C)	Pure Ge (cm.$^{-3}$ X 10^{15})	As Doped Ge (cm.$^{-3}$ X 10^{16})	X^{α}/X^1 (X 10^{-7})	γ^1
900	37.		68.	1.72
850	33.	4.0	28.	1.38
800	16.5	2.6	10.	1.18
750	9.3	1.75	4.4	1.10
700	4.3	1.30	1.70	1.0
650	2.0	0.61	0.48	1.0

Table B.5. Solubility of gold in pure single crystal and boron doped (5 X 10^{18} atoms/cm.^{3}) silicon. The distribution and activity coefficients were calculated as before.

Temperature (^{o}C)	Prue Si (cm.$^{-3}$ X 10^{16})	B Doped Si (cm.$^{-3}$ X 10^{15})	X^{α}/X^1 (X 10^{-6})	γ^1
1300	9.2		10.5	0.49
1200	6.8		4.7	0.48
1100	2.7		1.35	0.49
1000	1.10	7.0	0.47	0.49
900	0.32	2.1	0.130	0.48

Table B.6. Precipitation kinetics of copper in silicon at 30°C, 40°C, and 50°C after saturation at temperatures ranging from 700°C to 1000°C.

$t^{2/3}$ (hrs.)	900°C to 30°C	900°C to 40°C	900°C to 50°C	700°C to 30°C	800°C to 30°C	1000°C to 30°C
0.15			1.14			
0.25			1.33			
0.30		1.10				
0.35			1.60			
0.45			2.00			
0.50		1.25	2.28			
0.60	1.14		2.68	1.20	1.12	
0.70		1.43	3.20			
0.90			4.00			
1.00		1.67				
1.10			5.36			
1.20	1.33					
1.3		2.00				1.33
1.4			8.0			
1.6				1.40		
1.7		2.50				1.47
1.9				1.68		
2.0		2.87				
2.1	1.60					
2.3		3.33				1.65
2.5					1.87	
2.7		4.0				1.90
2.9	2.0			2.10		
3.2		5.1				
3.4						2.20
3.8		6.7				
4.0						2.65
4.1				2.73		
4.2						
4.3	2.65				2.80	
4.5						3.3
5.6				4.17		4.4
6.1	3.5					
6.8						6.7
7.5					5.6	
8.2				8.3		
9.0	7.0					

APPENDIX C

EFFECT OF HEAT CAPACITY DIFFERENCES BETWEEN LIQUID AND SOLID SOLUTE ON $\ln(k^e/\gamma^l)$ vs. $1/T$ RELATIONSHIPS FOR COPPER AND GOLD

Taking into account the temperature dependence of the enthalpy and entropy of fusion of a solute, Euqation 4.1 may be written as

$$\ln \frac{k^e}{\gamma^l} = \frac{\Delta H^f\ (T_m) - \Delta\overline{H}^{\alpha}}{RT} + \frac{\Delta\overline{S}^{ex,\alpha} - \Delta S^f\ (T_m)}{R} + f_1(T)\ ,$$

where

$$f_1(T) = \frac{1}{R}\Big[\ (T - T_m)\ \Big(\frac{C_p - a}{T} + b\ \Big) +$$

$$(a - C_p)\ln\frac{T}{T_m} - \frac{b}{2T}\,(T^2 - T_m^{\ 2})\ \Big]$$

and the specific heat of the liquid and solid are C_p and $(a + bT)$, respectively. These values per mole are: (Smithells, 1962)

Cu - $a = 5.41$ cal., $b = 1.40 \times 10^{-3}$ cal./°K, $C_p = 7.5$ cal.

Au - $a = 5.66$ cal., $b = 1.24 \times 10^{-3}$ cal./°K, $C_p = 7.0$ cal.

The following is a tabulation of calculated $f_1(T)$ values.

	T(°K)	$T - T_m$	$f_1(T)$
Cu	800	- 556	- .01
	1000	- 356	- .008
	1200	- 156	- .002

	T(°K)	T - T_m	$f_1(T)$
	1200	- 136	- .0015
Au	1400	64	- .001
	1600	264	-

BIBLIOGRAPHY

- Ainslie, N.G., Hoffman, R.E., and Seybold, A.V., 1960[a], Acta Met., 8, 523; 1960[b], Ibid., 8, 528.
- Arkharov, V.I., Ivanovskaya, S.I., Kolesnikova, N.M., and Fovanova, T.A., 1956, Fizika Metallov i Metallovedenie, 2, 57.
- Bauer, C.L., 1966, J. Phys. Chem. Solids, 27, 1133.
- Bernard, W., Roth, W., Schmid, A.P., and Zeldes, P., 1963, Phys. Rev., 131, 627.
- Bjerrum, N., 1926, Kgle. Danske Vidensk. Selskab., 7, No. 9.
- Blakemore, J.S., 1962[a], "Semiconductor Statistics" (New York: Pergamon Press), Chapter 1; 1962[b], Ibid., Chapter 3.
- Boltaks, B.I., 1963[a], "Diffusion in Semiconductors" (New York: Academic Press), Chapter 7; 1963[b], Ibid., Chapter 4
- Boltaks, B.I., Julikov, G.S., Malkovich, R.Sh., 1960-61, Sov. Phys. - Solid State, 2, 2134.
- Brooks, M.S., and Kennedy, J.K., 1962, "Ultrapurification of Semiconductor Materials" (New York: MacMillan), Chapter 2.
- Bullis, W.M., 1966, Solid State Elect., 9, 143.
- Bullough, R., and Newman, R.C., 1959, Proc. Roy. Soc., A249, 427; 1961, Phil. Mag., 6, 403; 1962, Proc. Roy. Soc., A266, 209; 1963, Prog. in Semicond., 7, 99.
- Bullough, R., Newman, R.C., Wakefield, J., and Willis, J.B., 1960, J. Appl. Phys., 31, 707.

- Burke, J., 1965^{a}, "The Kinetics of Phase Transformations in Metals" (New York: Pergamon Press), Chapter 6; 1965^{b}, Ibid., Chapter 5.
- Burton, J.A., Hull, G.W., Morin, F.J., and Severiens, J.C., 1953^{a}, J. Phys. Chem., 57, 853.
- Burton, J.A., Kolb, E.D., Slichter, W.P., and Struthers, J.D., 1953^{b}, J.Chem. Phys., 21, 1991.
- Burylev, B.P., 1963, Russ. J. Phys. Chem., 37, 1120.
- Cahn, J.W., 1957, Acta Met., 5, 169.
- Callen, H.B., 1960, "Thermodynamics" (New York: John Wiley), Chapter 2.
- Cardona, M., Paul, W., and Brooks, H., 1959, J. Phys. Chem. Solids, 8, 204.
- Carpenter, S.H., and Baker, G.S., 1965, Acta. Met., 13, 917.
- Carslaw, H.S., and Jaeger, J.C., 1959, "Conduction of Heat in Solids", 2nd. ed. (Oxford: Clarendon Press), p. 332.
- Caryl, D.B., and Ward, R.G., 1967, J. Iron and Steel Inst., 205, 28.
- Castaing, R., 1951, Rescherche Aeronaut., 23, 41.
- Christian, J.W., 1965, "The Theory of Transformations in Metals and Alloys" (Oxford: Pergamon Press), Chapter 6.
- Collins, C.B, and Carlson, R.O., 1957, Phys. Rev., 108, 1409.
- Collins, C.B., Carlson, R.O., and Gallagher, C.J., 1957, Phys. Rev., 105, 1168.
- Cottrell, A.H., 1953, "Dislocations and Plastic Flow in Crystals" (Oxford: Clarendon Press), Chapter 4; 1955, "Theoretical Structural Metallurgy", 2nd. Ed. (London: Edward Arnold), Chapter 7.
- Cottrell, A.H., and Bilby, B.A., 1949, Proc. Phys. Soc., A62, 49.

- Cox, G.W., 1965, Ph.D. Thesis, Univ. of N.S.W., Australia.
- Crank, J., 1956, "Mathematics of Diffusion" (Oxford: Clarendon Press), Chapter 7.
- Darken, L.S., and Gurry, R.W., 1953, "Physical Chemistry of Metals" (New York: McGraw-Hill), p. 264.
- Dash, W.C., 1956, J.Appl. Phys., 27, 1193.
- Davenport, E.S., and Bain, E.C., 1935, Trans. Amer. Met. Soc., 23, 1047.
- Dean, F.V., Kerr, J.R., and Hellawell, A., 1961-62, J. Inst. Metals, 90, 234.
- Denbigh, K., 1966, "The Principles of Chemical Equilibrium", 2nd. Ed. (Cambridge: University Press), Section 2.13.
- Dekker, A.J., 1957, "Solid State Physics" (Englewood Cliffs: Prentice Hall), Chapter 12.
- Doremus, R.H., 1960, Trans. AIME, 218, 596.
- Dunlap, W.C., 1955, Phys. Rev., 97, 614.
- Elliott, R.P., 1965, "Constitution of Binary Alloys", 1st. Supp. (New York: McGraw-Hill).
- Fiermans, L., and Vennik, J., 1965, Phys. Stat. Sol., 12, 277.
- Frank, F.C., 1953, Phil. Mag., 44, 854.
- Frank, F.C., and Turnbull, D., 1956, Phys. Rev., 104, 617.
- Freedman, J.F., and Nowick, A.S., 1958, Acta Met., 6, 176.
- Fritzsche, H., 1958, J. Phys. Chem. Solids, 6, 69.
- Fuller, C.S., 1959, "Semiconductors", Ed. N.B. Hannay (New York: Reinhold), Chapter 5.
- Fuller, C.S., and Ditzenberger, J.A., 1956, J. Appl. Phys., 27, 544.

- Fuller, C.S., Struthers, J.D., Ditzenberger, J.A., and Wilfstirn, K.B., 1954, Phys. Rev., 93, 1182.
- Fuoss, R.M., 1934, Trans. Faraday Soc., 30, 967.
- Gallagher, C.J., 1957, J. Phys. Chem. Solids, 3, 82.
- Geballe, T.H., 1959, "Semiconductors", Ed. N.B. Hannay (New York: Reinhold), Chapter 8.
- Gibbs, J.W., 1906, Scientific Papers, Vol. I (Thermodynamics), p. 219.
- Guggenheim, E.A., 1935, Proc. Roy. Soc., A148, 304.
- Hall, R.N., 1957, J. Phys. Chem. Solids, 3, 63.
- Hall, R.N., and Racette, J.H., 1964, J. Appl. Phys., 35, 379.
- Ham, F.S., 1958, J. Phys. Chem. Solids, 6, 335; 1959, J. Appl. Phys., 30, 915.
- Hansen, M., 1958, "Constitution of Binary Alloys", 2nd. Ed. (New York: McGraw-Hill).
- Harper, S., 1951, Phys. Rev., 83, 709.
- Hartley, S., 1966, Acta Met., 14, 1237.
- Heumann, T., and Heinemann, F., 1956, Z Elektrochem., 20, 222.
- Hildebrand, J.H., 1929, J. Am. Chem. Soc., 51, 66.
- Hildebrand, J.H., and Scott, R.L., 1950, "The Solubility of Non-electrolytes" (New York: Reinhold), Chapter 23.
- Hume-Rothery, W., and Raynor, G.V., 1962, "The Structure of Metals and Alloys", 4th. Ed. (London: Institute of Metals), Part 1.
- Huntington, H.B., Shirn, G.A., and Wajda, E.S., 1955, Phys. Rev., 99, 1085.

- Ing, S.W., Morrison, R.E., Alt, L.L., and Aldrich, R.W., 1963, J. Electrochem. Soc., 110, 533.
- Irvin, J.C., 1962, Bell Syst. Tech. J. 41, 387.
- Jaccodine, R.J., 1964, Appl. Phys. Lett., 4, 114.
- Johnson, W.A., and Mehl, R.F., 1939, Trans. AIME, 135, 416.
- Joshi, M.L., and Dash, S., 1966, J. Appl. Phys., 47, 2453.
- Kidson, G.V., and Miller, G.D., 1964, J. Nucl. Mat., 12, 61.
- Kirkaldy, J.S., 1958, Can. J. Phys., 36, 899.
- Kirkaldy, J.S. and Brown, L.C., 1963, Can. Met. Quart., 2, 89.
- Kirkaldy, J.S., and Purdy, G.R., 1962,[a] Can. J. Phys., 40, 202; 1962,[b] Ibid., 40, 208.
- Kirkaldy, J.S., Brigham, R.J., and Weichert, D.H., 1965, Acta Met., 13, 907.
- Knight, G., 1956, "Handbook of Semiconductor Electronics", Ed. L.P. Hunter (New York: McGraw-Hill), Section 20.
- Koch, R.C., 1960, "Activation Analysis Handbook" (New York: Academic Press).
- Kofstad, P., 1963, J. Electrochem. Soc., 110, 491.
- Kooi, E., 1964, J. Electrochem. Soc., 111, 1383.
- LaChapelle, T.J., and Heller, H.B., 1964, Trans. AIME, 230, 311.
- Lehovec, K., 1962, J. Phys. Chem. Solids, 23, 695.
- Leymonie, C., 1963, "Radioactive Tracers in Physical Metallurgy" (New York: John Wiley).
- Lifshin, E., and Hanneman, R.E., 1965, General Electric Report No. 65-RL-3944M (The Knolls, Schnectady, N.Y. : Research Information).
- Lifshitz, I.M., 1956, Nuovo cimento Suppl., 3, 716.
- Lücke, K., and Detert, K., 1957, Acta Met., 5, 628.

- Lupis, C.H.P., and Elliott, J.F., 1966[a], Acta Met., 14, 529; 1966[b], Ibid., 14, 1019.
- Maradudin, A.A., Montroll, E.W., and Weiss, G.H., 1963, Solid State Physics, Suppl. 3 (New York: Academic Press).
- McCaldin, J.O., 1965, J. Appl. Phys., 36, 211.
- McLean, D., 1957[a], "Grain Boundaries in Metals" (Oxford: Clarendon Press), Chapter 2; 1957[b], Ibid., Chapter 5.
- McSkimin, H.J., 1953, J. Appl. Phys., 24, 988.
- Millea, M.F., 1966, J. Phys. Chem. Solids, 27, 315.
- Mima, G., and Hasegawa, M., 1960, Technol. Repts. Osaka Univ., 10, 157.
- Morin, F.J., and Maita, J.P., 1954, Phys. Rev., 94, 1525.
- Mott, N.F., and Gurney, R.W., 1948, "Electronic Processes in Ionic Crystals", 2nd. Ed. (Oxford: Clarendon Press), Chapter 2.
- Onsager, L., 1944-45, Ann. N.Y. Acad. Sci., 46, 241.
- Oriani, R.A., and Hall, R.N., 1958, J. Phys. Chem. Solids, 6, 97.
- Paul, W., and Brooks, H., 1963, Prog. in Semicond., 7, 135.
- Pearson, G.L., and Bardeen, J., 1949, Phys. Rev., 75, 865.
- Penning, P., 1958[a], Philips Res. Repts., 13, 79; 1958[b], Ibid., 13, 17.
- Plumb, R.C., and Lewis, J.E., 1955, Nucleonics, 13, 42.
- Potemkin, A.Ya., and Potapov, V.I., 1960, Sov. Phys. - Solid State, 2, 1668.
- Prigogine, L., and Defay, R., "Chemical Thermodynamics" (New York: Longman's, Green), P. 357.
- Reiss, H., 1953, J. Chem. Phys., 21, 209.

- Reiss, H., and Fuller, C.S., 1956, J. Metals, 12, 276; 1959, "Semiconductors", Ed. N.B. Hannay (New York, Reinhold), Chapter 6.
- Reiss, H., Fuller, C.S., and Morin, F.J., 1956a, Bell Syst. Tech. J., 35, 535.
- Reiss, H., Fuller, C.S., and Pietruszkiewitz, A.J., 1956b, J. Chem. Phys., 25, 650.
- Rieger, H., 1964, Phys. Stat. Sol., 7, 685.
- Safranek, W.H., and Winkler, J.H., 1953, "Modern Electroplating", Ed. A.G. Gray (New York; John Wiley), p. 231.
- Schwuttke, G.H., 1961, J. Electrochem. Soc., 108, 163.
- Seitz, F., 1952, "Imperfections in Nearly Perfect Crystals", Ed. W. Shockley (New York: John Wiley), Chapter 1.
- Sheasby, J., 1963, Ph.D. Thesis, Univ. of N.S.W., Australia.
- Shockley, W., 1950, "Electrons and Holes in Semiconductors" (Princeton: D. Van Nostrand), Chapter 16.
- Shockley, W., and Last, J.J., 1957, Phys. Rev., 107, 392.
- Shockley, W., and Moll, J.L., 1960, Phys. Rev., 119, 1480.
- Sittner, W.R., 1956, "Handbook of Semiconductor Electronics", Ed. L.P. Hunter (New York: McGraw-Hill), Section 8.6.
- Slater, J.S., 1960, M.Sc. Thesis, McMaster University.
- Smithells, C.J., 1962, "Metals Reference Book", 3rd. Ed., Vol. II, (London: Butterworths).
- Smits, F.M., 1958, Proc. I.R.E., 46, 1049.
- Sosnowski, L., 1959, J. Phys. Chem. Solids, 8, 142.
- Sprokel, G.J. and Fairfield, J.M., 1965, J. Electrochem. Soc., 112, 200.

- Struthers, J.D., 1956, J. Appl. Phys., **27**, 1560.
- Stull, D.R., and Sinke, G.C., 1956, "Thermodynamic Properties of the Elements" (Washington: American Chemical Society).
- Swalin, R.A., 1961, J. Phys. Chem. Solids, **18**, 290.
- Swalin, R.A., 1962, "Thermodynamics of Solids" (New York: John Wiley), Chapter 14.
- Syed, A.S., 1964, Ph.D. Thesis, University of British Columbia.
- Thomas, W.R., and Leak, G.M., 1955, J. Iron and Steel Inst., **180**, 155.
- Thurmond, C.D., 1959, "Semiconductors", Ed. N.B. Hannay (New York, Reinhold), Chapter 4.
- Thurmond, C.D., and Kowalchik, M., 1960, Bell Syst. Tech. J., **39**, 169.
- Tiller, W.A., 1958, J. Appl. Phys., **29**, 611.
- Trumbore, F.A., 1956, J. Electrochem. Soc., **103**, 597.
- Trumbore, F.A., 1960, Bell Syst. Tech. J., **39**, 205.
- Trumbore, F.A., Isenberg, C.R., and Porbansky, E.M., 1958, J. Phys. Chem. Solids, **9**, 60.
- Trumbore, F.A., Porbansky, E.M., and Tartaglia, A.A., 1959, J. Phys. Chem. Solids, **11**, 239.
- Trumbore, F.A., Spitzer, W.G., and Logan, R.A., 1962, J. Electrochem. Soc., **109**, 734.
- Tweet, A.G., 1957, Phys. Rev., **106**, 221.
- Tyler, W.W., 1959, J. Phys. Chem. Solids, **8**, 59.
- Van Bueren, H.G., 1960[a], "Imperfections in Nearly Perfect Crystals" (Amsterdam: North Holland), Chapter 1; 1960[b], Ibid., Chapter 9; 1960[c], Ibid., Chapter 31.

- Wagner, C., and Schottky, W., 1930, Z. phys. Chem., B11, 163.
- Wagner, C., 1952^{a}, "Thermodynamics of Alloys" (Reading, Mass: Addison-Wesley), Chapter 1; 1952^{b}, Ibid., Chapter 2.
- Wallwork, G.R., 1959, Ph.D. Thesis, Univ. of N.S.W., Australia.
- Wallwork, G.R., and Jenkins, A.E., J. Electrochem. Soc., 106, 10.
- Watkins, G.D., 1963, J. Phys. Soc. Japan, 18, Suppl. II, 22.
- Webb, W.W., 1957, Acta Met., 5, 89.
- Weertman, J., 1957, Phys. Rev., 107, 1259.
- Weisberg, L. and Graham, A.K., "Modern Electroplating", Ed. A.G. Gray (New York: John Wiley), p. 252.
- Weiser, K., 1962, Phys. Rev., 126, 1427.
- Wertheim, G.K., 1959, Phys. Rev., 115, 37.
- Westbrook, J.H., 1964, Met. Rev., 9, 415.
- Westbrook, J.H., and Wood, D.L., 1961, Nature, 192, 1280.
- Wilcox, W.R., and LaChapelle, T.J., 1964, J. Appl. Phys., 35, 240.
- Wilcox, W.R., LaChapelle, T.J., and Forbes, D.H., 1964, J. Electrochem. Soc., 111, 1377.
- Wittry, D.B., Axelrod, J.M., and McCaldin, J.O., 1960, "Properties of Elemental and Compound Semiconductors", Ed. H.C. Gatos, Met. Soc. AIME Conf., Vol. 5 (New York: Interscience), p. 89.
- Woodbury, H.H., and Ludwig, G.W., 1960, Phys. Rev., 117, 102.
- Woodbury, H.H., and Tyler, W.W., 1957, Phys. Rev., 105, 84.
- Wong, M.C., 1965, Metals Progress, 87, No 5., 5.
- Worthing, A.G., and Geffner, J., 1943, "Treatment of Experimental Data" (New York: John Wiley), Chapter 11.

- Zaromb, S., 1957, I.B.M. Journal of Res. and Dev., 1, 57.
- Zener, C., 1949, Acta Cryst., 2, 163; 1950, "Symposium on Thermodynamics in Physical Metallurgy" (Cleveland: American Society for Metals), p. 16; 1952, "Imperfections in Nearly Perfect Crystals", Ed. W. Shockley (New York: John Wiley), p. 289.